COPY 1

Report No.: FAA-RD-74-125, II-I

CORE ENGINE NOISE CONTROL PROGRAM

Volume II, Supplement I - IDENTIFICATION OF NOISE GENERATION and SUPPRESSION MECHANISMS

FAA WJH Technical Center
00026768

R.K. Matta
P.R. Mingler

AIRCRAFT ENGINE GROUP
GENERAL ELECTRIC COMPANY
CINCINNATI, OHIO 45215

NAFEC
LIBRARY
SEP 28 '76

July, 1976

FINAL REPORT

Document is available to the public through the
National Technical Information Service,
Springfield, Virginia 22151

Prepared for

U.S. DEPARTMENT OF TRANSPORTATION
FEDERAL AVIATION ADMINISTRATION
Systems Research & Development Service
Washington, D.C. 20590

NOTICE

This document is disseminated under the sponsorship of the Department of Transporation in the interest of information exchange. The United States Government assumes no liability for its contents or use thereof.

1. Report No.	2. Government Accession No.	3. Recipient's Catalog No.
FAA-RD-74-125, II-I		

4. Title and Subtitle	5. Report Date
Core Engine Noise Control Program Volume II Supplement I - Identification of Noise Generation and Suppression Mechanisms	July 1976
	6. Performing Organization Code R76AEG341
7. Author(s) R.K. Matta (Ed.), S.B. Kazin (Prog. Tech. Dir.), P.R. Mingler	8. Performing Organization Report No.
9. Performing Organization Name and Address General Electric Company Advanced Engineering and Technology Programs Department Aircraft Engine Group Evendale, Ohio 45215	10. Work Unit No. 36310
	11. Contract or Grant No. DOT-FA72WA-3023
12. Sponsoring Agency Name and Address U.S. Department of Transportation Federal Aviation Administration Systems Research and Development Service / Washington, D.C. 20590	13. Type of Report and Period Covered Final - Jan.- July 1975
	14. Sponsoring Agency Code

15. Supplementary Notes

Volume I - Identification of Component Noise Sources, FAA-RD-74-125, I
Volume II - Identification of Noise Generation and Suppression Mechanisms, FAA-RD-74-125, II
Volume III and Volume III Supplement I - Prediction Methods, FAA-RD-74-125, III and III-I

16. Abstract

The work reported herein is supplemental to the earlier investigations of the mechanisms of core engine noise generation and suppression which are reported in FAA-RD-74-125, III. The prediction models of Volume III were updated based on this effort.

TURBINE NOISE - Two source noise reduction mechanisms, blade row spacing, and vane lean, were exercised analytically to define the acoustic benefits associated with varying these parameters. It is shown how multi-stage turbines can be optimized through appropriate distribution of spacing between the blade pairs. The vane lean results indicate that very large reduction can be obtained in the acoustic energy associated with the dominant radial mode.

LOW FREQUENCY CORE NOISE - Three compact suppressor configurations were designed and tested in a hot flow, rectangular duct facility. Two of these (stacked and acoustic rectifier treatments) are recommended as engine compatible suppressors for low frequency core noise. The third configuration, side-branch resonator, yielded poor suppression results.

TURBINE TONE/JET STREAM INTERACTION - The turbulence scattering analysis defined earlier (Volume II) was exercised in a parametric study after using experimental data to model the shear layer turbulence. The scattered energy exhibits a strong dependence on the fan jet velocity, incident tone frequency, and the distance between the fan and core exhaust planes.

17. Key Words (Suggested by Author(s))	18. Distribution Statement
Core Engine Noise, Turbofan Engine Noise, Jet Engine Noise Control, Combustor Noise, Core Noise, Turbine Noise, Tone/Jet Stream Interaction	Document is available to the public through the National Technical Information Service, Springfield, Virginia 22151

19. Security Classif. (of this report)	20. Security Classif. (of this page)	21. No. of Pages	22. Price
Unclassified	Unclassified	154	

METRIC CONVERSION FACTORS

Approximate Conversions to Metric Measures

Symbol	When You Know	Multiply by	To Find	Symbol
		LENGTH		
in	inches	*2.5	centimeters	cm
ft	feet	30	centimeters	cm
yd	yards	0.9	meters	m
mi	miles	1.6	kilometers	km
		AREA		
in^2	square inches	6.5	square centimeters	cm^2
ft^2	square feet	0.09	square meters	m^2
yd^2	square yards	0.8	square meters	m^2
mi^2	square miles	2.6	square kilometers	km^2
	acres	0.4	hectares	ha
		MASS (weight)		
oz	ounces	28	grams	g
lb	pounds	0.45	kilograms	kg
	short tons (2000 lb)	0.9	tonnes	t
		VOLUME		
tsp	teaspoons	5	milliliters	ml
Tbsp	tablespoons	15	milliliters	ml
fl oz	fluid ounces	30	milliliters	ml
c	cups	0.24	liters	l
pt	pints	0.47	liters	l
qt	quarts	0.95	liters	l
gal	gallons	3.8	liters	l
ft^3	cubic feet	0.03	cubic meters	m^3
yd^3	cubic yards	0.76	cubic meters	m^3
		TEMPERATURE (exact)		
°F	Fahrenheit temperature	5/9 (after subtracting 32)	Celsius temperature	°C

*1 in = 2.54 exactly. For other exact conversions and more detailed tables, see NBS Misc. Publ. 286, Units of Weights and Measures, Price $2.25, SD Catalog No. C13.10:286.

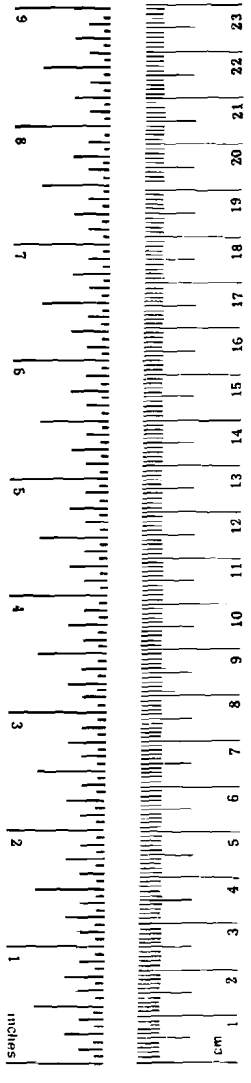

Approximate Conversions from Metric Measures

Symbol	When You Know	Multiply by	To Find	Symbol
		LENGTH		
mm	millimeters	0.04	inches	in
cm	centimeters	0.4	inches	in
m	meters	3.3	feet	ft
m	meters	1.1	yards	yd
km	kilometers	0.6	miles	mi
		AREA		
cm^2	square centimeters	0.16	square inches	in^2
m^2	square meters	1.2	square yards	yd^2
km^2	square kilometers	0.4	square miles	mi^2
ha	hectares (10,000 m^2)	2.5	acres	
		MASS (weight)		
g	grams	0.035	ounces	oz
kg	kilograms	2.2	pounds	lb
t	tonnes (1000 kg)	1.1	short tons	
		VOLUME		
ml	milliliters	0.03	fluid ounces	fl oz
l	liters	2.1	pints	pt
l	liters	1.06	quarts	qt
l	liters	0.26	gallons	gal
m^3	cubic meters	35	cubic feet	ft^3
m^3	cubic meters	1.3	cubic yards	yd^3
		TEMPERATURE (exact)		
°C	Celsius temperature	9/5 (then add 32)	Fahrenheit temperature	°F

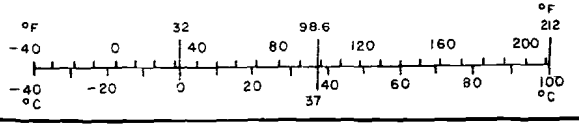

PREFACE

This report describes the work performed under the DOT/FAA Core Engine Noise Control Program (Contract DOT-FA72WA-3023). The original work under this contract is in Report Number FAA-RD-74-125, Volumes I,II, and III.

Supplements to Volumes II and III report additional work undertaken under this program after completion of the work reported in the original three volumes.

The objectives of the program were:

- Identification of component noise sources of core engine noise (Phase I).
- Identification of mechanisms associated with core engine noise generation and noise reduction (Phases II and III).
- Development of techniques for predicting core engine noise in advanced systems for future technology aircraft (Phase IV).
- Extension of the core noise prediction (Phase V).
- Update of the core engine noise control effort (Phase VI).

The objectives were accomplished in six phases as follows:

- Phase I - Analysis of engine and component acoustic data to identify potential sources of core engine noise and classification of the sources into major and minor categories.
- Phase II - Identification of the noise generating mechanism associated with each source through a balanced program of:

  Analytical studies

  Component and model tests

  Acoustic evaluation of data from existing and advanced engine systems.
- Phase III - Identification of noise reduction mechanisms for each source through a program with elements similar to Phase II.
- Phase IV - Development of improved prediction techniques incorporating the results obtained during the preceding two phases.

- Phase V - Analysis of low frequency noise transmission through turbine blade rows and addition of engine and component data to the prediction method for core noise.

- Phase VI - Analytical studies of turbine source noise suppression and parametric trends in turbine tone/jet stream interaction; an experimental study of compact low frequency noise suppressors and a prediction model update.

The work accomplished is reported in five volumes corresponding respectively to the five objectives stated above.

- Volume I - Identification of Component Noise Sources (FAA-RD-74-125, I).

- Volume II - Identification of Noise Generation and Suppression Mechanisms (FAA-RD-74-125, II).

- Volume III - Prediction Methods (FAA-RD-125, III).

- Volume III Supplement I - Extension of Prediction Methods. (FAA-RD-74-125, III-I)

- Volume II Supplement I - Extension to Identification of Noise Generation and Suppression Mechanisms. (FAA-RD-74-125, II-I)

A visual representation of the overall program and report organization is shown on pages v and vi.

This volume documents the results of the Phase VI activity which extended the initial core engine noise control work through:

1) Analytical studies of turbine noise reduction at the source through blade row spacing and through vane lean

2) Design and testing of three compact suppressors for low frequency noise attenuation.

3) A parametric study on turbine tone modulation by coannular jet flows.

CORE ENGINE NOISE CONTROL PROGRAM
OVERALL REPORT ORGANIZATION

Contract Phase		Contract Documentation
Phase I	Volume I	Identification of Component Noise Sources FAA-RD-74-125,I
Phase II and Phase III	Volume II	Definition of Mechanisms of Noise Generation Definition of Mechanisms of Noise Reduction FAA-RD-74-125,II
Phase IV	Volume III	Development of Prediction Techniques FAA-RD-74-125,III

CORE ENGINE NOISE CONTROL PROGRAM
OVERALL REPORT ORGANIZATION

Contract Phase		Contract Documentation
Phase V	Volume III, Supplement I	Extension of the Core Noise Prediction Technique FAA-RD-74-125, III-I
Phase VI	Volume II, Supplement I	Extension to the Definition of the Mechanisms of Noise Generation and Suppression FAA-RD-74-125, II-I

SUMMARY

The work reported in this Volume is supplemental to the efforts of Phases 2 and 3: Identification of Mechanisms of Noise Generation and Suppression. Three core engine noise sources were investigated: Turbine Noise, Low Frequency Core Noise, and Turbine Tone/Jet Stream Interaction.

Turbine Noise - Two source noise reduction mechanisms, blade row spacing and vane lean, were studied analytically to determine the relative acoustic benefit associated with varying these geometric parameters.

The spacing study shows how to allocate any given amount of spacing between the various blade pairs in a multi-stage turbine to achieve optimum noise reduction. The allocation follows from consideration of the noise generation by each set of interactions.

Spacing results in noise reduction due to the decay of the viscous wake. Vane leaning results in noise reduction by phasing the wake interaction across the blade span. The results of this study show that the benefits are optimized by curved vanes, providing over 20 dB attenuation for the dominant first radial mode. These curved vanes, which are radial at the hub, also avoid secondary flow problems which would be associated with the acute angles that follow from straight leaned vanes.

The prediction program for viscous wake interaction noise used in these source noise studies is provided in the appendices.

Low Frequency Core Noise Suppression - Three compact suppressor configurations compatible with aircraft engine installations were designed and tested in a hot flow, rectangular duct facility. The three configurations were stacked treatment, acoustic rectifier, and side-branch resonator. Design details and geometric definitions of each suppressor configuration are presented. The test results are shown and discussed for temperatures of 590° K and 720° K at Mach numbers of 0.2, 0.3, and 0.4.

The stacked treatment and the acoustic rectifier configurations are recommended as engine compatible suppressors having the ability to achieve 10 dB suppression over a resonable frequency range below 2000 Hz. The side-branch resonator is not recommended due to poor suppression test results.

Turbine Tone/Jet Stream Interaction - The outer shear layer of a coannular flow configuration was modeled using engine and model data, and the scaling laws for interaction were established. The turbulence scattering analysis defined in Volume II was exercised in a parametric study. The energy in the scattered wave (haystack) exhibits a strong dependence on the

tone frequency, fan velocity and the relative distance between the fan and core nozzle exhaust planes; increasing with all three. The fan velocity and the distance between the exhaust planes together serve to define the quality and quantity of the turbulence in the shear layer. At the same time, the influence of velocity ratio and area ratio appears to be minimal.

The results are in good agreement with the empirical prediction formulated using engine data in Volume III. This method is updated by formal inclusion of the frequency term as a prediction parameter in addition to the fan jet velocity and the relative distance between nozzle planes.

TABLE OF CONTENTS

Section		Page
	PREFACE	
	SUMMARY	
1.0	INTRODUCTION	1
2.0	TURBINE SOURCE NOISE REDUCTION	3
	2.1 Turbine Discrete Frequency Noise	3
	2.2 Spacing	3
	2.3 Leaned Vanes	13
	2.4 Discussion	27
	2.5 Conclusions	31
	2.6 Prediction Method Update	32
3.0	COMPACT SUPPRESSORS FOR LOW FREQUENCY NOISE	33
	3.1 Background	33
	3.2 Suppressor Concepts	33
	3.3 Experimental Procedure	38
	3.4 Test Results	51
	3.5 Discussion	61
	3.6 Conclusions and Recommendations	61
	3.7 Prediction Method Update	62
4.0	TURBINE TONE/JET STREAM INTERACTION	64
	4.1 Background and Objectives	64
	4.2 Parametric Study	66
	4.3 Discussion	74
	4.4 Conclusions	80
	4.5 Prediction Method Update	82
	APPENDICES/PROGRAM LISTINGS	
	A. Analytical Turbine Tone Prediction	87
	B. Interaction Effects	133

NOMENCLATURE

A	-	area, total resonator neck area
A_{nm}	-	coefficients for acoustic pressure associated with duct modes
A_o	-	incident wave amplitude
AR	-	exhaust nozzle area ratio, fan/core
$\hat{a}_r$	-	unit vector in direction of observer
B	-	number of blades in rotor
BPF	-	blade passing frequency
BPR	-	bypass ratio, fan/core
b	-	shear layer thickness
c	-	acoustic velocity
D	-	diameter
dB	-	decibel
$\mathcal{F}$,F	-	force induced by viscous wake interaction
f	-	frequency
f_c	-	correlation frequency
f_o	-	incident tone or resonance frequency
G_m	-	coefficient of unsteady upwash
Hz	-	Hertz, cycles/sec
h	-	radius ratio, hub/tip
I	-	acoustic intensity
IGV	-	inlet guide vane
i	-	$\sqrt{-1}$
$J_n(\ )$	-	Bessel function of 1st kind and nth order
$K_n(\ )$	-	modified Bessel function of nth order

NOMENCLATURE (continued)

k	-	integer index (Section 2)
kHz	-	kilo-Hertz
k_c	-	correlation wave number, ω_c/c
k_i	-	wave number of incident wave, ω_o/c
k_{nm}	-	$(n^2\omega^2 - \lambda_{nm}^2)^{1/2}$
L	-	distance between fan and core nozzle planes
L_{TL}	-	resonator transmission loss
ℓ	-	blade chord
ℓ_c	-	eddy size
M	-	number of rotating line vortices
M_j	-	jet stream Mach number
M_n	-	duct Mach number
M_t	-	turbulence Mach number
m	-	slope
N	-	rotational speed, rpm
n	-	circumferential mode number (Section 2); number of openings in treatment (Section 3)
n'	-	harmonic
OAPWL	-	overall power level
OASPL	-	overall sound pressure level
OGV	-	outlet guide vane
PWL	-	acoustic power level
p	-	acoustic pressure
R	-	flow resistance of resonator neck
R_o	-	tip radius

NOMENCLATURE (Continued)

R_{nm}	-	cylinder function
r	-	radial coordinate
S_1	-	area of main duct
SPL	-	sound pressure level
s	-	axial spacing between blade rows
T	-	temperature
T_n	-	BPF from nth stage
t	-	time
t_e	-	trailing edge thickness
t°	-	physical neck length
t'	-	equivalent neck length
U	-	blade speed
V	-	number of blades in stationary row (Section 2); volume (Sections 3 and 4)
VR	-	velocity ratio, fan/core
v	-	flow velocity
W	-	weight flow rate
WPS	-	worst possible situation-maximizing noise generation
$X/\rho c$	-	specific reactance component of impedance
$Y_n(\ )$	-	Bessel function of 2nd kind and nth order
y	-	normal coordinate
z	-	axial coordinate
α	-	$k_c \ell_c$
α_h	-	physical blade lean, re hub
α_R	-	resonator dimensionless resistance, $SR/A\rho c$
β	-	air flow angle

NOMENCLATURE (Continued)

β_x	-	resonator dimensionless reactance, $Sc/\pi f_o V$
$\gamma_\kappa, \gamma_\rho$	-	dimensionless perturbations in compressibility and density
Γ	-	unsteady circulation due to viscous wake interaction
Δ	-	difference or increment
Δ_s	-	$\omega - \omega_o$
Δ_5	-	drop in tone intensity due to turbulence scattering
δ	-	drop in tone SPL due to "haystacking"
ε	-	total wake lean, $\theta_e + \Psi$
ζ	-	ratio of flight velocity to jet velocity
η	-	f_o/f_c
η_{nm}	-	norm for cylinder functions
θ	-	angle
θ_e	-	effective aerodynamic lean
κ	-	compressibility, $\frac{1}{\rho}\left(\frac{\partial\rho}{\partial p}\right)$
λ	-	wave length
λ_{nm}	-	eigenvalue
$\vec{\mu}_s$	-	$\frac{\omega}{c}\hat{\alpha}_r - \vec{k}_i$
Θ	-	angle factor, $\cos^2\theta \exp\left[-\frac{1}{2}\mu_s^2 \ell_c^2 - \frac{1}{2}\left(\frac{\Delta_s}{\omega_c}\right)^2\right]$
ρ	-	density
ρc	-	acoustic impedance
σ	-	blade row solidity, $\frac{\text{pitch}}{\text{chord}}$
τ	-	time delay
ϕ	-	angle
ψ	-	blade geometrical lean, re turbine axis
Ω	-	angular velocity, rad/sec

NOMENCLATURE (Concluded)

ω	-	circular frequency
ω_o	-	incident tone frequency, $k_i c$
$(\ )_{abs}$	-	value in stationary coordinate frame
$(\ )_c$	-	correlation value
$(\ )_{core}$	-	primary (core) nozzle or jet parameter
$(\ )_{fan}$	-	secondary (fan) nozzle or jet parameter
$(\ )_{rel}$	-	value in rotating coordinate frame
$(\vec{\ })$	-	vector quantity
$\overline{(\ )}$	-	mean, time-averaged value
$(\ )'$	-	derivative
$\langle\ \rangle$	-	time and space-average of mean square quantity
$\lvert\ \rvert$	-	magnitude, absolute value

SECTION 1.0

INTRODUCTION

The various sources of core engine noise generation were identified and rank ordered in Volume I of the Core Engine Noise Control Program. The major sources were shown to include turbine noise, turbine tone interaction with jet stream turbulence, and low frequency core (combustor) noise. The work reported herein seeks to extend some of the results obtained during the three succeeding phases for these three components.

Turbine Noise - One of the major achievements of the Core Engine Program was the development of an analytic prediction method for turbine tone power (Volume II, Section 4). Not only was the absolute power level accurately predicted, but also the change in level due to increased spacing between the turbine third stage rotor and nozzle. This analysis was also extended to circumferentially leaned turbine nozzles. In effect when a vane is leaned, the angle between the wake of a nozzle or rotor is increased relative to the leading edge of a downstream blade row. The result is a time phased interaction which reduces the peak pressure pulse leaving the downstream blade.

Leaning and spacing can be used as source noise reduction techniques in turbines to produce noise reduction with a minimized impact on the engine system. This analytic prediction method provided the capability to conduct parametric studies which were used in this supplemental study to obtain design trade-off comparisons of the relative acoustic benefits associated with varying these geometric parameters.

Combustor Noise - The combustor noise tests of Phase 3 (Volume II, Section 3) included successful demonstration of a low frequency suppressor configuration. The configuration, however, was not compatible with an actual aircraft engine installation due to its size. Several ideas for potential low frequency suppressor configurations were identified which offer promise of being compatible with an actual installation. These configurations were tested in an existing rectangular duct facility which is capable of using heated flow to represent temperature conditions existing in the core nozzle. This effort established the configuration of a viable core noise suppressor and provided for the expansion of the range of acoustic treatment design parameters which will result in significant core noise suppression.

Turbine Tone/Jet Stream Interaction - An analysis was formulated in Phase 2 (Volume II, Section 5) to describe the turbulence scattering phenomenon which leads to "haystacking" of turbine tones as they propagate through the exhaust jet mixing region(s). The analysis indicated that the pertinent parameters in this interaction would include the tone frequency, the jet velocity, the size of the mixing region, and the quality and quantity of the turbulence in the shear layer. A model of the shear layer and the turbulence encountered permitted an analytical study which isolated the most significant

parameters. Also, the study served to validate the empirical prediction method developed in Phase 4 (Volume III), Section 5) and to scope the applicable range of this method.

In each element, the additional effort increased the utility of the results obtained under the initial program effort by exploring factors that were not apparent when the program was originally formulated.

SECTION 2.0

TURBINE SOURCE NOISE REDUCTION

2.1 TURBINE DISCRETE FREQUENCY NOISE

Viscous wake interaction between adjacent blade rows in the dominant tone generating mechanism in turbines. This mechanism is analytically modeled in Volume II (Section 4) and used to predict the discrete frequency acoustic power level (PWL). A brief description of the prediction method is provided in Volume III (Section 4). A listing of the computer program, the input required and a typical output are shown herein in Appendix A.

This analytical model is useful for turbine source noise reduction studies because it "recognizes" and accounts for variations in the internal aerodynamics and mechanical configuration occurring in the turbine.

The objectives of this effort were to:

- Conduct parametric investigations varying blade row spacing in order to gain insight leading into optimizing configurations in multistage turbines.
- Define the effects of leaned vanes in turbines.

2.2 SPACING

The viability of opened blade row spacing as a noise reduction technique for multi-stage fan turbines is reported in Volume II, Section 4. A highly loaded, 3-stage, fan turbine (Figure 1, Table 1 was tested using the design spacing between blade rows (the baseline configuration) and then with additional spacing inserted in the last two stages. Significant noise reduction was obtained along with minimal performance losses.

A parametric investigation of opened blade row spacing was conducted using the above-mentioned fan turbine. Such a study becomes necessary in a multi-stage turbine not only because the spacing can be split up between stages in different ways, but also because the choice exists of inserting spacing either upstream or downstream of the rotor for each blade passing frequency (BPF) (except, perhaps, that associated with last stage). Wakes from an upstream nozzle row interacting with the rotor, and those from the rotor interacting with a downstream nozzle row both generate the same tone frequency. Hence, two blade pairs, nozzle-rotor (N-R) and rotor-nozzle (R-N), account for the acoustic energy in each BPF (except, of course, that arising from the last stage when there is no outlet guide vane).

INTERACTION	BASELINE (S/C)t	SPACED (S/C)t
N2-R2	.19	.83
R2-N3	.32	1.143
N3-R3	.29	.89

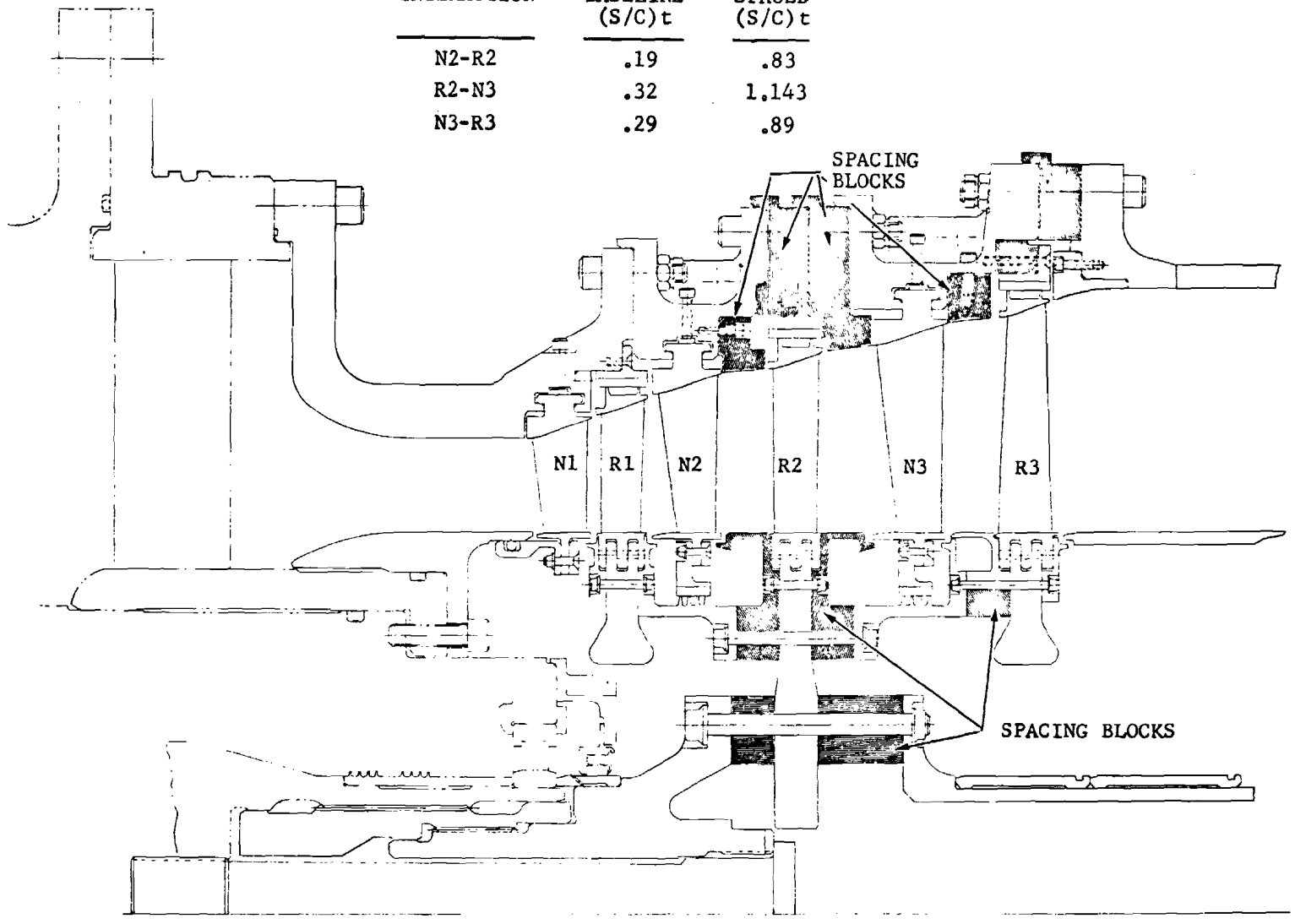

Figure 1 3-Stage Turbine Showing the Increased Spacing

Table 1. 3-Stage Turbine Rig Basic Turbine Data at Design

Average Pitch Loading, $\frac{gJ\Delta h}{2\Sigma U_p^2}$	1.5
Equivalent Specific Work, E/θ_{cr}	33.0 Btu/lb (76753 J/kg)
Equivalent Rotative Speed, $N/\sqrt{\theta_r}$	3169.0 rpm
Equivalent Weight Flow, $W\sqrt{\theta_{cr}}\ \epsilon/\delta$	28.0 lb/sec (12.7 kg/sec)
Inlet Swirl Angle	0 degrees
Exit Swirl Angle Without Guide Vanes	$\leq$ 5 degrees
Maximum Tip Diameter	28.4 inches (72.1 cm)
Number of Stages	3
$\dot{W}\sqrt{T_T}/P_T$ at Inlet	43.16
$\Delta h/T_T$	0.0635
$N/\sqrt{T_T}$	138.98

Design Parameters	Stage 1	Stage 2	Stage 3
Pitch Loading, $\frac{gJ\Delta h}{2U_p^2}$	2.07	1.76	0.85
Exit Axial Mach No.	0.424	0.459	0.407
Exit Absolute Mach No.	0.593	0.602	0.408
Exit Swirl Angle (Degrees)	44	40	3
Number of Blades	106	102	112
Number of Vanes	64	108	100
Tip Speed (Ft/Sec)	384	418	456
Blade Row Spacing $(s/\ell)_p$	.237	.258	.298

s: Axial Spacing Between Blade Rows ℓ: Nozzle Chord Length

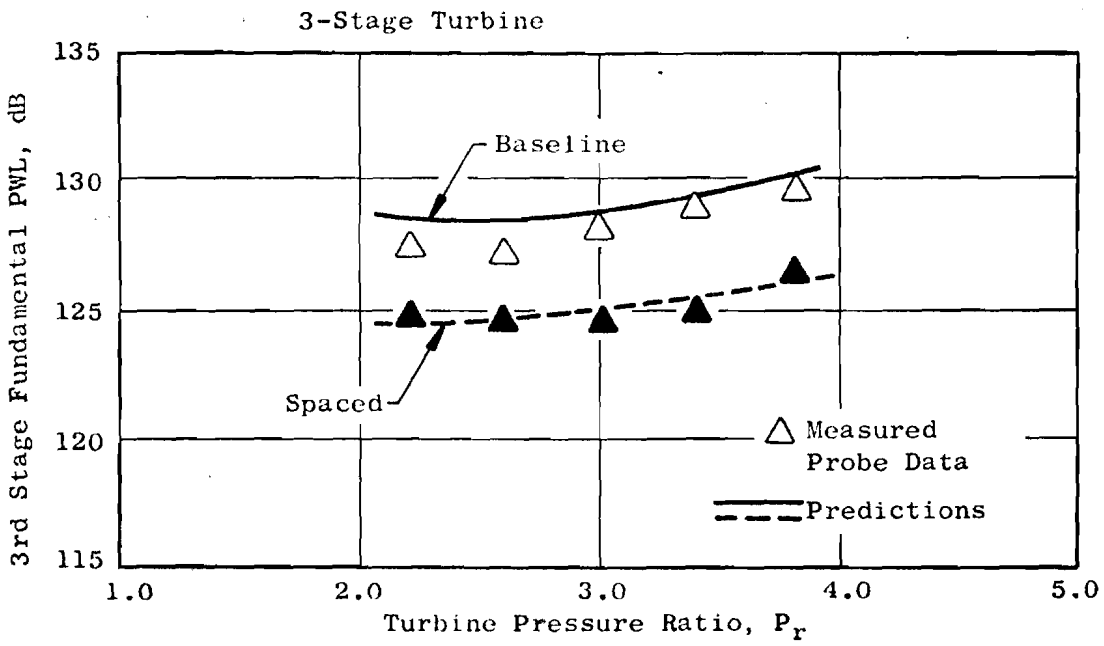

Figure 2 Noise Generation by the Last Stage of a Low Pressure Turbine

This study provides a technique which permits evaluation of multi-stage fan turbines to define optimum placement of any given spacing and the amount of tone noise reduction to be expected.

Up to 7 inches (17.78 cm) additional spacing was introduced between each blade pair. The tone power levels at the source were predicted using the computer program of Appendix A. The predictions shown are for the design point. However, since the exhaust air angles for turbines remain relatively constant over the operating range, the attenuation due to spacing also remains relatively constant (Figure 2). The tone PWL's for the three stage turbine rig are shown in Figures 3(a), (b) and (c) as functions of the blade spacing. Figure 3(a) shows that the N1R1 viscous wake interaction is almost entirely responsible for energy in the first stage tone. This is due to the large chord of the first stage nozzle blades (spacing/chord ratio for the N1R1 interactions are small, Table 2). Turbine tone noise reduction is best accomplished, based on the above, by increasing the spacing between the rotor (R1) and the upstream nozzle (N1).

Suppression of the 2nd stage BPF however, requires spacing to be introduced on either side of the rotor, because the two interactions contribute almost equally as is shown in Figure 3(b).

Curves were generated to define the optimum rotor location for any given amount of blade row spacing by moving the rotor from one extreme position to the other between the upstream and downstream nozzles. The results are shown in Figure 6 for the 1st and 2nd stage. Initially, the entire available spacing was inserted downstream of the rotor and the tone PWL was then generally controlled by the N-R interaction. Then, with the two nozzle rows fixed, the rotor was moved downstream. This results in a decrease of the N-R noise, but increases in the R-N noise. Since the tone is assumed to be the incoherent sum of the two interactions, an optimum location can be located. There is no R-N interaction for the last stage, and, therefore, no optimum. To illustrate how such a study might be used, assume two inches (5.08 cm) of additional spacing is available for stage 2. The minimum tone PWL for this spacing occurs with the rotor 1.43 inches (3.63 cm) from the upstream nozzle. Since the baseline spacing was 0.33 inches (0.84 cm), this means 1.10 inches (2.79 cm) should be introduced upstream of the rotor and the other 0.90 inches (2.29 cm) downstream.

The locus of the minimums for each spacing was curve-fitted and a small study conducted to determine the optimum spacing distribution between the stages for any given overall turbine length increase. The governing criterion was to obtain the maximum reduction possible in turbine noise for any given spacing. Such a study would normally be done on a PNL basis, but in this case, all three (3) tones fall into the same 1/3 octave band and the total tone PWL is a sufficient indicator.

The attenuation suffered by a tone as it propagates through downstream blade rows must be known before source PWL predictions can be used to define the radiated PWL's. These data will be generated under contract DOT-FA75WA-3688 which is now in progress. However, until then empirical estimates must be used.

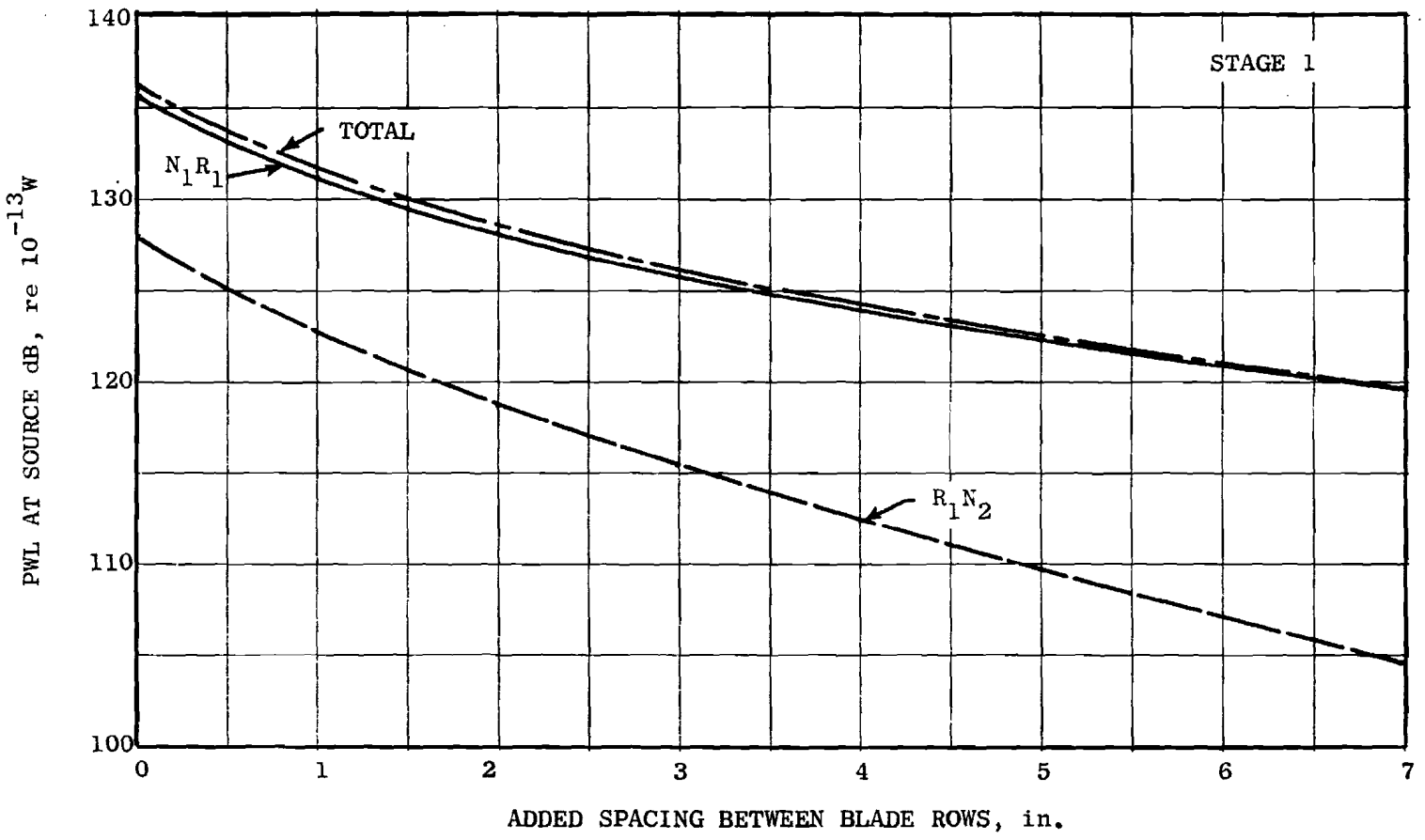

Figure 3 (a) PWL Reduction with Spacing - 1st Stage BPF

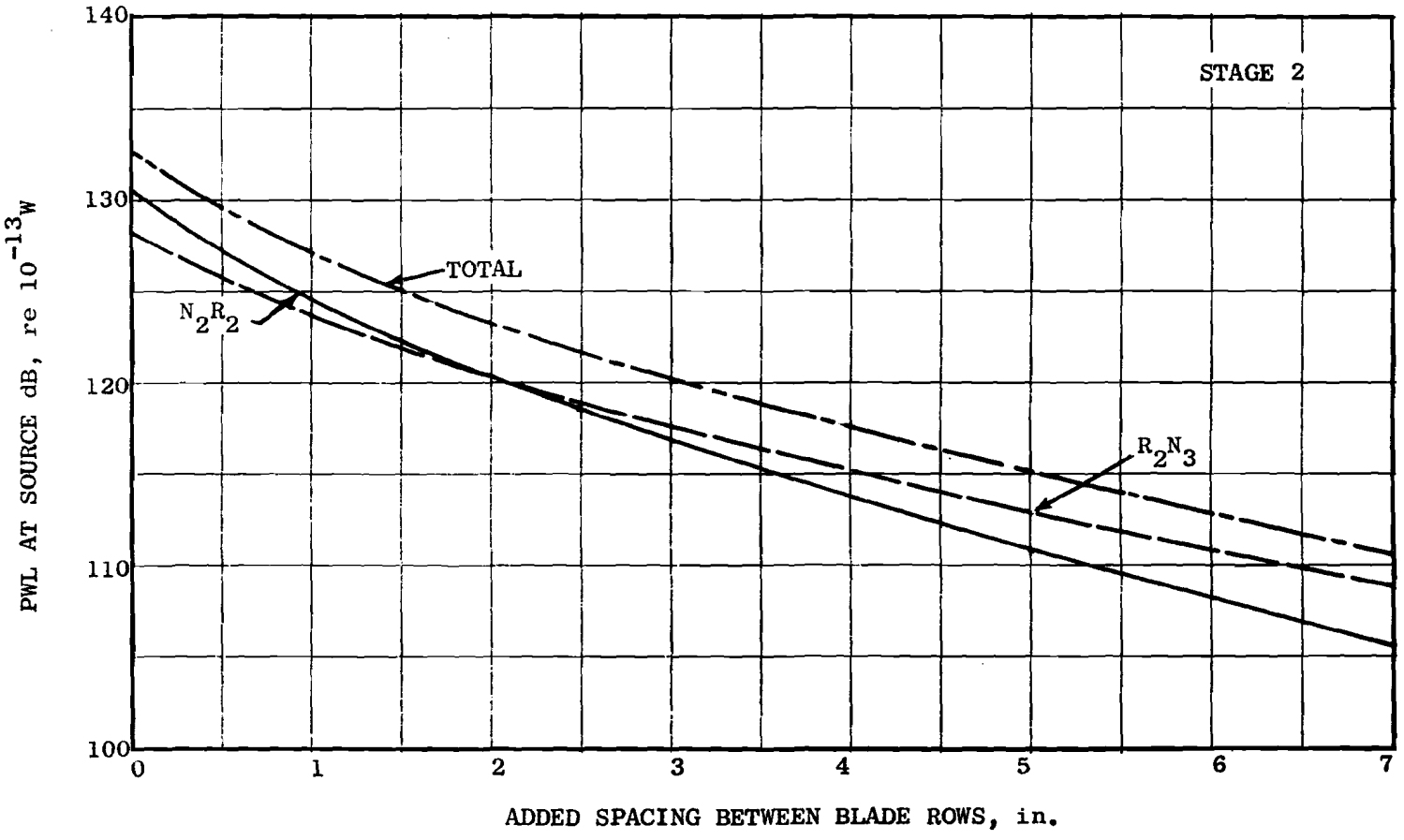

Figure 3 (b) PWL Reduction with Spacing - 2nd Stage BPF

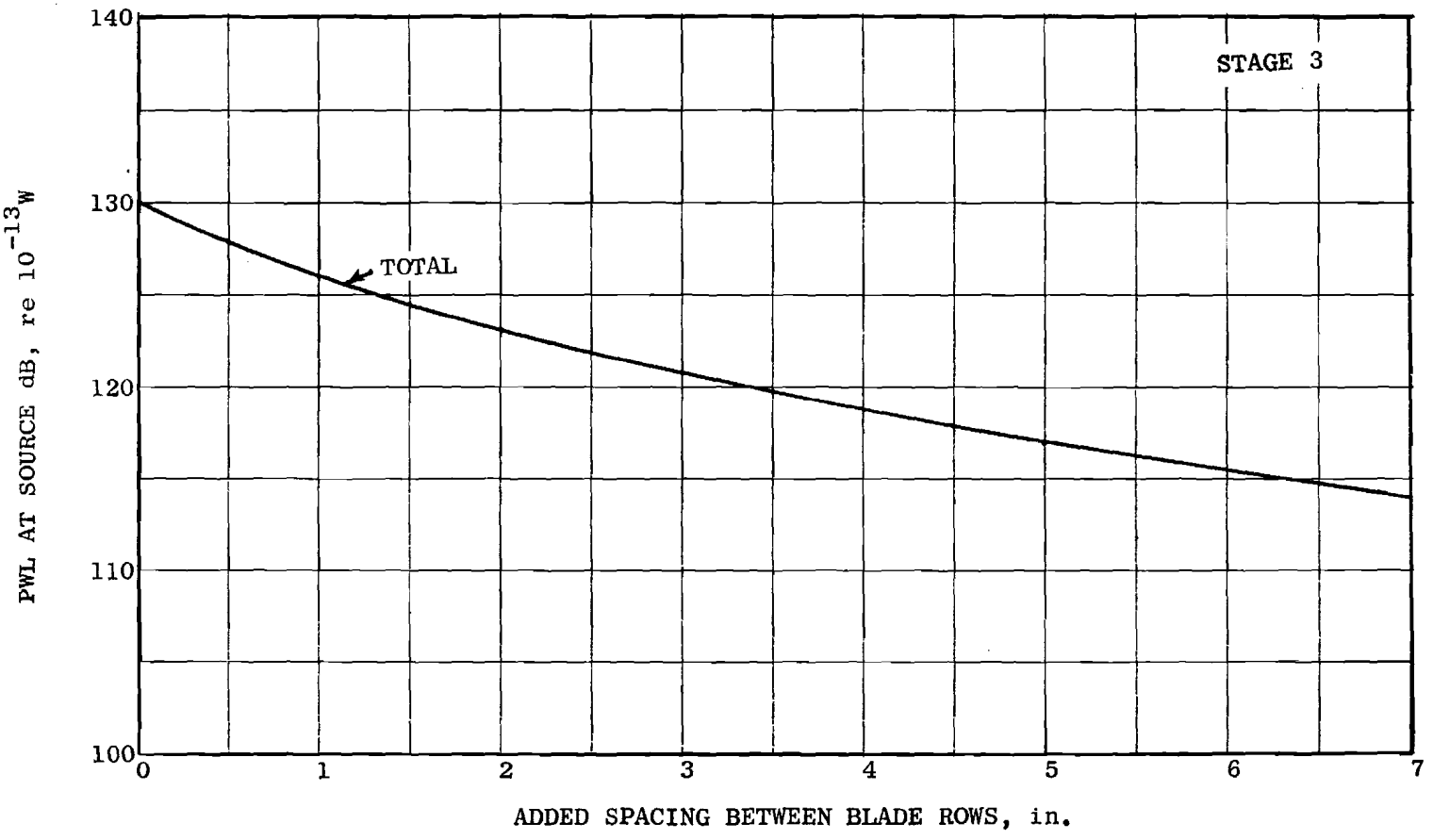

Figure 3 (c) PWL Reduction with Spacing - 3rd Stage BPF

Table 2. Effects of Spacing/Chord Ratio on Source Power Levels.

- 3- Stage Turbine
- Discrete Frequency Noise Only

Effect of Spacing on Source PWL

Stage 1

S/C	N-R PWL	Delta	S/C	R-N PWL	Delta	S/C	Tone PWL	Delta
.28	135.0	.0	.70	127.9	.0	.98	135.3	.0
.68	133.0	-2.6	1.29	125.1	-2.8	1.98	133.7	-2.6
1.08	131.1	-4.5	1.87	122.8	-5.1	2.95	131.7	-4.6
1.48	129.5	-8.1	2.45	120.7	-7.2	3.93	130.0	-6.2
1.88	128.2	-7.4	3.04	118.8	-9.1	4.92	128.2	-7.6
2.68	125.8	-9.8	4.21	115.5	-12.4	6.88	126.2	-10.1
4.28	122.4	-13.2	6.54	109.8	-18.1	10.82	122.6	-13.6
5.88	119.6	-16.0	8.88	104.7	-23.2	14.75	119.7	-16.5

Stage 2

S/C	N-R PWL	Delta	S/C	R-N PWL	Delta	S/C	Tone PWL	Delta
.27	130.6	.0	.70	128.1	.0	.97	132.6	.0
.68	127.2	-3.4	1.24	125.7	-2.4	1.93	129.5	-3.0
1.10	124.6	-6.0	1.79	123.7	-4.4	2.89	127.2	-5.4
1.51	122.3	-8.3	2.34	121.9	-6.2	3.84	125.1	-7.4
1.92	120.3	-10.3	2.88	120.4	-7.7	4.80	123.4	-9.2
2.75	116.8	-13.8	3.97	117.6	-10.5	6.72	120.2	-12.3
4.39	110.9	-19.7	6.16	112.9	-15.2	10.55	115.0	-17.5
6.04	105.8	-24.8	8.34	108.8	-19.3	14.38	110.6	-22.0

Stage 3

S/C	N-R PWL	Delta	S/C	R-N PWL	Delta	S/C	Tone PWL	Delta
.34	130.1	.0	***	0	0	***	130.1	.0
.76	127.8	-2.3						
1.18	126.0	-4.1						
1.60	124.6	-5.6						
2.02	123.1	-7.0						
2.85	120.8	-9.3						
4.53	117.1	-13.0						
6.20	114.1	-16.0						

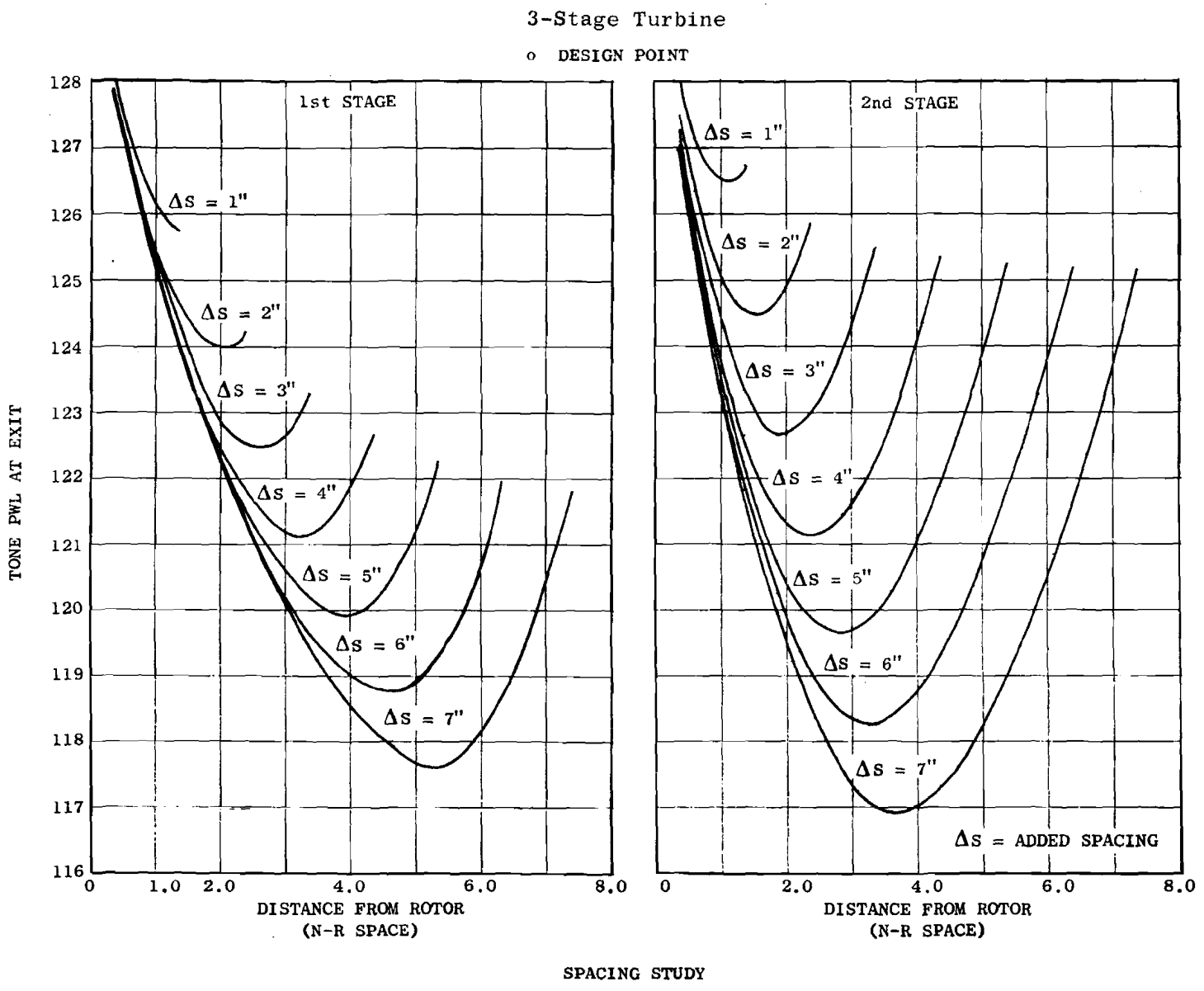

Figure 4 Optimum Rotor Location for a Given Spacing

The turbine noise correlations shown in Volume III indicate very little attenuation due to the last stage (data from both the last and second-to-last stage fall on the same correlating line). Data from stages further upstream lie considerably below, however, suggesting significant attenuation (up to 10 dB) by the blade rows upstream of the final stage.

The measured tone PWL's downstream of the turbine (Volume II, Section 4) were used as a starting point in the study. At design operating point, these were found to be:

Stage BPF	Tone PWL (dB, re 10^{-13} Watt)
1 (T1)	129.3
2 (T2)	136.5
3 (T3)	129.6
Total	137.9

The optimized spacing distribution between the blade rows for total given turbine elongations of 1, 2, and 3 inches, respectively, are given in Table 3. The maximum benefits obtainable for this particular turbine are total tone PWL of 2.7, 4.0, and 5.1 dB, respectively, for the three spacings.

The corresponding effect on the core engine EPNL is shown in Figure 5 for approach power. Four bypass ratio of 4 engines were used as powerplants on a 770,000 lb (349580 kg) TOGW aircraft. The 5.1 dB reduction in turbine tone OAPWL translated into 4.3 EPNdB reduction of the core engine EPNdB. Since the core engine noise levels in this case are dominated by the turbine noise, smaller OAPWL reductions would result in even more favorable PWL to EPNL conversions.

This process can be duplicated for any multi-stage turbine to define an optimum spaced configuration for a given total amount of spacing or for a desired reduction in noise levels.

2.3 LEANED VANES

The primary purpose of blade lean is to phase the viscous wake interaction radially from hub to tip along the downstream blading (Figure 6). At the same time the upwash velocity component is reduced by a factor $\cos(\alpha)$ where α is the local lean angle. Both effects tend to reduce the discrete frequency noise, but the latter effect is small in most cases.

The objective here was to define and detail (computerize) a leaned vane analysis to facilitate design and selection of leaned vanes for noise reduction in turbines.

The word lean is used to denote azimuthal deviation from a radial line (see Figure 7). A leaned wake can result from a physically leaned blade, from aerodynamic flow considerations radially, or from blade twist along the leading or trailing edge. The lean which results from blade twist is normally about one order of magnitude smaller than the existing aerodynamic lean and can be ignored. Aerodynamic lean is a twisting of the wake due to varying exit angles from hub to tip.

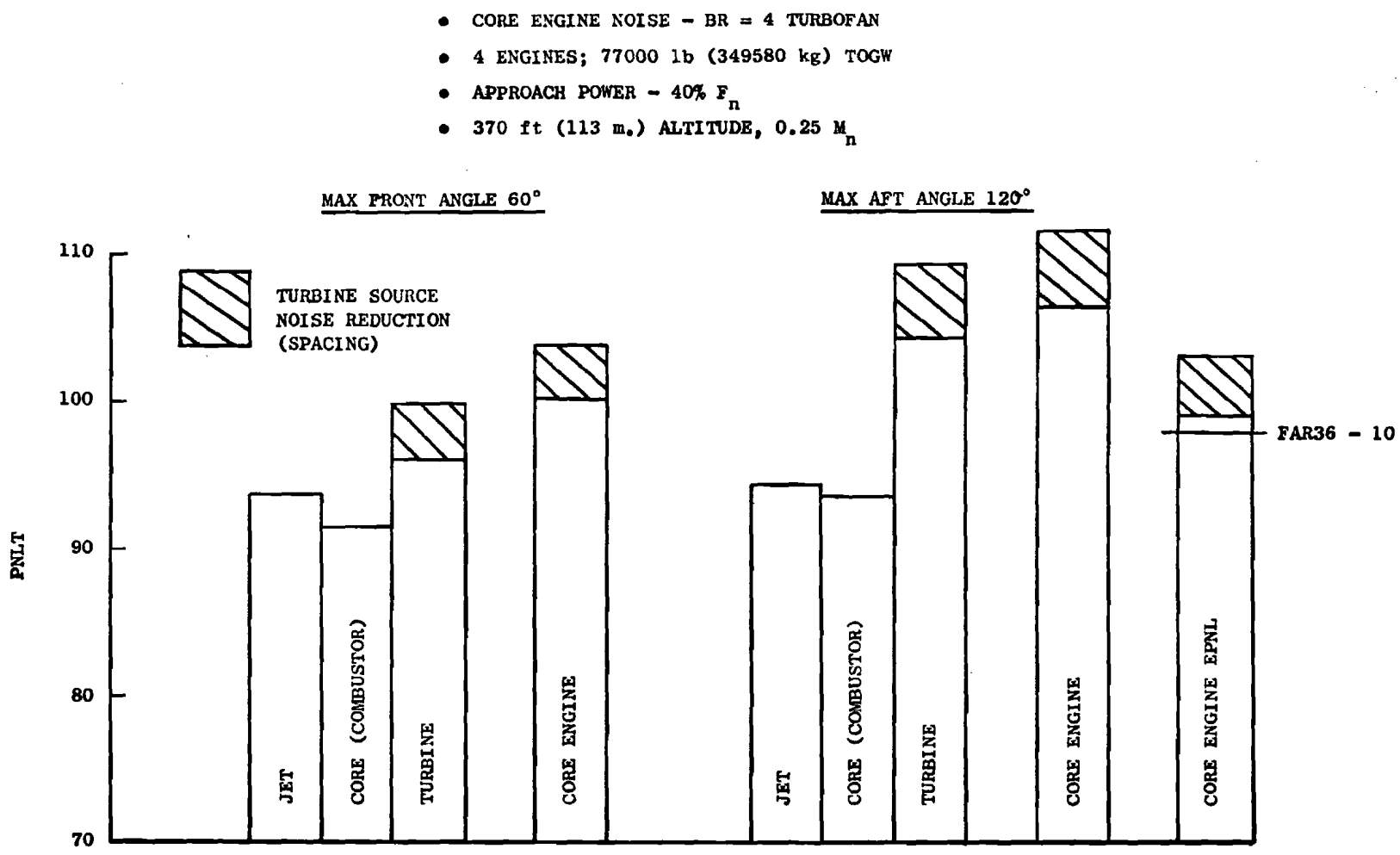

Figure 5 Effect of Turbine Spacing on Core Engine Noise

Table 3. Spacing Study.

(a) Baseline Spacing

		Tone PWL (re 10^{-13} Watt)
T_1	=	129.3 dB
T_2	=	136.5 dB
T_3	=	129.6 dB
OAPWL	=	137.9 dB

(b) 1 in. (2.54 cm.) Extra Space;

Use in Stage 2 + 0.75" N2R2
+ 0.25" R2N3

and T_1 = 129.3
T_2 = 132.0
T_3 = 129.6
OAPWL = 135.2
ΔOAPWL = 2.7 dB

(c) 2 in. (5.08 cm.) Extra Space;

Stage 1 + 0.25" + 0.25" N1R1
Stage 2 + 1.50" + 1.0" N2R2, 0.5" R2N3
Stage 3 + 0.25" + 0.25" N3R3

T_1 = 127.9
T_2 = 130.6
T_3 = 128.4
OAPWL = 133.9
ΔOAPWL = 4.0 dB

(d) 3 in. (7.62 cm.) Extra Space;

Stage 1 + 0.5" + 0.5" N1R1
Stage 2 + 1.75" + 1.0" N2R2, + 0.75" R2N3
Stage 3 + 0.75" + 0.75" N3R3

T_1 = 126.7
T_2 = 130.1
T_3 = 126.4
OAPWL = 132.8
ΔOAPWL = 5.1 dB

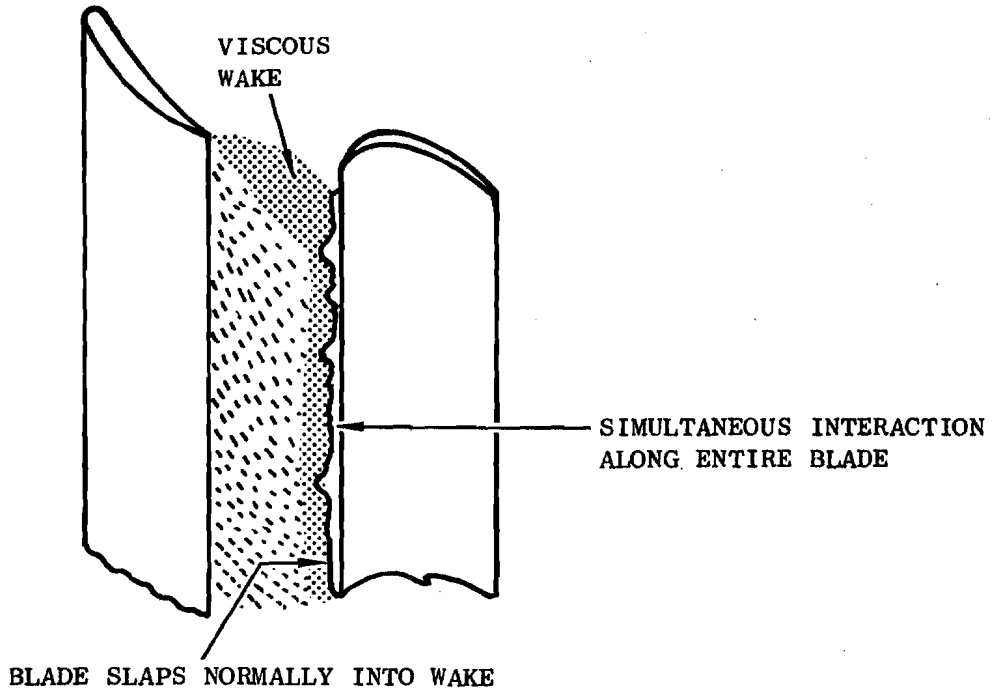

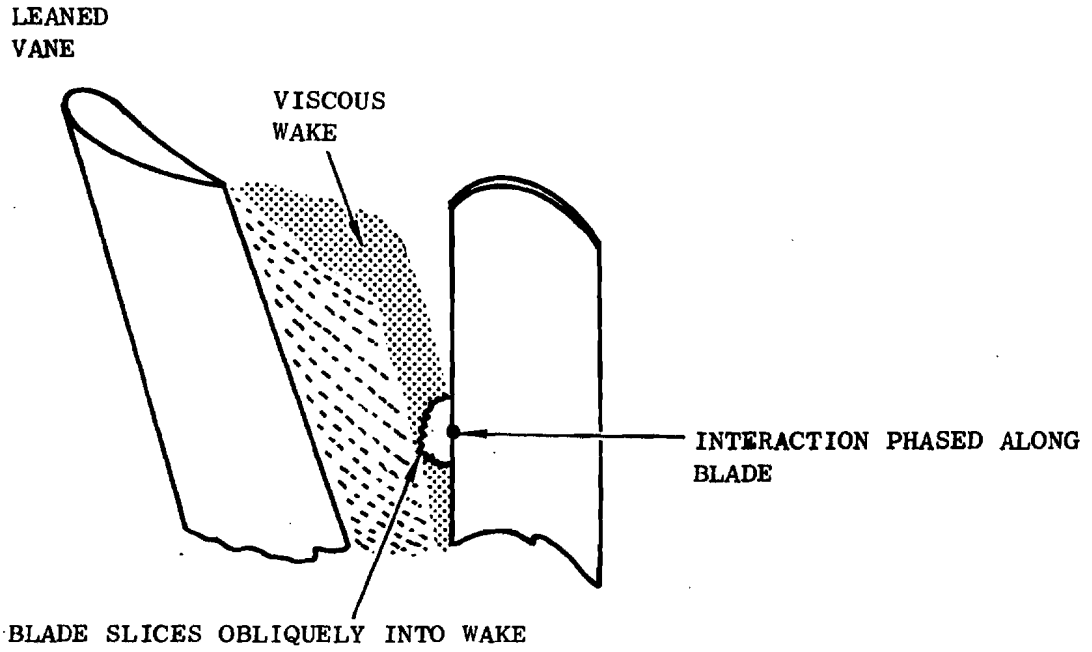

Figure 6 Noise Reduction Using Leaned Vanes

ROTOR-OGV INTERACTION

$$\vec{F}_{\ell} = \vec{F}(r)\,\delta(z)\,\delta\left(\theta - \frac{2\pi\ell}{V}\right)e^{-jnB\Omega\left(t-\frac{2\pi\ell}{V\Omega}\right)}$$

$$\ell = 0, 1, 2, \ldots\ldots (V-1)$$

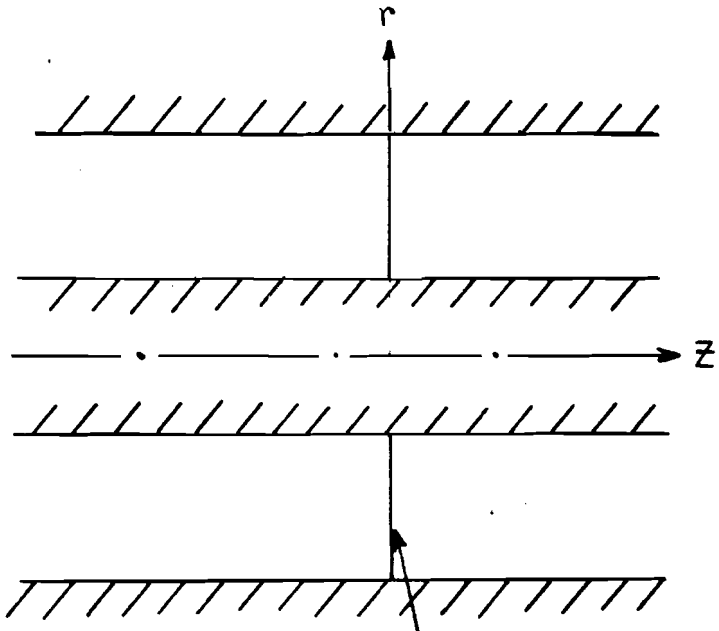

Downstream Blade Row [z = 0]

B = Number of Rotor Blades

V = Number of Stator Blades

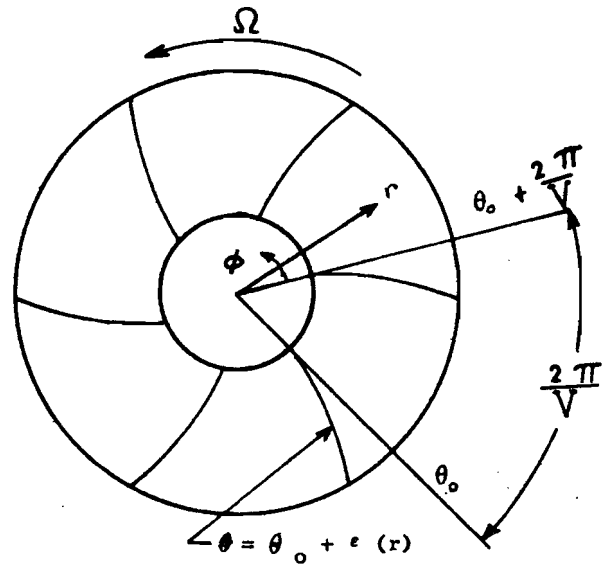

[Negative Curvature Shown]

Figure 7 Definition of Source Plane for Viscous Wake Interaction

Physical lean of stationary blades is considered desirable due to mechanical problems in leaning rotor blades.

Initial consideration of an axisymmetric geometry (Figure 7) and a Rotor-OGV case will help illustrate the principles involved. The analysis may be extended to an IGV-Rotor if desired.

The wave equation in a duct can be expressed as

$$\Box p = -\rho_o \nabla \cdot \vec{\mathcal{F}} \tag{2-1}$$

where $\Box$ is the wave operator ($\partial^2/\partial_t{}^2 - 1/C^2 \nabla^2$, in the case of no mean flow), p is the acoustic perturbation and $\vec{\mathcal{F}}$ the driving force. In the case of noise generation by rotating turbomachinery, $\vec{\mathcal{F}}$ is zero except at the plane of noise generation, i.e., at the blade row. Further, a compact source assumption permits the driving force to be expressed in terms of delta functions.

The Dirac delta function is formally defined as a generalized function by the relationship:

$$\int_{-\infty}^{\infty} \delta(x-\xi)\ F(x)dx = F(\xi) \tag{2-2}$$

Here F(x) is a "good" function (differentiable anywhere and any number of times).

Also,
$$\int_{-\infty}^{\infty} \delta(x) = 1 \tag{2-3}$$

Hence, using a cylindrical coordinate system (Figure 7), the force at the zeroeth blade for a rotor - outlet guide vane (R-OGV) interaction can be expressed as

$$\vec{\mathcal{F}}_o = \vec{F}(r)\delta(z)\delta(\theta)e^{-i\ n'B\Omega t} \tag{2-4}$$

where n' = harmonic number, B = number of rotor blades, Ω = angular velocity, and t are functions of r for leaned vanes as shown in Figure 7. The force on the ℓ-th blade is given by:

$$\vec{\mathcal{F}}_\ell = \vec{F}(r)\delta(z)\delta(\theta - \frac{2\pi\ell}{V})e^{-\ i\ n'B\Omega(t\ -\ \frac{2\pi\ell}{V\Omega})} \tag{2-5}$$

where V = number of stator blades.

Further, θ and t can be expressed as

$$\left.\begin{aligned} \theta(n) &= \theta_o - \varepsilon(r) \\ t(r) &= t_o - \varepsilon(r)/\Omega \end{aligned}\right\} \tag{2-6}$$

in order to separate out the radial dependency. Note that ε is positive in the direction of rotation and θ_o and t_o are independent of r (the case of radial vanes).

Summing over the entire blade row and using the expansion formula

$$\delta(\theta - \frac{2\pi\ell}{V}) = \frac{1}{2\pi} \sum_{n=-\infty}^{\infty} e^{i\,n\,(\theta - \frac{2\pi\ell}{V})}$$

equation (2-5) gives

$$\vec{\mathcal{F}} = \sum_{\ell=0}^{V-1} \vec{\mathcal{F}}_\ell$$

$$= \vec{F}(r)\,\frac{\delta(z)}{2\pi} \sum_{\ell=0}^{V-1} \sum_{n=-\infty}^{\infty} e^{i(n\theta - n'B\Omega t)}\, e^{-i\,\frac{2\pi\ell}{V}\,(n-n'B)} \qquad (2\text{-}7)$$

But $\sum_{\ell=0}^{V-1} e^{-i\,\frac{2\pi\ell}{V}\,(n-n'B)}$

$= V$ for $n-n'B = kV$, $k = 0, \pm 1, \pm 2, \ldots$

$= 0$ otherwise

Hence, Equation (2-7) reduces to

$$\vec{\mathcal{F}} = \frac{V}{2\pi}\,\vec{F}(r)\,\delta(z) \sum_{k=-\infty}^{\infty} e^{i(n\theta_o - n'B\Omega t)} \qquad (2\text{-}8a)$$

$$= \frac{V}{2\pi}\,\vec{F}(r)\,\delta(z) \sum_{k=-\infty}^{\infty} e^{i(n\theta_o - n'B\Omega t_o)}\, e^{ikV\varepsilon(r)} \qquad (2\text{-}8b)$$

Equation (2-8b) shows that the driving force for leaned vanes is similar to that for radial vanes other than for the phasing provided by the exp ($ikV\varepsilon$) factor. The system can literally be "tuned", through the ε (r), to yield minimum integrated driving force.

A similar equation can be derived for inlet guide vane - rotor (IGV-R) interactions using a rotor-fixed coordinate system and then converting back to a stationary system:

$$\vec{\mathcal{F}} = \frac{B}{2\pi}\,\vec{F}(r)\,\delta(z) \sum_{n=\infty}^{\infty} e^{-i(n\theta_o - n'B\Omega t_o)}\, e^{-i\,n'B\varepsilon(r)} \qquad (2\text{-}9)$$

It should be noted that the term $\vec{F}(r)$ itself arises from a Fourier Series expansion expressing the viscous wake interaction effect summed over the blades in the upstream row (see Volume II, Section 4).

Away from Z = 0, Equation (2-1) is homogeneous and may be solved by standard separation of variable techniques as in Volume II, Section 4.

In case a 2-D solution (Reference 1) is required, the coordinate θ is replaced by y/a where 'a' is the mean radius and y the azimuthal circumferential coordinate. Also, the expansion formula becomes:

$$\delta(y-y_o) = -\frac{1}{2\pi a} \sum_{m=-\infty}^{\infty} e^{i\frac{n}{a}(y-y_o)} \tag{2-10}$$

As an example of application of this analysis, the Fourier coefficients (A_{nm}) for the acoustic pressure expression in the analytical noise prediction [Volume III, Equation (4.2.1-6)] now include the phasing term:

$$A_{nm} = \frac{M}{4\pi n R_o c\, \eta_{nm}} \int_h^1 r\, \Gamma(r)\, R_{nm}(\lambda_{nm} r)\, e^{ikV\varepsilon(r)} dr \tag{2-11}$$

for a R-OGV case.

Equation (2-11) permits the vanes to be tuned for minimum noise radiation to the far-field. The blade number (B or V) tends to be rather high for a typical turbine stage and thus a small amount of lean can lead to rather substantial phasing.

The equivalent lean, ε, includes both physical lean (ψ) and effective aerodynamic lean (θ_e), that is

$$\varepsilon = \psi + \theta_e$$

All three, ε, ψ and θ_e, are referenced to the rotor axis and are taken to be positive in direction of rotation. ψ is computed from the local vane lean (α_h) as given in Volume III, Section 4:

$$\psi(r) = \alpha_h(r) - \sin^{-1}\left[\frac{r_{hub}}{r} \sin \alpha_h(r)\right] \tag{2-12}$$

The local vane lean is referenced to the hub as shown in Figure 8.

The aerodynamic lean is determined through consideration of the wake-downstream blade interaction. The varying exit angles from hub to tip impart a twist to the wake leaving the upstream blade row. The twist seen by the downstream blade row is a function of the axial spacing between the blade rows. For example, for an IGV-R case, the wakes are fixed to the vanes and therefore stationary. As the rotor blades slice through these, the following effective lean is generated:

$$\theta_e(r) = \left(\frac{s}{r} \tan \beta_{abs}\right)\Big|_r - \left(\frac{s}{r} \tan \beta_{abs}\right)\Big|_{hub} \tag{2-13a}$$

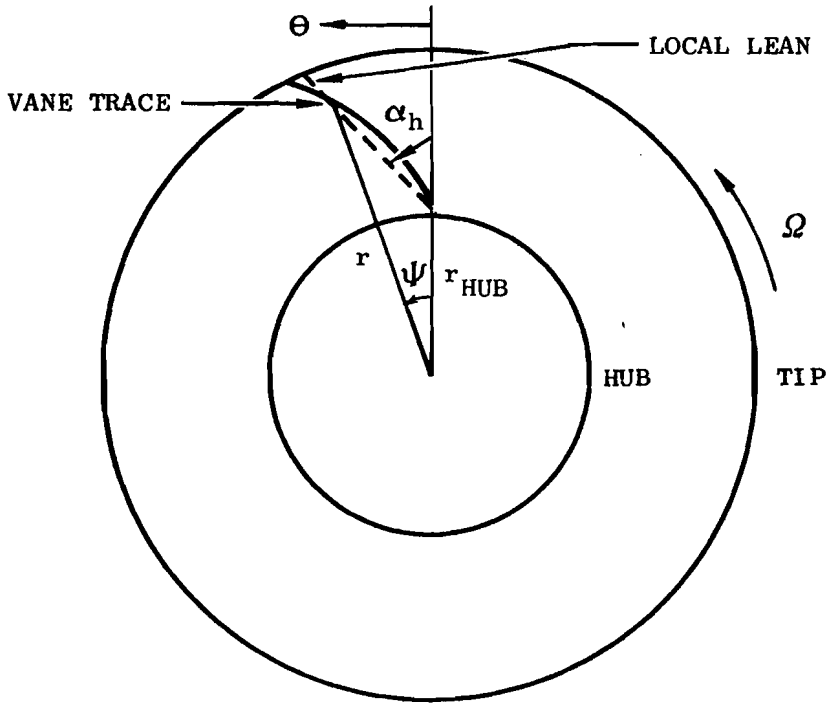

Figure 8 Determination of the Physical (or Geometrical) Lean

where s = axial spacing between the blade rows

r = radius

β_{abs} = (absolute) air angle exiting from the upstream row

and $|_r$ and $|_{hub}$ denote evaluation at any radial location and at the hub, respectively. The term (s/r tan β) simply denotes the wake swirl between the upstream blade trailing edge and the downstream blade leading edge.

However, for a R-OGV case, the wakes are fixed to the rotor blades and the effective lean must be computed using the relative exit angles, β_{rel}:

$$\theta_e\ (r) = (\frac{s}{r} \tan \beta_{rel})|_r - (\frac{s}{r} \tan \beta_{rel})|_{hub} \qquad (2\text{-}13b)$$

Strip Theory. The solution to the viscous wake interaction problem is considerably simplified by use of a two-dimensional flow assumption. The 2-D problem is solved at several fixed radial locations by unwrapping the annulus out into flat infinite strips at each fixed radius. The total acoustic power is then computed by integrating over the annulus area. A case can be made for the use of strip theory, especially for high radius ratio annulii (see, for example, References 1 and 2). The latter reference compares the modal distribution resulting from strip theory and axisymmetric analysis for a radius ratio (hub/tip) of 0.75 and demonstrates good agreement for low circumferential mode numbers. As either the radius ratio decreases or mode number increases, the approximation eventually breaks down. The degradation results from the fact that the cylinder function in the axisymmetric solution skews the energy towards the tip as the mode number increases, while the two dimensional solution is incapable of incorporating any such weighted (skewed) distribution.

Estimations of the unsteady forces responsible for the noise generation however, are all on a two dimensional basis. This coupled with the inherent simplicity of the strip theory approach makes it an attractive tool to many investigators. Results herein are supplied for both a strip and an axisymmetric analysis.

The two-dimensional analysis provided by Mani (Reference 1) was used with the turbine viscous wake model (Volume II, Section 4) to predict the noise generation by the last two blade pairs for the 3-stage turbine. This turbine was described earlier in the spacing study (Section 2.2). Using conventional turbine nomenclature, the R2N3 case provides a rotor-outlet guide vane interaction, and the N3R3 case an inlet guide vane-rotor interaction.

The force at each radial location was associated with a phase angle given by cos ϕ where ϕ is either kVε or nBε, depending on the interaction pair. A mean force was computed by integrating this force over the blade height. This roughly corresponds to attributing all the acoustic energy to the first (zeroeth order) radial mode in the duct. The higher order radial modes were neglected in this two-dimensional analysis because their distinctive property that the pressure disturbances average to zero over the blade span results in

comparatively inefficient sound transmission (this effect is particularly pronounced for wavelengths large compared to the radial inflexion distance). To use an analogy, monopoles are in general more efficient radiators of sound than dipoles, and dipoles more efficient than quadrapoles.

Results are shown in Figures 9 and 10 for the R2N3 and N3R3 interactions for both straight and curved leaned vanes (N3).

Looking first at straight vanes and local lean angles of less than 15° the results suggest significant suppression for both cases (over 10 dB), over the worst possible situation (WPS), i.e., when the wake interaction occurs in phase over the entire downstream blade. Note that the WPS does not necessarily occur for radial vanes, though it was very close to this for the N-R case used in this study. Due to the large inherent aerodynamic lean in the R-N case selected, the WPS was encountered near 16° lean.

The attenuation indicated can be enhanced through curved vanes tuned for optimum lean. Examples of such tuning are shown in Figures 9 and 10. Over 20 dB improvement was obtained for the R2N3 case and about 10 dB for the N3R3 case. The tuning was accomplished by looking at the indicated force phasing over the blade and selecting approximate lean angles to provide maximum cancellation effect (Figure 11). The blade was then fine tuned through iteration on the computer. A simple way to pick an optimum curve is to design for 180° phasing between hub and pitch and pitch and tip when the hub, pitch and tip forces are of the same order of magnitude.

Axisymmetric Solution. The analysis presented in Volumes II and III was conveniently adapted to accommodate phasing through relationships like Equation (2-11). The phasing effect being confined to the blade row plane, the wave equation remains separable, the eigenvalues are real, and the solution can be expressed as:

$$p \sim \sum_{n=-\infty}^{\infty} \sum_{m=1}^{\infty} \rho C^2 \, n\omega \, A_{nm} \, e^{i\,n(\theta-\omega t)} e^{ik_{nm}z} \, R_{nm}(\lambda_{nm} r) \tag{2-14}$$

with

$$A_{nm} = \frac{M}{4\pi n R_o C} \, \eta_{nm} \int_h^1 r \, \Gamma(r) \, R_{nm}(\lambda_{nm} r) \, e^{i\phi} \, dr \tag{2-15}$$

where

p = pressure perturbation

ρ = density perturbation

c = acoustic velocity

R_o = tip radius

h = nondimensionalized hub radius, r_{hub}/R_o.

$\Gamma(r)$ = circulation around the blade row of interest

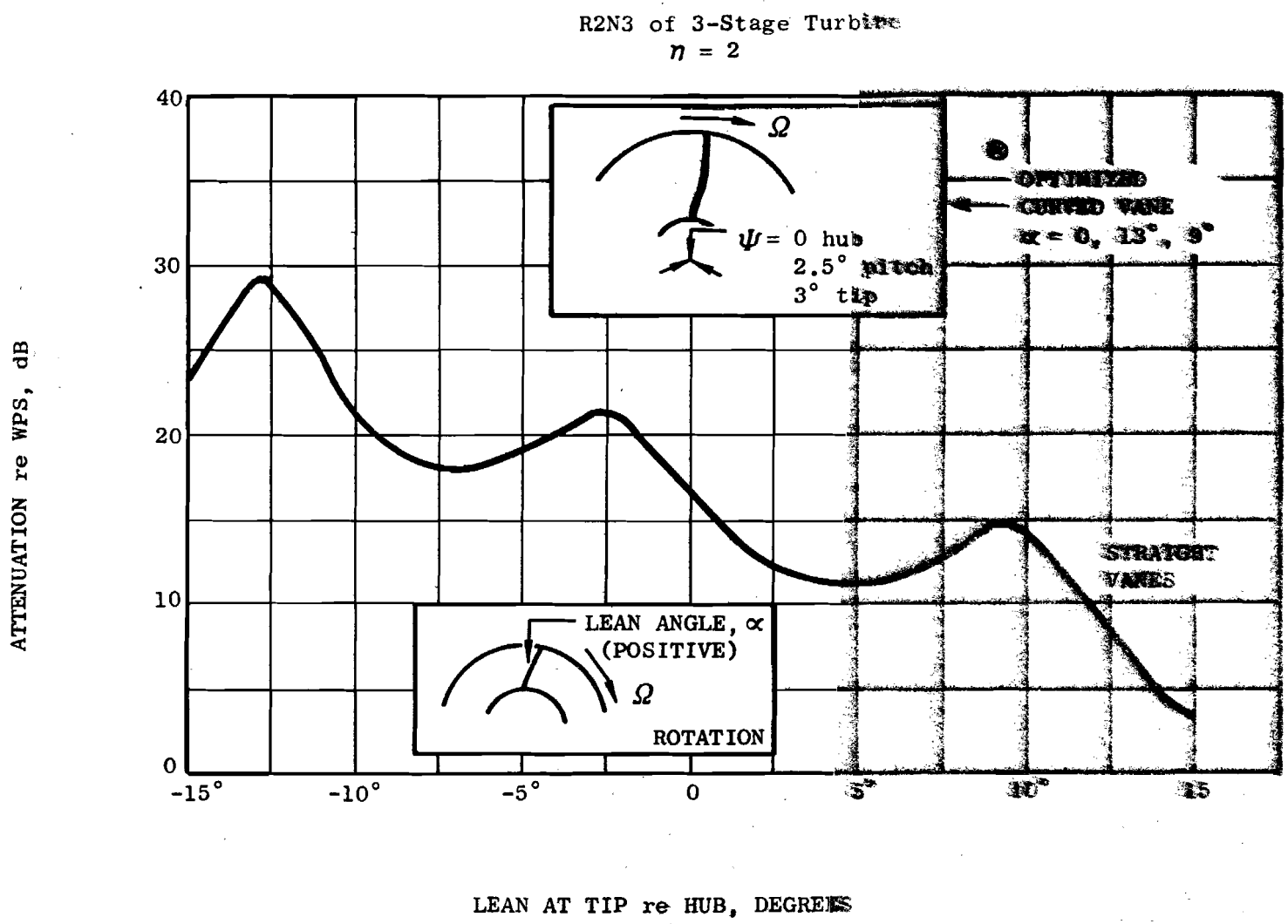

Figure 9 Noise Reduction for a Rotor-Nozzle Interaction

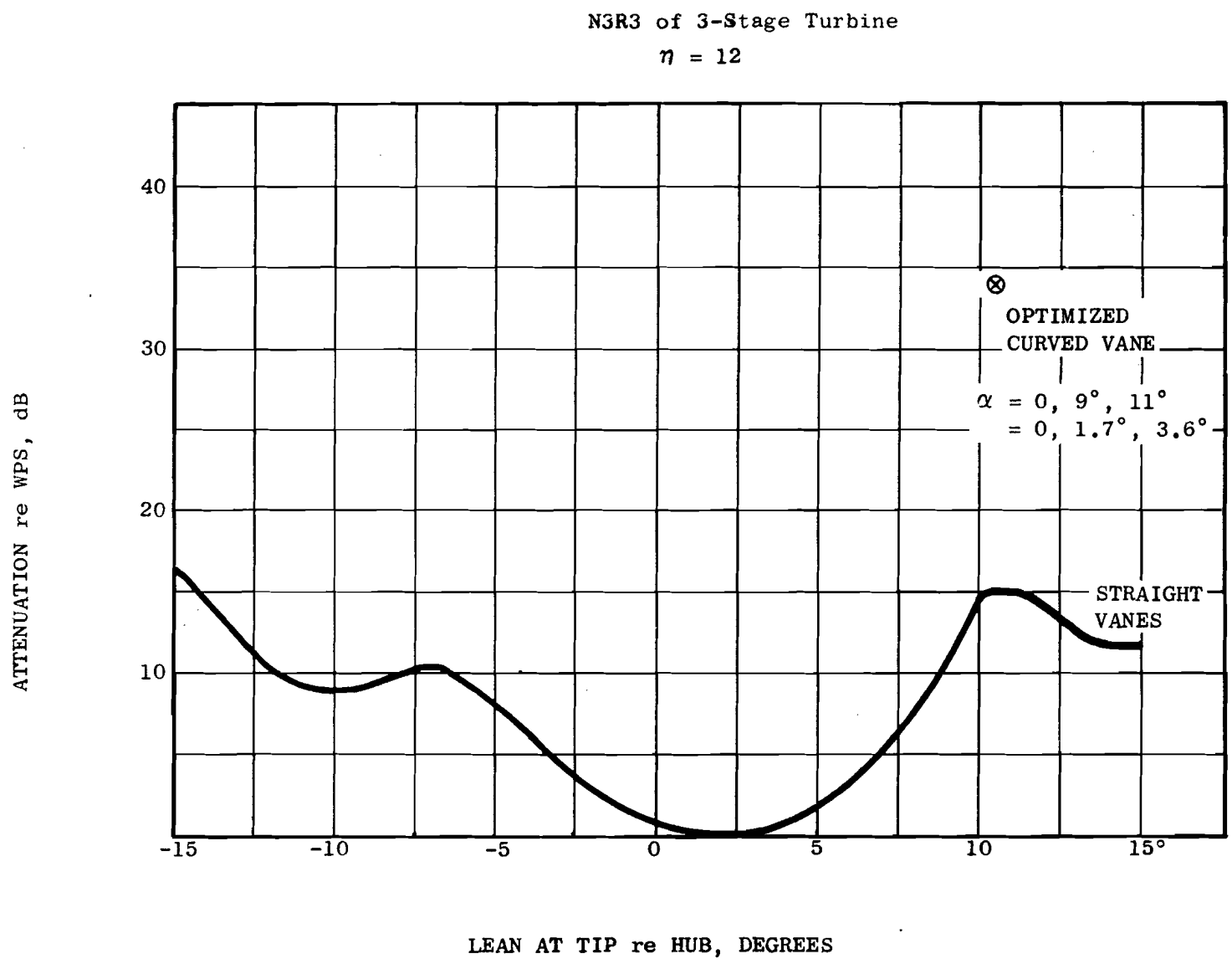

Figure 10 Noise Reduction for a Nozzle-Rotor Interaction

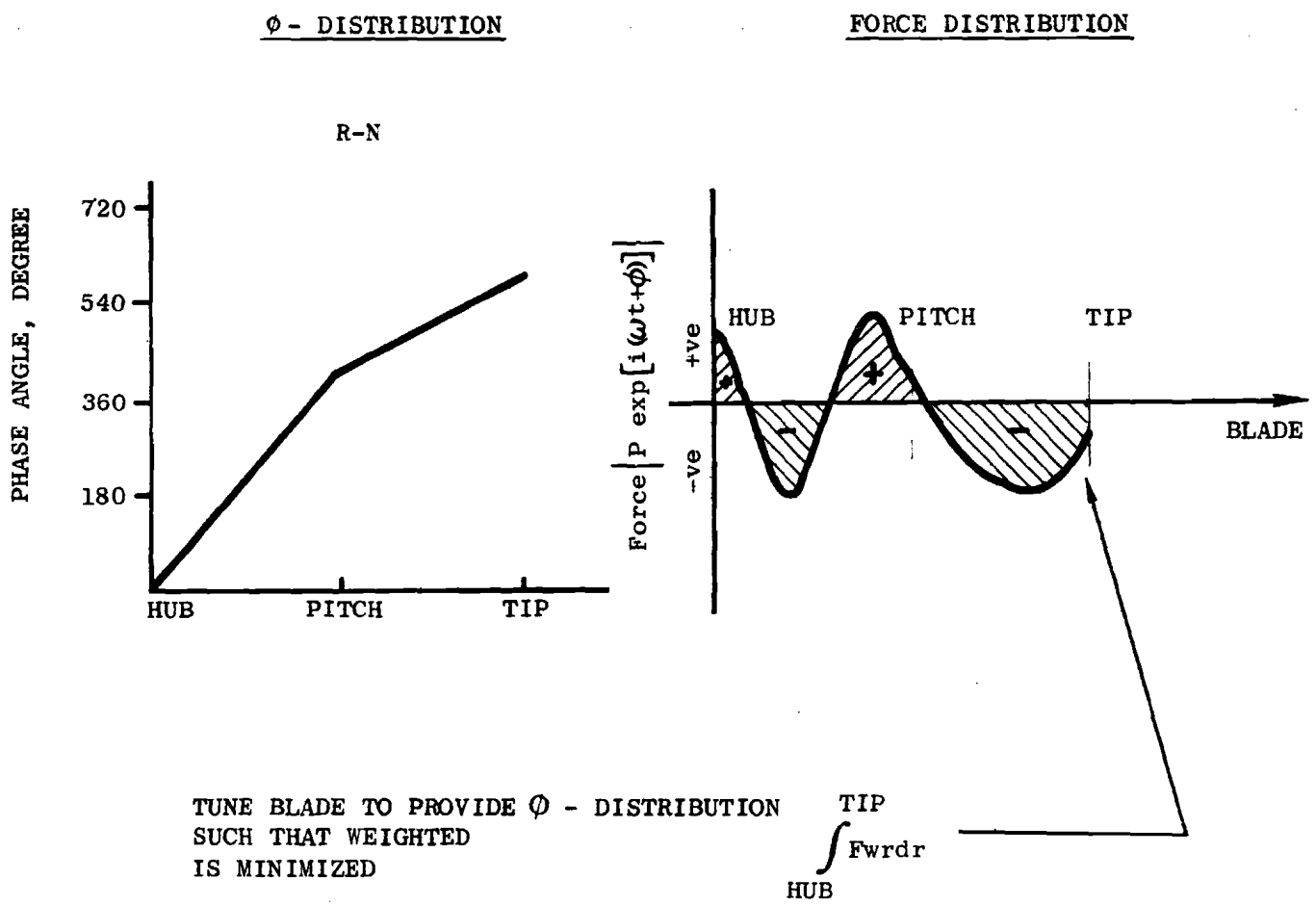

Figure 11 Phasing and Force Cancellation Due to Lean

$$|k_{nm}| = (n^2\omega^2 - \lambda^2_{nm})^{1/2}$$

$$\eta_{nm} = \int_h^1 r\, R^2_{nm}\,(\lambda_{nm}{}^2)\, dr$$

$$= \frac{1}{2\lambda^2_{nm}}[(\lambda^2_{nm} - n^2)\, R^2_{nm}(\lambda_{nm}) - (\lambda^2_{nm}h^2 - n^2)\, R^2_{nm}\,(\lambda_{nm}h)]$$

$$R_{nm}(\lambda_{nm}r) = \left\{J_n\,(\lambda_{nm}r) - \frac{J_n'(\lambda_{nm})}{Y_n'(\lambda_{nm})}\, Y_n\,(\lambda_{nm}R)\right\}$$

J_n = Bessel functions of the first kind and nth order

Y_n = Bessel functions of the second kind and nth order

ϕ = phase angle = $kV\varepsilon$ for R-N interactions and $-n'B\varepsilon$ for N-R interactions

$(\ )'$ denotes a derivative with respect to the argument

The unsteady force fluctuations driving the acoustic waves can only be computed on a two-dimensional basis, hence the circulation is found at a number of discrete radial stations and curve-fitted before the integration indicated in (2-15) is carried out.

Tables 4 and 5 show the noise reduction in the first (zeroeth order) radial mode resulting from vane lean for the R2N3 and N3R3 cases. Both, straight and curved vanes were considered. The trends are similar to those from strip theory. There are some differences in the attenuation levels, but this is only to be expected considering the differences in the two models and that the radius ratio for the two test cases was about 0.65. The important detail is that both models indicate significant (more than 20 dB) attenuation of the first radial mode through leaned vanes.

Assuming for the moment that only half of this attenuation is actually realized, that is the turbine noise is reduced by 10 PNdB, over 6 EPNdB improvement is obtained in the core engine noise levels, possibly without weight or performance penalties, for the 770,000 lb (349580 kg) TOGW aircraft discussed earlier in Section 2.2. The core engine component levels are shown in Figure 12. It must be remembered that fan and airframe noise levels must be added to obtain the full system EPNL.

2.4 DISCUSSION

The viability of using opened blade row spacing as a source noise reduction mechanism has been amply demonstrated through tests. The testing has been accomplished on high and low pressure turbines in single and multi-stage configurations (See Volume II, Section 4). The associated performance loss

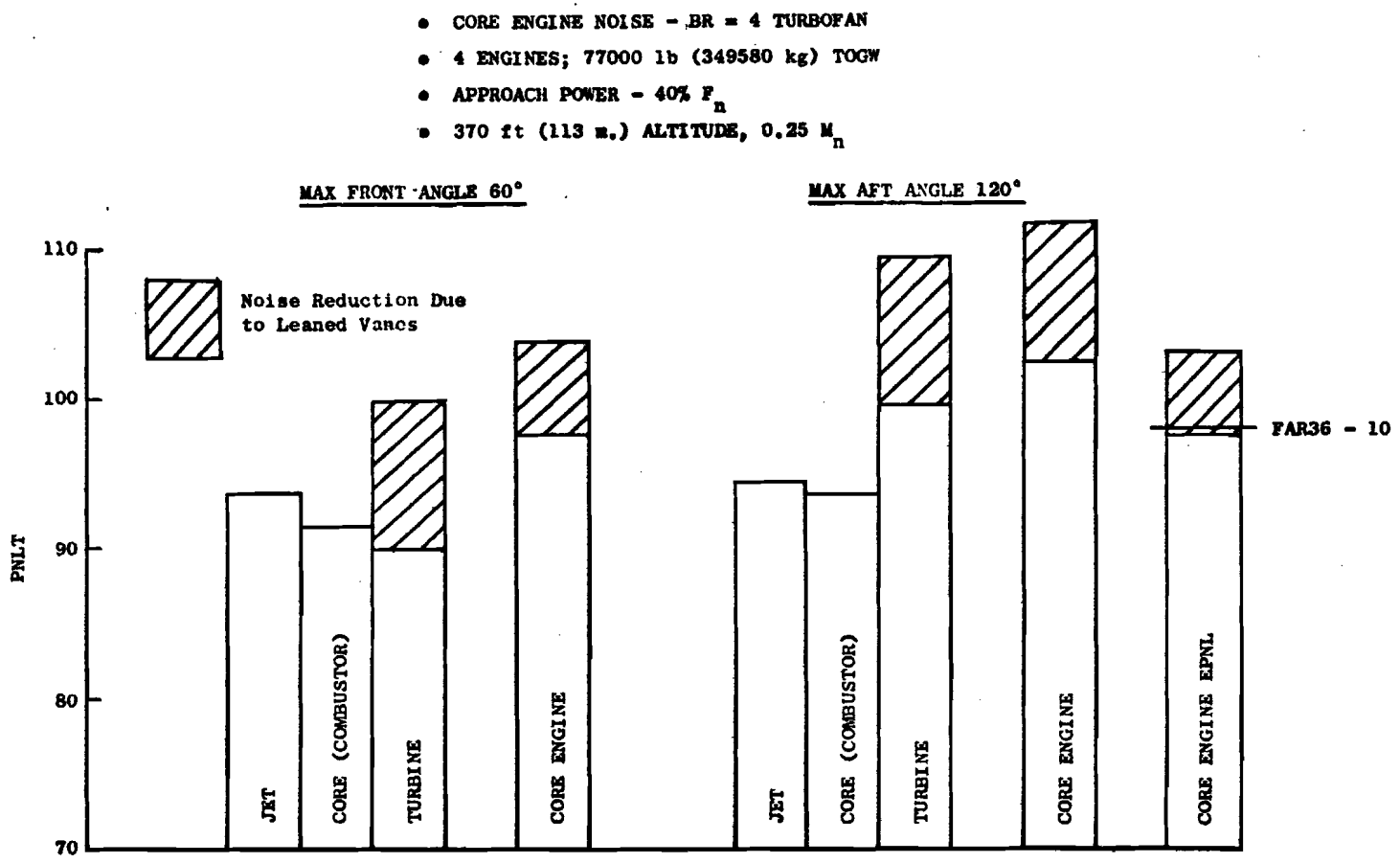

Figure 12 Effect of Leaned Vanes on Core Engine Noise

appears to be small and, possibly, recoverable. Section 2.2 now shows how to define optimum configurations for any given spacing in a multi-stage turbine. The same scheme may be used to obtain the necessary spacing to achieve a desired amount of noise reduction. The reduction is a direct consequence of wake decay with distance.

Vane lean seeks to obtain noise reduction by destructive interference of forces over a blade span. The relationship defined in Section 2.3 between the force phasing and blade lean permits selection of blade lean to achieve maximum cancellation. In general, the optimized blades tend to be curved. The

Table 4. Noise Attenuation Due to Leaned Vanes.

- R2N3
- First Radial Mode Only
- Axisymmetric Analysis

Local Lean (Degrees)	PWL Attenuation Over WPS, dB
h p t	
Curved Vane	
0, 13°, 9°	20.0
Straight Vanes	
-15°	19.2
-10°	15.4
-5°	14.7
0	12.7
5°	9.3
10°	8.9
15°	7.5

curved blades are properly designed with zero lean at the hub in order to avoid acute corners and associated aerodynamic performance problems.

The phase cancellation was aimed at the first (zeroeth order) radial mode for three reasons. First, this is the dominant mode for typical spinning lobe numbers. For example, Table 6 shows the modal energy distribution for the n=12 spinning lobe arising from the N3R3 interaction. As can be seen, the energy in higher order radial modes decreases rapidly, being down by 54 dB in the fifth radial mode. This effect is enhanced by decreasing lobe number.

Table 5. Noise Attenuation Due to Leaned Vanes.

- N3R3
- First Radial Mode Only
- Axisymmetric Analysis

Local Lean (Degrees) h p t	PWL Attenuation Over WPS, dB
Curved Blade	
0, 5, 10	27.9
Straight Blades	
-15°	10.1
-10°	6.7
-5°	3.8
0	0.4
5°	1.2
10°	6.6
15°	9.7

Table 6. Energy Distribution in Radial Modes.

- n = 12 spinning lobe, N3R3
- Zero lean

Radial Mode Number (m)	Radial Inflexions	Acoustic PWL dB re 10^{-13} Watt
1	0	130.1
2	1	122.1
3	2	102.6
4	3	110.5
5	4	86.2

Secondly, the higher radial modes include one or more inflexions in the spanwise force distribution; they tend to average out to zero, being exactly zero in strip theory, and result in relatively inefficient energy transfer. As the ratio of the BPF wavelength to the radial inflexion distance increases, the efficiency drops further.

Finally, the higher order modes attenuate far more rapidly while propagating down ducts. For example, lining effectiveness is greatly augmented by increasing radial mode number (Reference 3). Also, since the cut-off speed increases with the mode number, cut-off effects are obviously enhanced. This is particularly important since cut-off effects seem to extend over a gray area rather than being sharply defined.

The strip theory and axisymmetric results are in good agreement on the optimized curved vane for the low lobe number case (R2N3). However, there is some divergence in the N3R3 case because of the higher lobe number, as was expected. The cylinder function R_{nm} heavily weights the tip in the axisymmetric analysis; thus a 0 to 360° phasing from hub to tip no longer provides maximum cancellation. Instead, the optimum vane design requires roughly 0, 90° and 270° phasing at hub, pitch and tip, respectively.

As stated earlier, an axisymmetric modeling is preferred to a two-dimensional model, especially where higher order modes and low radius ratios are involved. The axisymmetric analysis also permits inclusion of the phasing effect in the Fourier coefficient computations (Equation [2-15]) as an integral part of the analysis (the lean effect had to be artifically inserted into the strip theory results by adding the indicated phase angle to the acoustic pressure at each radial location).

Considering the low radius ratio (0.65) and the above differences, the agreement between the two prediction sets is fairly good.

The full predicted attenuation may not be realized because of the assumptions made in the analysis and the idealization imposed on the flowfield. The accuracy of the results, of course, depend on the performance data input. Turbine testing has shown that the actual flowfield fluctuates rather randomly about the mean predicted values (which are used as input to the leaned vane program). The fluctuations are small, but their effect on the force phasing over the blade is multiplied by the number of blades in the row of interest. Since turbine stages typically contain 100 blades, the deviation from ideal conditions can be considerable. The predicted attenuations are too large to be ignored, however, but this concept merits further investigation.

Leaned vane theory also permits computation of the worst possible situation (maximum base generation), a condition which should be avoided.

2.5 CONCLUSIONS

Opened blade row spacing and vane lean both appear to be promising concepts in turbine source noise reduction. Using the former mechanism, optimized

multi-stage turbine configurations can be defined through consideration of the individual interactions and the BPF acoustic power levels. A small amount of spacing can then yield significant overall noise relief when the spacing is distributed parametrically between and within the different stages.

The second mechanism, vane lean, indicates that very large (above 20 dB) reduction may be obtained in the energy in the first (zeroeth order) radial mode by tuning the vanes to obtain force cancellation over the blade span through appropriate phasing. The tuning generally results in curved vanes, though the curvature is small. This effect is predicted by both strip theory and axisymmetric models.

The tuning tends to increase the energy content in the higher order radial modes, but the sound transmission through these modes is a relatively inefficient phenomenon and far more amenable to suppression.

The strip theory appears to provide a good approximation to the axisymmetric optimum vane results for the low lobe number case, but shows some divergence for the higher lobe number case (illustrating the inherent limitations of a two-dimensional approach to an annular flow field - especially where low radius ratios are involved).

The potential benefits of leaned vanes, as derived from these analytical studies, suggest a comparatively superior noise source reduction mechanism. The spacing benefits, however, have been demonstrated on several actual turbines, whereas the leaning benefits still remain to be demonstrated.

2.6 PREDICTION METHOD UPDATE

The analysis for viscous wake interaction in turbines was programmed and the coding is provided in Appendix A, along with a logical flow chart. This program was updated to accommodate the leaned vane analysis of Section 2.3 as an option. The option is exercised by setting FLEAN1=T in the input. Due to the extreme complexity of the programming, the reader is referred to Appendix A for further discussion of this prediction method. A very detailed input sheet is also provided, along with a typical output. The output format is explained in the same appendix.

The strip theory computations are carried out as indicated in Reference 1, with the phasing inserted as explained in Section 2.3.

SECTION 3.0

COMPACT SUPPRESSORS FOR LOW FREQUENCY NOISE

3.1 BACKGROUND

Core engine noise is composed of low frequency noise, probably associated with the combustor, and higher frequency turbine noise. Core engine noise is becoming more important as the system noise level is reduced to meet the lower noise limits that are now being proposed for aircraft certification. To meet the more restricted limits, suppression of not only combustor noise but also turbine noise might be required. In Phase 3 of this program a low frequncy core noise suppressor was designed and tested. Although considerable suppression was obtained, the suppressor was more than 12 in. (30.5 cm) deep. The current effort was directed toward decreasing the depth of the suppressor to achieve a flightworthy design. To achieve this goal three different design concepts were built and acoustically tested.

3.2 SUPPRESSOR DESIGN CONCEPTS

A typical spectrum including turbine and combustor noise is given in Figure 13. The NOY weighted spectrum shows that both low and high frequency suppression is desired. The NOY weighted low frequency noise peaks at 400 Hz and the turbine noise around 3150 Hz; the peaks are not sharp but are broadband in nature such that the suppressor must be effective over a relative wide frequency range.

A typical core engine exhaust envelope is shown in Figure 14. The available depth and length for the treatment are limited, but four suppressor concepts which can fit within these limits are shown in Figure 15. These include: (a) stacked treatment, (b) folded quarter-wave, (c) side-branch resonator, and (d) an acoustic rectifier concept.

(a) Stacked Treatment

The stacked treatment concept combines high and low frequency Helmholtz resonator (SDOF) dissipative panels by stacking the first on top of the second such that the thin treatment panel serves as the facesheet for the low frequency panel. Because the neck lengths involved in the openings to the low frequency panel cavities are relatively long, the thickness of the cavities is relatively small. For example, with a neck length of about 1.0 in. (2.54 cm), the low frequency treatment can be tuned-in with a cavity depth in the range of 4.0 in. to 5.0 in. (10.2 cm - 12.7 cm). Such a depth is much smaller than would be required if a simple faceplate were used. As a result of these features, the stacked treatment is very compact.

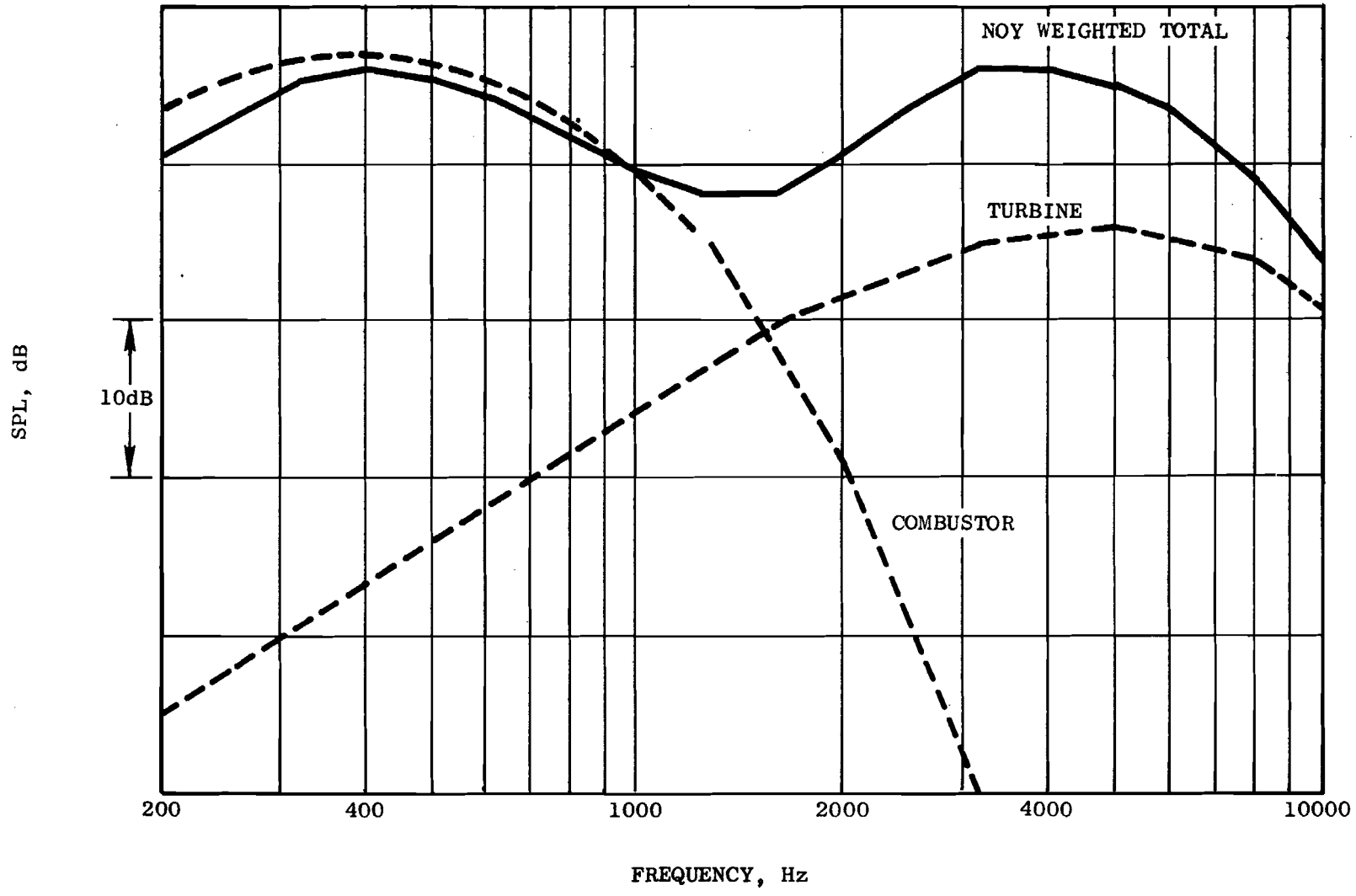

- 120° ACOUSTIC ANGLE
- 152.4 m SIDELINE; 61.m ALTITUDE
  (500') (200')

Figure 13 Core Noise Spectra

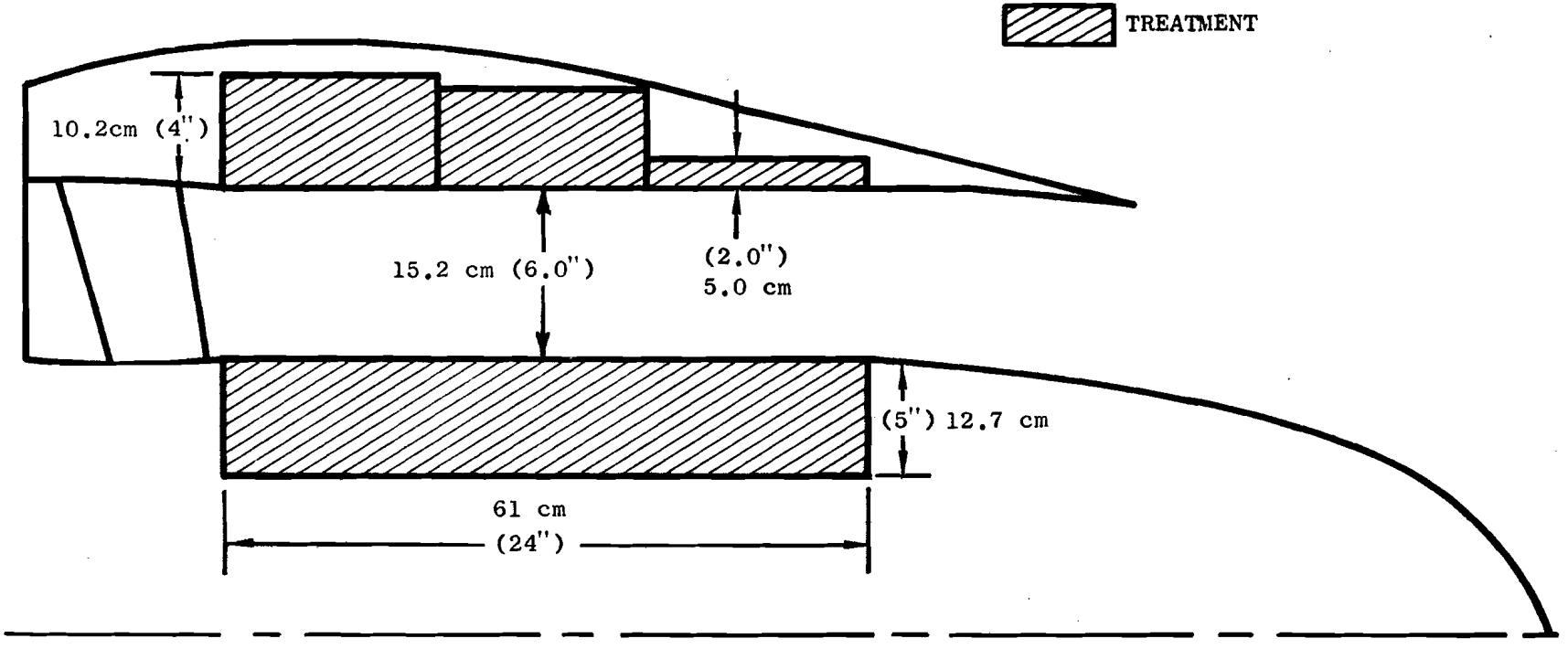

- TYPICAL DIMENSIONAL CONSTRAINTS

Figure 14 Core Suppressor Envelope Definition

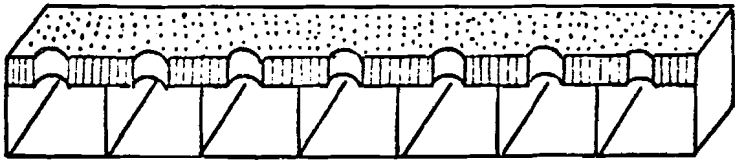

(a) STACKED TREATMENT CONCEPT

DISSIPATIVE HELMHOLTZ RESONATOR

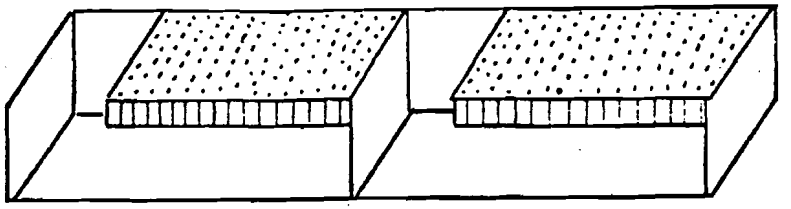

(b) FOLDED QUARTER-WAVE CONCEPT

REACTIVE

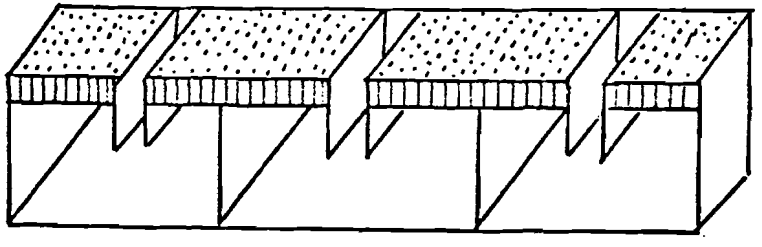

(c) SIDE-BRANCH RESONATOR CONCEPT

REACTIVE HELMHOLTZ RESONATOR

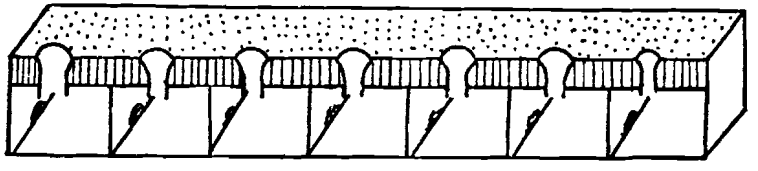

(d) ACOUSTIC RECTIFIER CONCEPT

DISSIPATIVE RESONATOR

Figure 15 Compact Core Suppressor Concepts

(b) Folded-Quarter Wave

The folded-quarter wave concept places the high frequency SDOF treatment atop a low frequency panel which makes use of the quarter-wave resonance. In this case, the length required for the resonance is incorporated axially rather than radially; again the thickness is constrained to be within practical limits. The length needed to achieve the required low frequency suppression depends upon the effectiveness of one or more such cavities placed in series along the axis of the duct. As a result, the folded quarter-wave concept is generally less compact than the stacked treatment concept.

(c) Side-Branch Resonator

The side-branch resonator concept for low frequency noise reduction is based on the reactive rather than dissipative mechanism. This means it reflects the noise back toward the source by introducing a large impedance change across the whole duct cross-section. This requires a matching of the volume in the resonator realtive to the duct cross-sectional area, but it does not require multiple segments in series (except for the purpose of tuning to different frequencies). The advantage of this concept is that it can make use of the volume in the core plug (for the low frequency cavities) which is otherwise wasted. Because the local impedance change extends across the whole duct, the low frequency resonator cavities are required on one side only. Slots rather than holes, are used to cause the local impedance change to be uniform in the circumferential direction. The effect of such a slot arrangement has not been evaluated in terms of aerodynamic losses. The side-branch resonator concept therefore permits the use of otherwise wasted space to obtain a reasonably compact suppressor.

(d) Acoustic Rectifier

This concept is similar in principle to stacked treatment but differs from it in that the neck between the duct and cavity is tapered to provide a flow coefficient which is higher on entering the cavity than leaving it. Left unchecked, this baising would raise the steady state pressure in the cavities and effectively introduce a higher resistance and consequently a higher tuning frequency than desired. By bleeding air from the cavities the steady-state static pressure can be controlled so that the desired resistance can be maintained. Preliminary calculations indicate that for the sound pressure levels to be suppressed (allowing for the pressure amplification within the cavity which is expected at the Helmholtz resonace) the amount of bleed air required is essentially insignificant in its effect on engine performance.

3.3 EXPERIMENTAL PROCEDURE

Testing Goals

The goal was to develope a design for an engine compatible suppressor capable of a maximum suppression of approximately 10 dB across a 400 Hz bandwidth in a frequency range below 2000 Hz. The suppressor was determined by testing three suppressor concepts at two temperatures and three Mach numbers between 500° K - 1100° K and 0.1 - 0.4 respectively. The following test points were selected:

Temperature	Mach Number
590° K (600° F)	0.2
920° K (1200° F)	0.3
	0.4

The low frequency suppressors were designed for frequencies between 500 Hz and 1000 Hz. Thin treatment was included in the hardware designs to take advantage of the suppression bandwidth available below 2000 Hz.

Hardware Design

Three of the four concepts were built and tested, excluding the folded quarter-wave concept because estimated length requirements were excessive. Design parameters for the three remaining suppressor concepts are defined in the following paragraphs.

The stacked treatment suppressor is pictured in Figure 16 and geometrically defined in Figures 17 & 18. Since the test conditions cover a range of temperatures and Mach numbers, a design point of 1000° F (810° K) and $M_n = 0.4$ was selected. The low frequency panel was designed with three sections tuned to 500 Hz, 630 Hz, and 800 Hz: the thin treatment panel acted as the facesheet. Figure 19 shows the calculated reactance values versus the optimum reactance for the plane-wave mode. The intersections marked by the black circles identify the Helmholtz tuning frequencies. The black triangles indicate the quarter wave resonances of the cavities.

The side-branch resonator concept pictured in Figure 20 and defined in Figures 21 & 22, was designed for the same operating conditions and tuning frequencies as the stacked treatment design. The low frequency tuning frequencies were determined by the following equation (Reference 1).

$$f_o = \frac{C}{2\pi} \sqrt{\frac{A}{Vt'}} \qquad (3\text{-}1)$$

where $f_o \triangleq$ tuning frequency (Hz)
$c \triangleq$ speed of sound (m/sec,ft/sec)

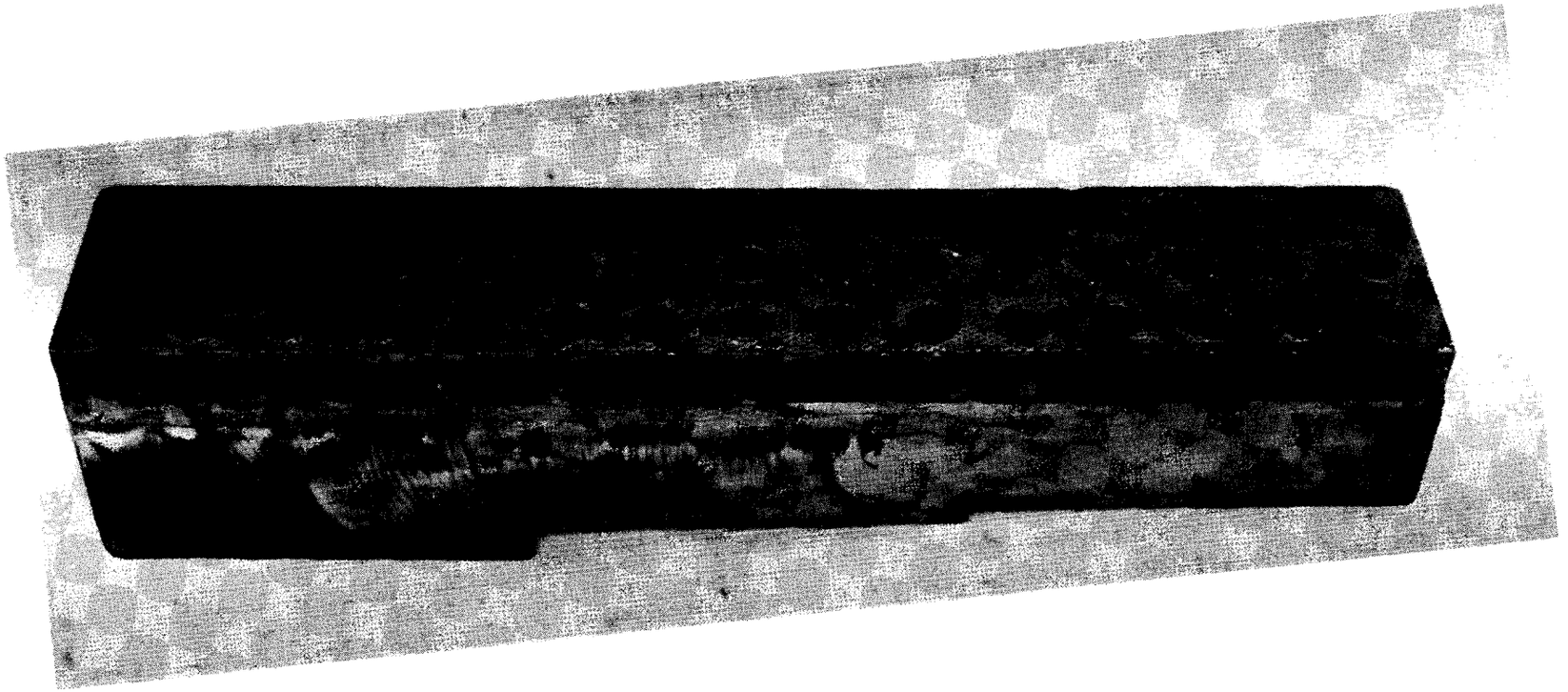

Figure 16 Photo of Staked Treatment Suppressor

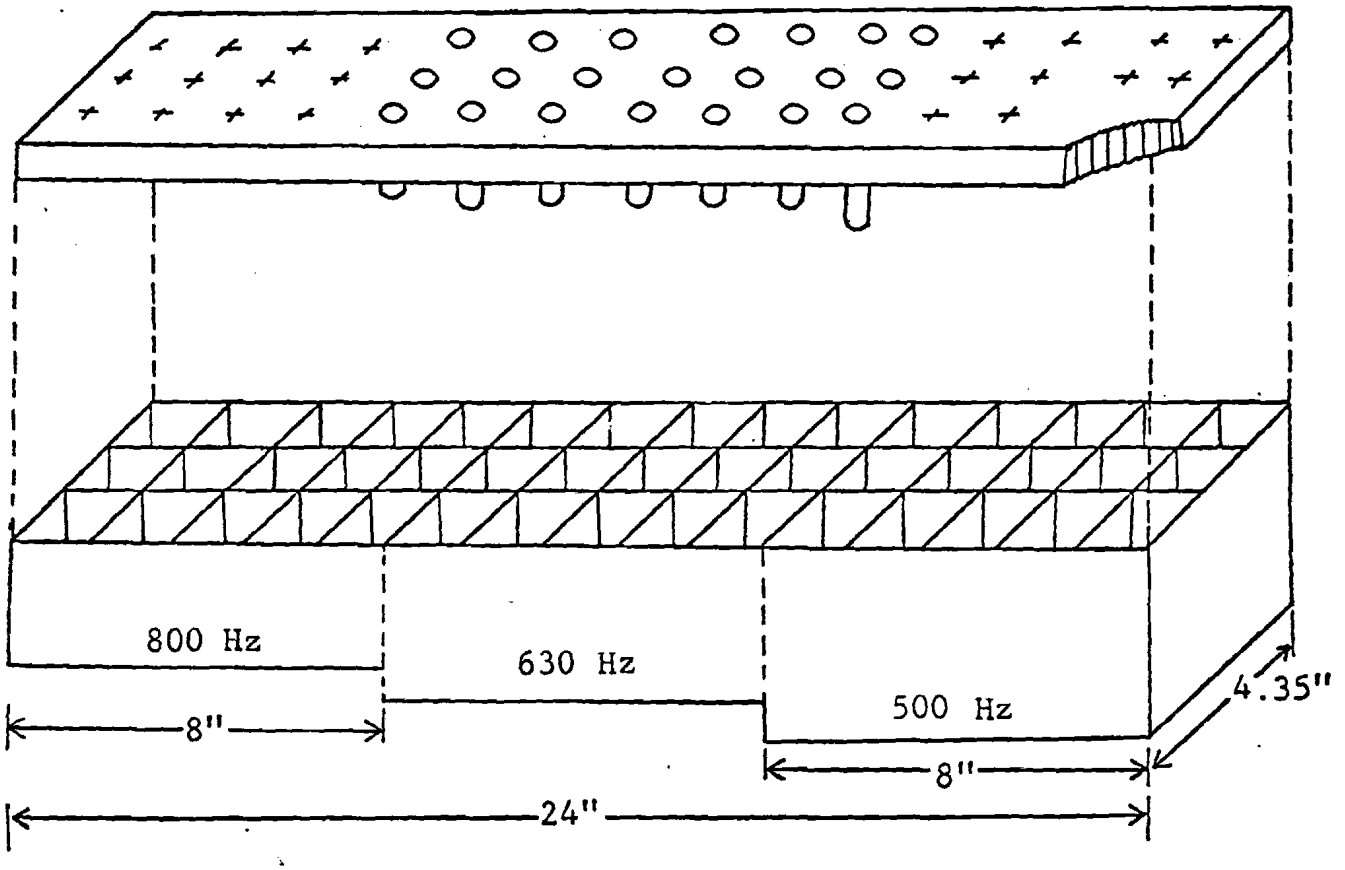

Figure 17 Stacked Treatment Suppressor (Geometrically Defined)

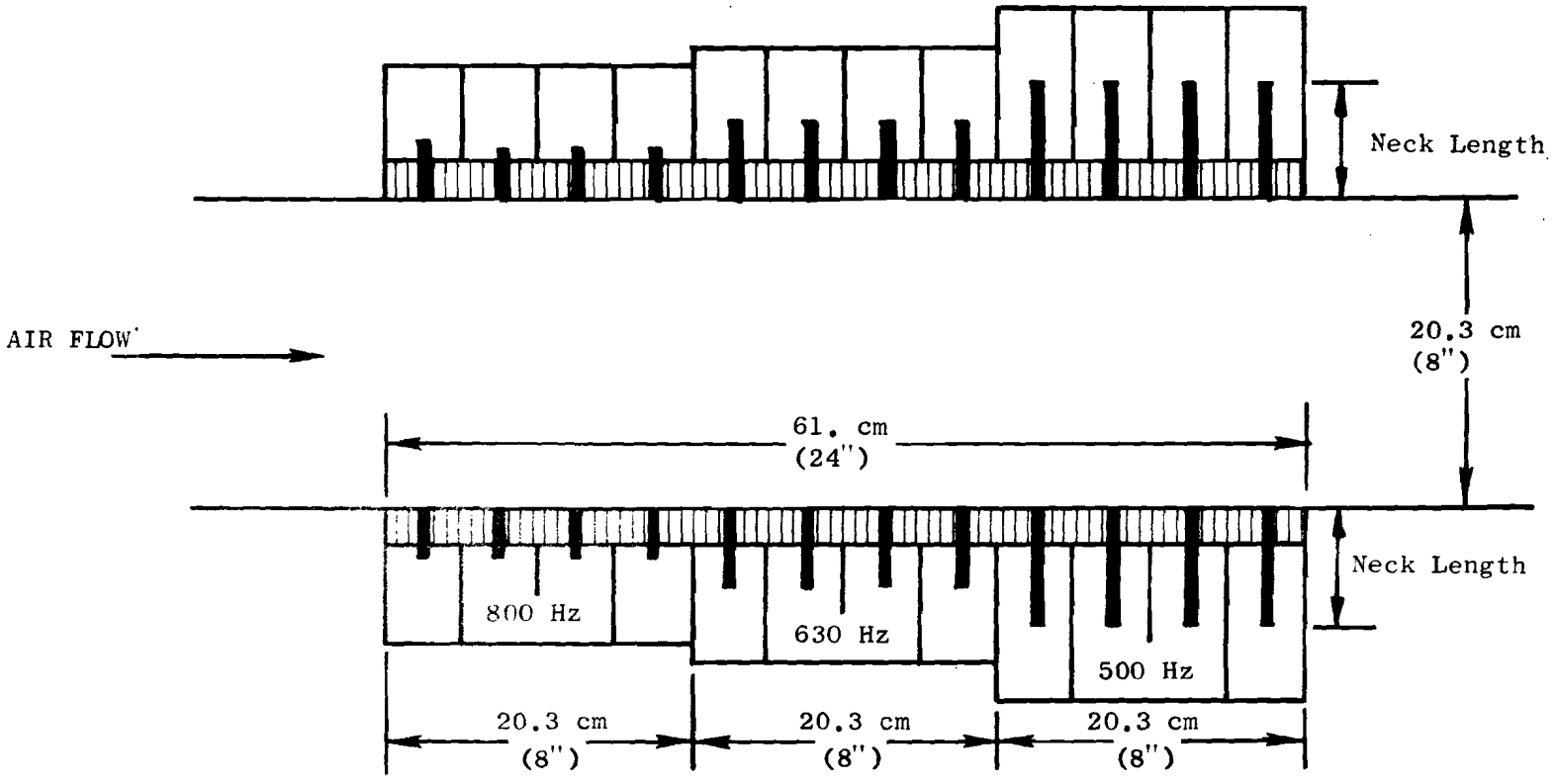

THIN TREATMENT

POROSITY: 22.5%
FACEPLATE THICKNESS: (.032") 0.8 mm
HOLE DIAMETER: (.062") 1.6 mm
CAVITY DEPTH: (1.0") 2.54 cm

COMBUSTOR TREATMENT

TUNING FREQUENCY (Hz)		800	630	500
POROSITY (%)		20	20	20
NECK LENGTH	cm	3.2	4.4	5.7
	(IN)	(1.25)	(1.75)	(2.25)
CAVITY DEPTH	cm	6.4	7.6	10.2
	(IN)	(2.5)	(3.0)	(4.0)
HOLE DIAMETER	cm	1.9	(1.9)	(1.9)
	(IN)	(0.74)	(0.74)	(0.74)

Figure 18 Stacked Treatment Definition

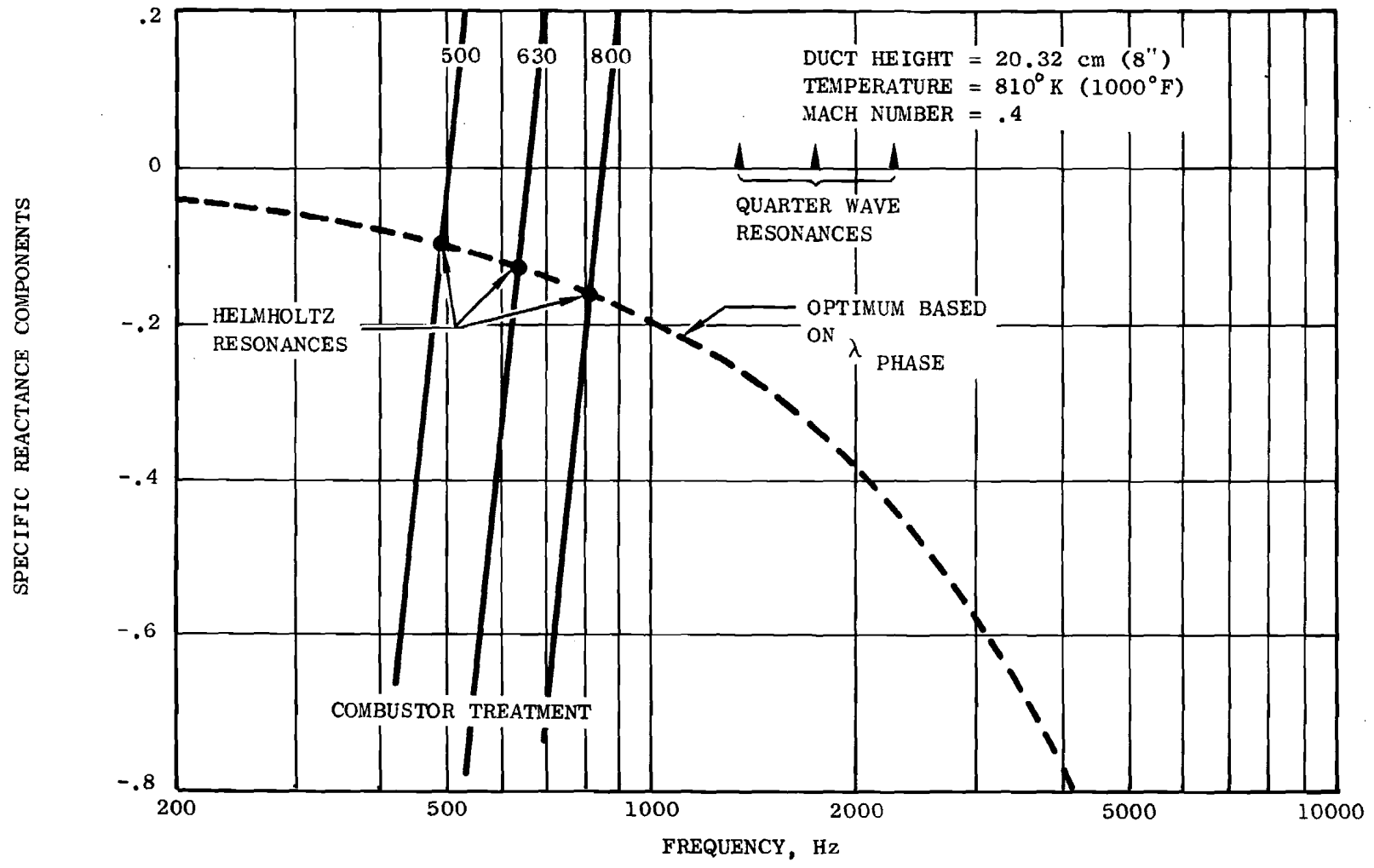

Figure 19 Stacked Treatment Reactance Curves

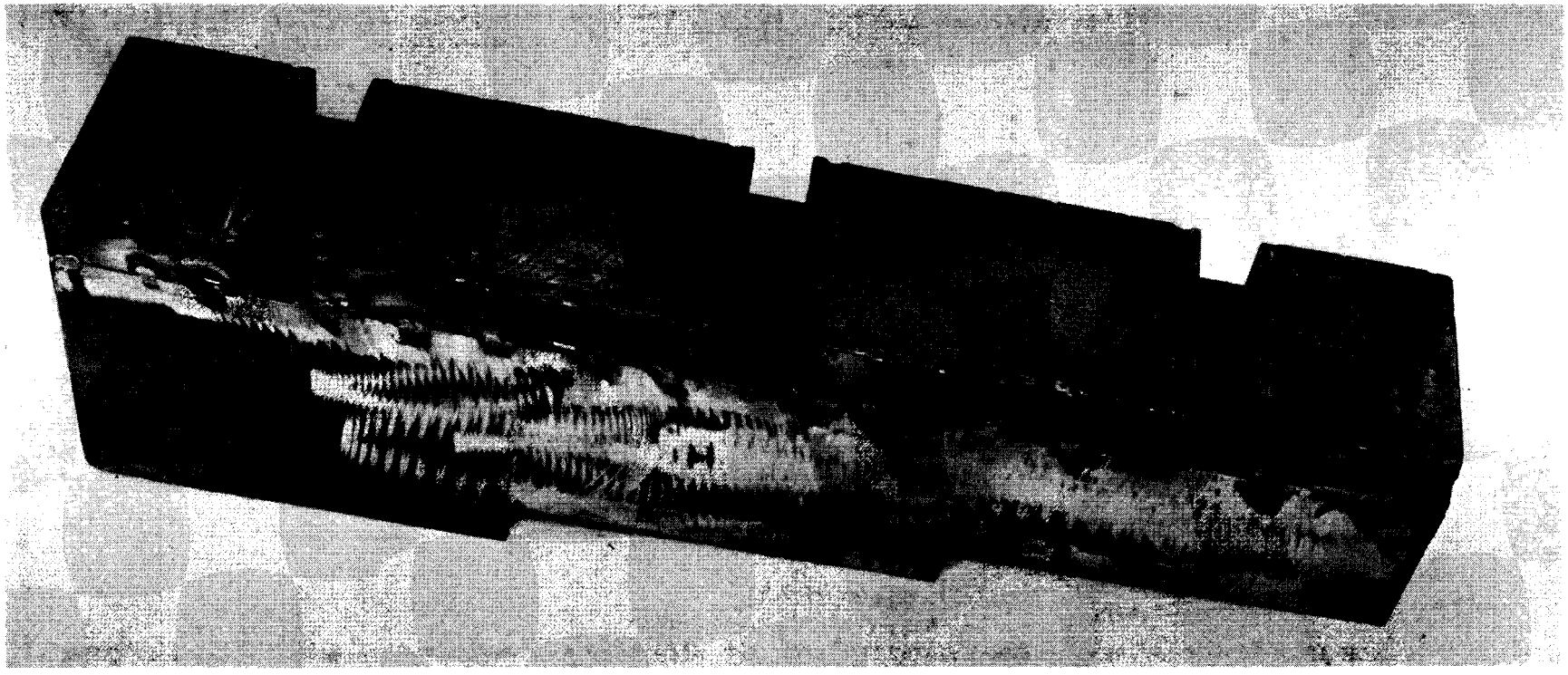

Figure 20 Photo of Side Branch Resonator Suppressor

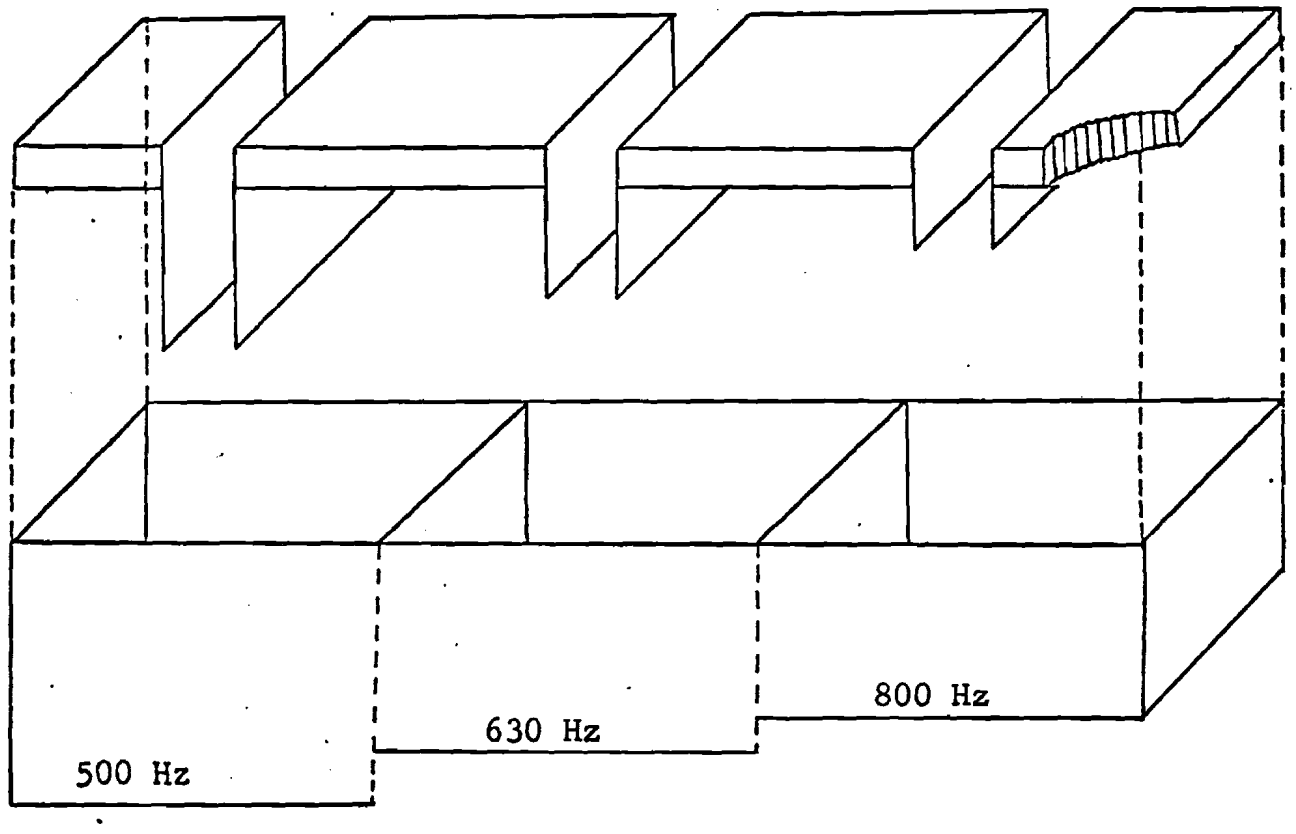

Figure 21 Side-Branch Resonator Suppressor (Geometrically Defined)

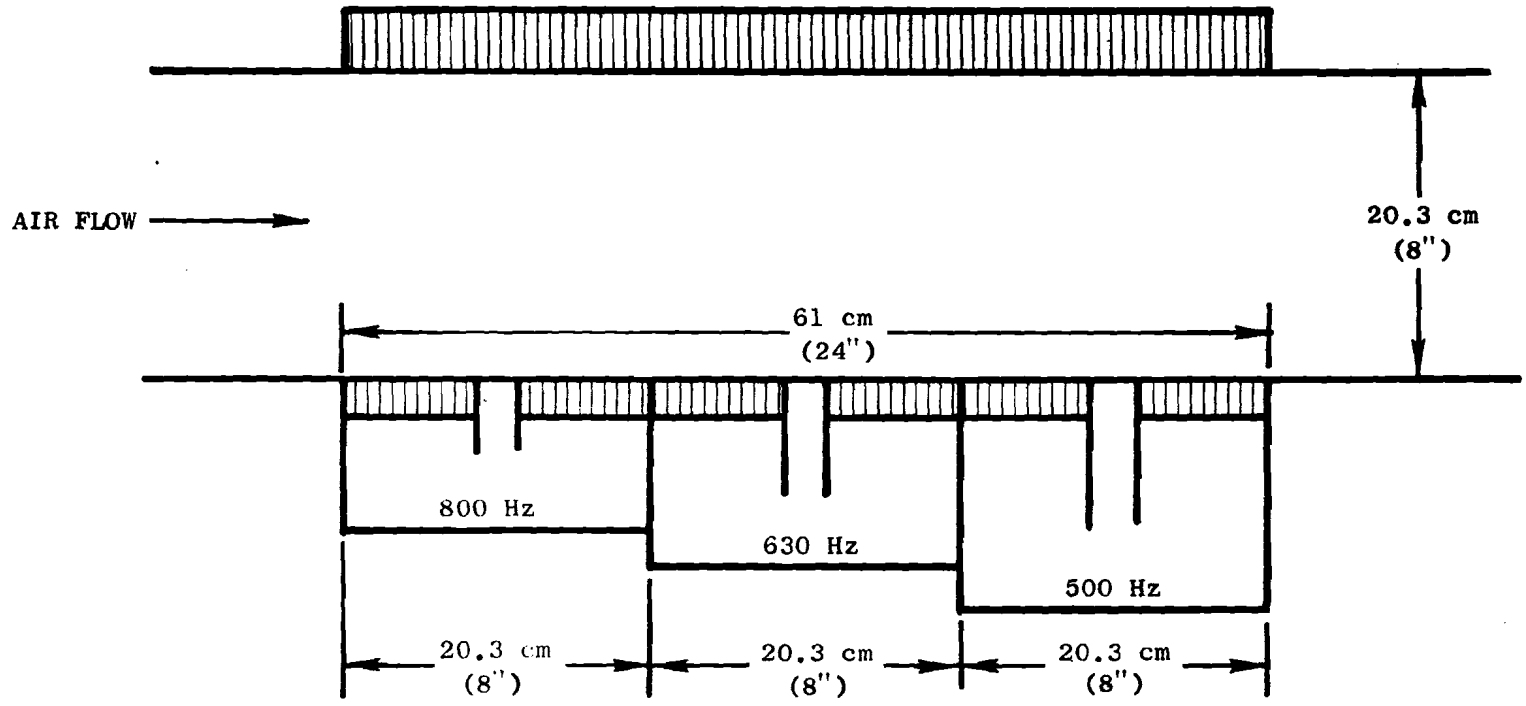

THIN TREATMENT

POROSITY: 10%
HOLE DIAMETER: (.0625") 1.6 mm
FACEPLATE THICKNESS: (.032") 0.8 mm
CAVITY DEPTH: (1.0") 2.54 cm
OPPOSITE PANEL
CAVITY DEPTH (1.5") 3.8 cm

COMBUSTOR TREATMENT

TUNING FREQUENCY (Hz)		800	630	500
POROSITY (%)		12.5	12.5	12.5
SLOT LENGTH	cm	2.54	5.0	7.6
	(IN)	(1.0)	(2.0)	(3.0)
CAVITY DEPTH	cm	7.6	10.2	12.7
	(IN)	(3.0)	(4.0)	(5.0)
SLOT WIDTH	cm	5.0	(5.0)	(5.0)
	(IN)	(1.0)	(1.0)	(1.0)

Figure 22 Side-Branch Resonator Treatment Definition

$A \triangleq$ resonator neck area (m^2, ft^2)
$V \triangleq$ resonator cavity volume (m^3, ft^3)
$t' \triangleq$ adjusted neck length (m, ft) = $t^o + .8\sqrt{A}$

The obtainable transmission loss for a side-branch resonator however is related to the duct and suppressor geometry by the following equation: (Reference 1):

$$L_{TL} = 10 \log_{10} \left[1 + \frac{\alpha_R + .25}{\alpha_R^2 + \beta_X^2 (f/f_o - f_o/f)^2} \right] \qquad (3\text{-}2)$$

where $\alpha_R \triangleq$ resonator resistance = $S_1 R_s / A\rho c$
$\beta_X \triangleq$ resonator reactance = $S_1 c / 2\pi f_o V$
$S_1 \triangleq$ area of main duct (ft^2, M^2)
$L_{TL} \triangleq$ resonator transmission loss (dB)

Using the above two equations, variations were made on the low frequency suppressor geometry to obtain 10 dB suppression over a large frequency range.

The third suppressor, the acoustic rectifier, is pictured in Figure 23 and defined in Figures 24 and 25. In designing this type of suppressor the low frequency tuning frequencies were difficult to define due to the tapered necks as a stacked treatment configuration with straight necks and reactance calculated at the design conditions of 1000° F (810° K) and $M_n = 0.4$ by standard SDOF calculations. This indicated the tuning frequency to be around 700 Hz. Next it was assumed that the system of tapered necks and bleed system would lower the tuning frequency and possibly vary the frequency along the suppressor length as a result of varying amounts of bleed.

A check of the suppressor at the test site indicated the tuning frequencies to be lower to the range of 500 Hz to 700 Hz. Thin treatment serving of a facesheet was omitted in this design so as not to confuse the evolution of the acoustic rectifier performance.

Test Set-Up

The hardware was tested on the High Temperature Duct Facility (HITAD) shown in Figure 26. The duct used two J79 type combustor cans to obtain and hold test temperatures. A siren noise source was used to achieve the required signal-to-noise ratio for the frequency range of 200 Hz to 2000 Hz. Data was acquired using a farfield array of half inch B&K microphones to measure the sound pressure levels at the radius and angles shown in Figure 26. Since the duct centerline height is 5 ft (1.52 m) and the microphones were located at a height of 4 in (10.2 cm) on a 25 ft (7.62 m) arc, the first ground null does not appear until past 2000 Hz. The microphone signal was then filtered at the one-third octave band of interest and recorded on a level recorder while being monitored on an oscilloscope.

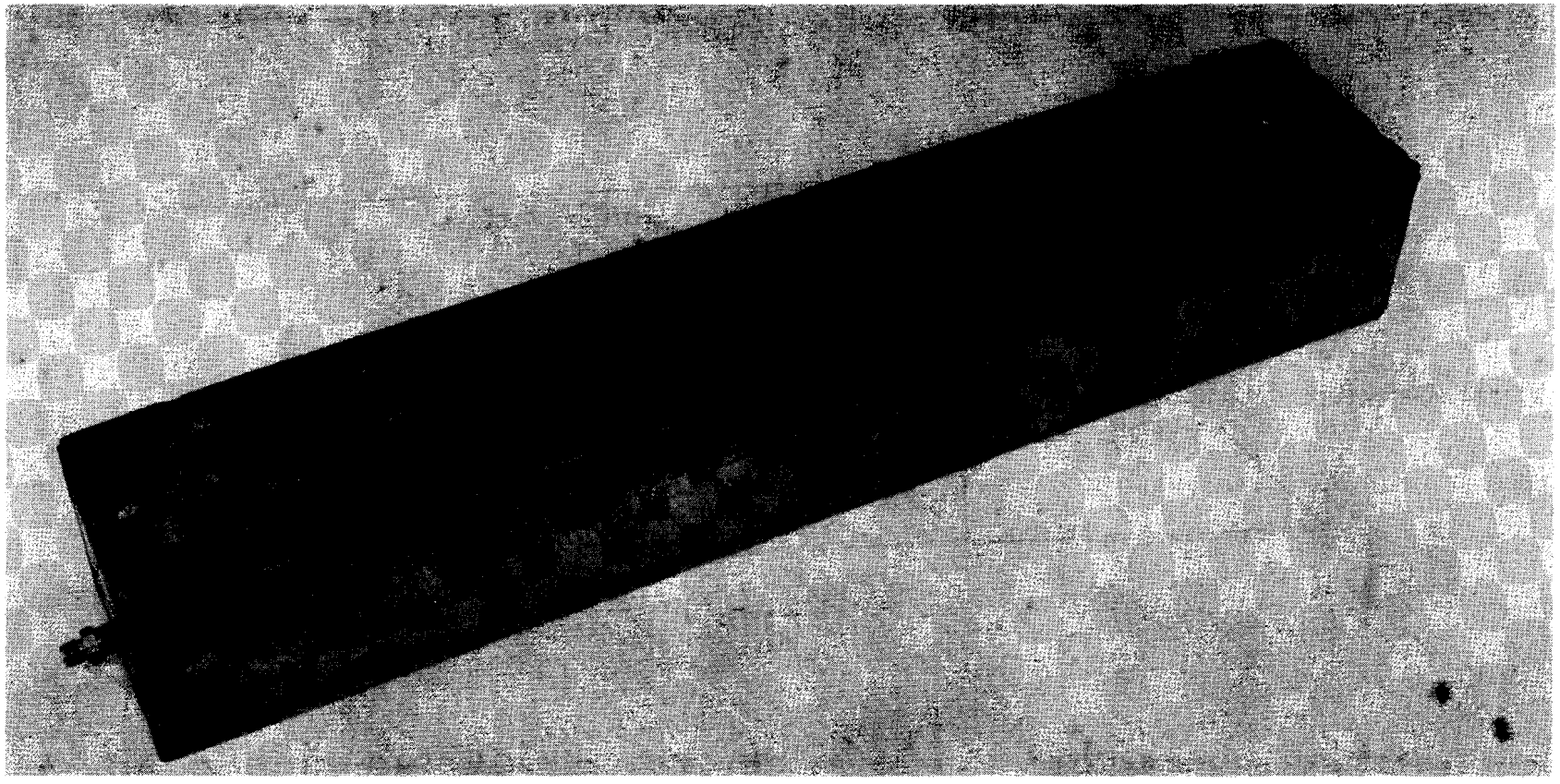

Figure 23 Photo of Acoustic Rectifier

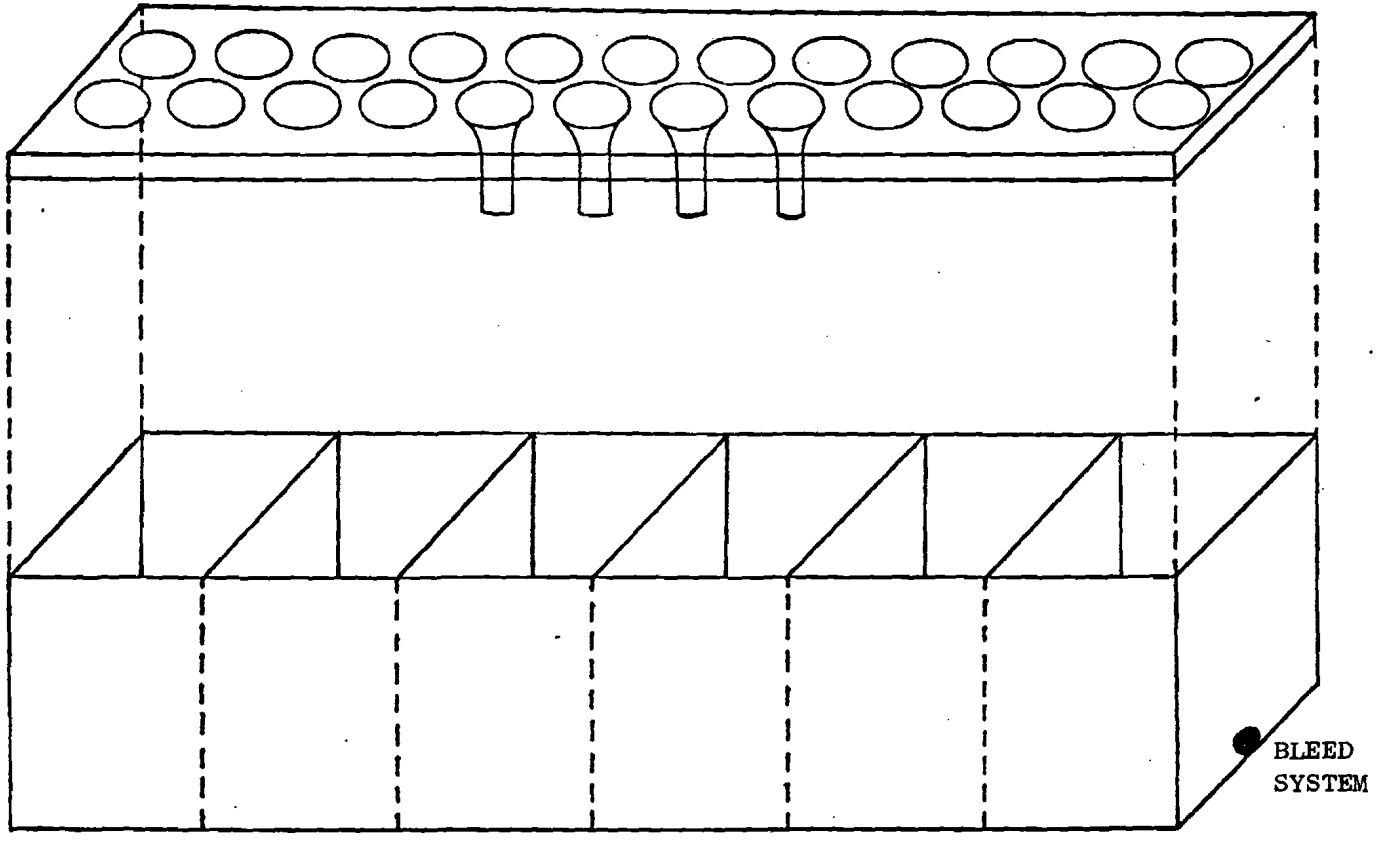

Figure 24 Acoustic Rectifier Suppressor (Geometrically Defined)

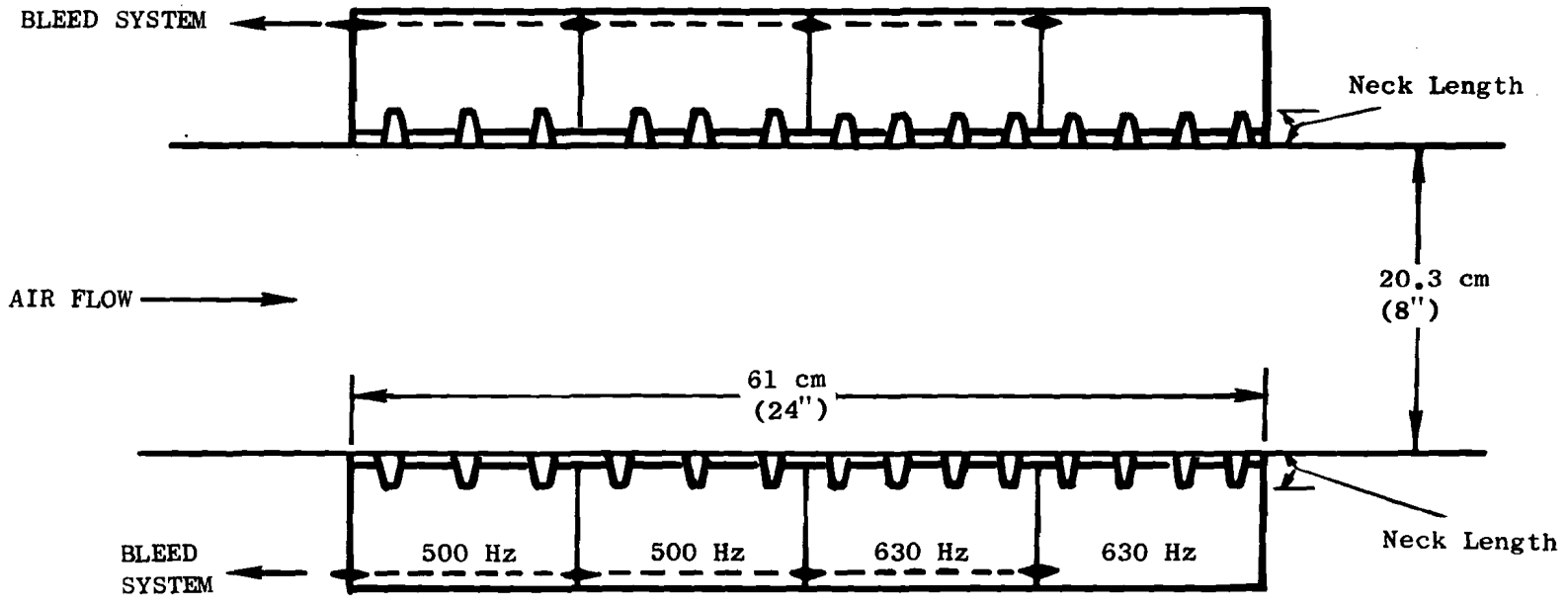

COMBUSTOR TREATMENT

TUNING FREQUENCY (Hz)	500	630
POROSITY (%)	7.0	10.0
NECK LENGTHS (cm, in)	2.54 cm (1.0")	2.54 cm (1")
CAVITY DEPTHS (cm, in)	8.9 cm (3.5")	8.9 cm (3.5")
MEAN HOLE DIAMETER (cm, in) (HOLES TAPERED FROM .75" to .5")	1.6 cm (.625")	1.6 cm (.625")

Figure 25 Acoustic Rectifier Treatment Definition

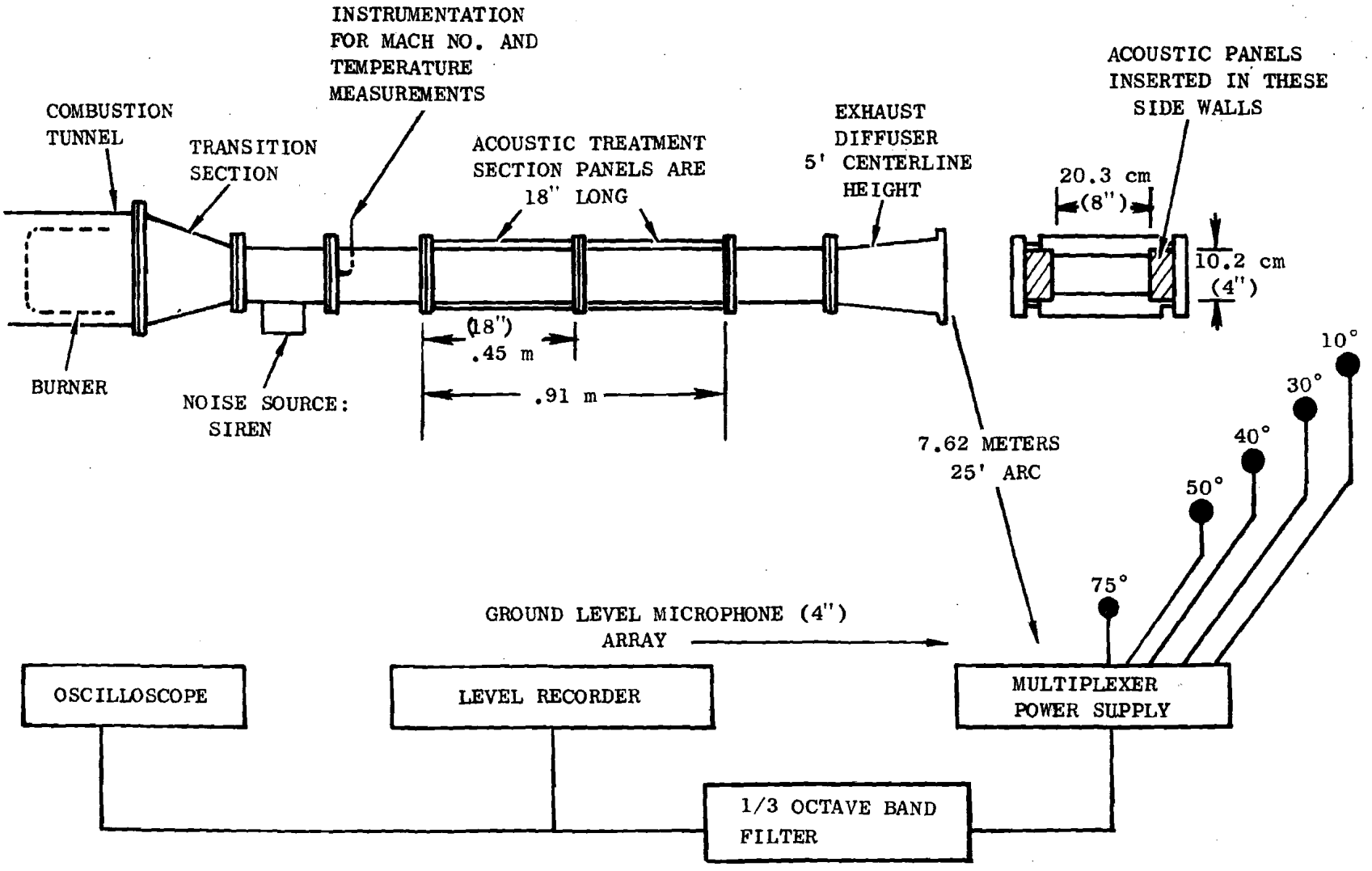

Figure 26 Schematic of Building 306 High Temperature Acoustic Duct Facility

Test Procedure

Prior to each test, all instrumentation was checked using a calibrated B&K piston phone. The test points were set by first centering the siren at the midpoint of each one-third octave band in the range of 200 Hz to 2000 Hz and then adjusting the Mach number and temperature conditions. The measured sound pressure levels were recorded on the level recorder and input to the computer for conversion to sound power levels. The sound power levels were calculated in a two step process. First a strip area weighting was calculated for the microphone locations based on spherical radiation. Then, using the strip areas and sound pressure levels, the sound power level was determined. The corrected transmission loss was calculated from the sound power level differences, with and without treatment installed in the duct.

3.4 TEST RESULTS

The corrected transmission loss results are presented in Figures 27 through 35. These results are grouped according to suppressor configuration, Mach number, temperature, and cover a frequency range of 200 Hz to 2000 Hz.

The stacked treatment results are shown in Figures 27, 28, and 29. At the lower test temperature, 590° K, the Helmholtz tuning frequencies peak at 630 Hz and a quarter wave resonance is seen at 1250 Hz. Over 10 dB suppression is obtained approximately over a 300 Hz frequency range between 500 and 800 Hz for all Mach numbers. At the 920° K test points, the stacked treatment Helmholtz frequencies peak at 800 Hz. However, at Mach 0.2 the suppressor obtains a peak suppression of 30 dB, and 10 dB suppression bandwidth from 500 Hz to 1100 Hz. This suppression peak and frequency range decrease however with increasing Mach number, yielding a peak of 15 dB at $M_n = 0.4$ and 10 dB suppression over a frequency range of 550 Hz to 900 Hz for the range of Mach numbers.

Results for the side-branch resonator treatment are shown in Figures 30, 31, and 32. All temperatures and Mach numbers show no suppression around 800 Hz and intermittent or poor suppression below 800 Hz. Above 1000 Hz, the suppression increases to 20 - 23 dB at 2000 Hz for both temperatures at the higher Mach numbers.

Figures 33, 34, and 35 show the acoustic rectifier suppressor transmission losses. The Helmholtz tuning frequencies peak at 630 Hz and a quarter wave resonance appears at 1250 Hz. The peak suppressions range between 20 and 30 dB with 10 dB suppression available over a frequency range of 300 Hz centered at 630 Hz as shown for all temperatures and Mach numbers except $M_n = 0.2$ at 590° K. At this test condition, much less peak suppression is seen.

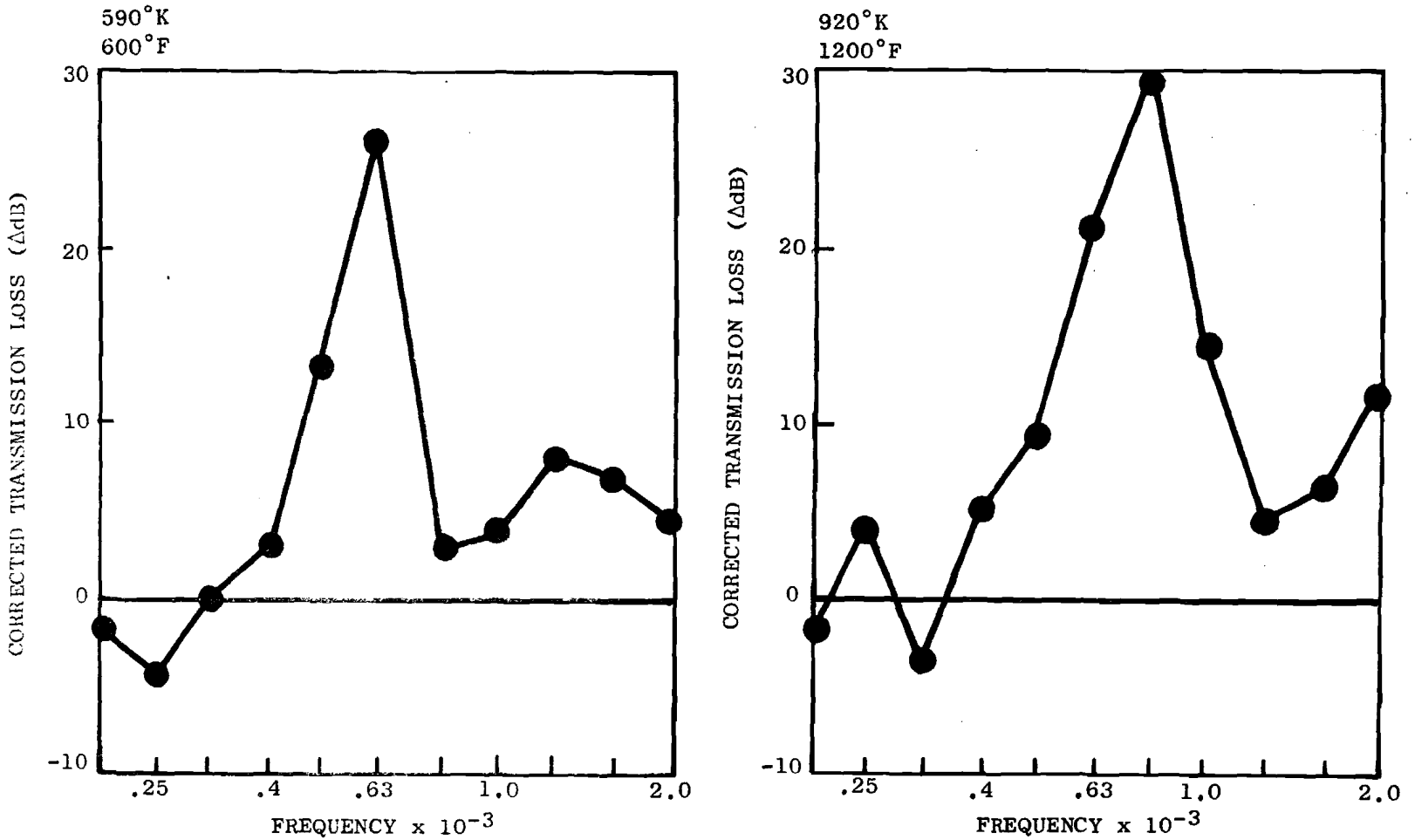

DUCT TEMPERATURES = 590°K & 920°K

Figure 27 Suppression Spectra (ΔT.L. vs Frequency) for Stacked Treatment Suppressor at Duct MACH NO. = 0.2

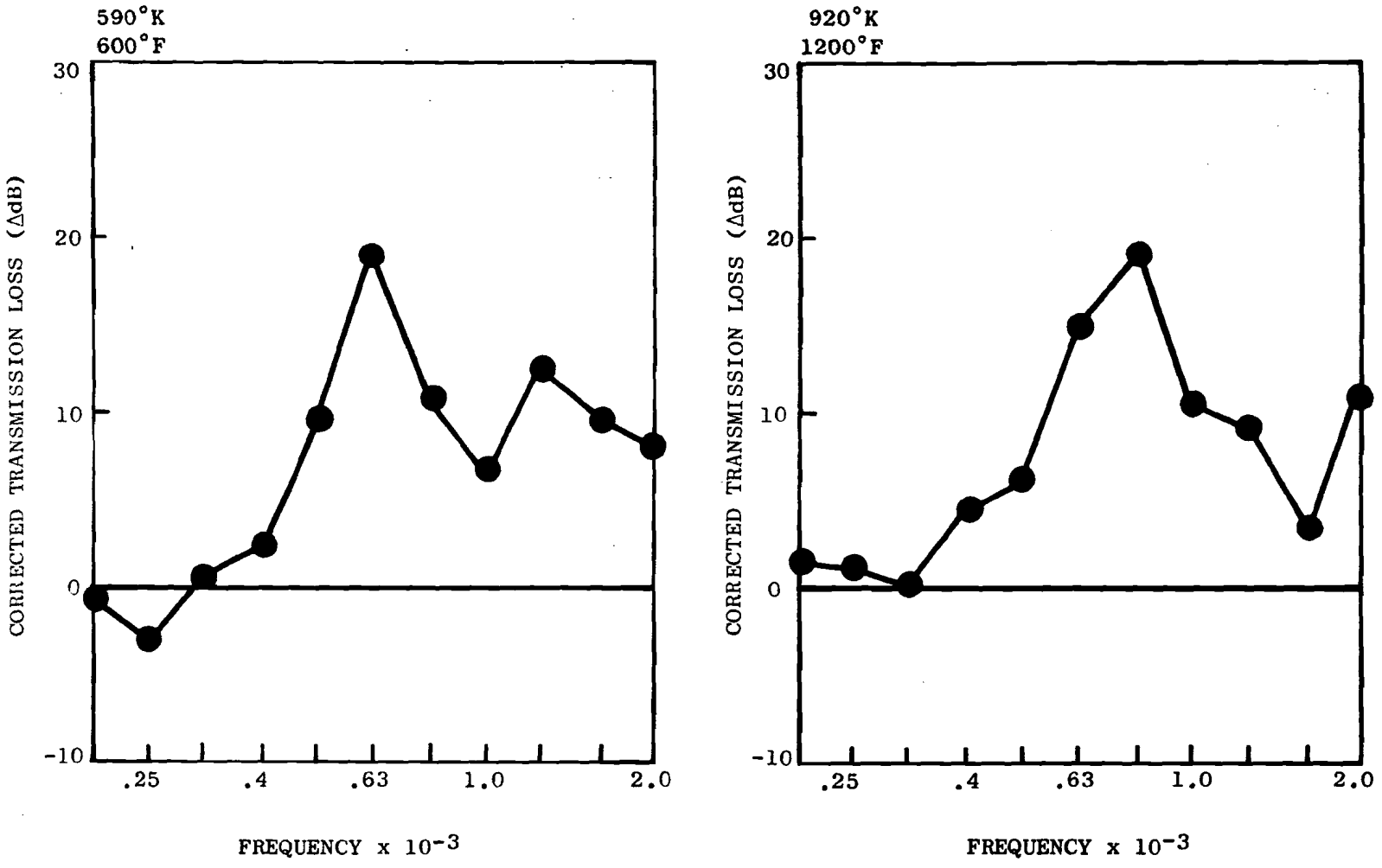

DUCT TEMPERATURES = 590°K & 920°K

Figure 28 Suppression Spectra (ΔT.L. vs Frequency) for Stacked Treatment Suppressor at Duct MACH NO. = 0.3

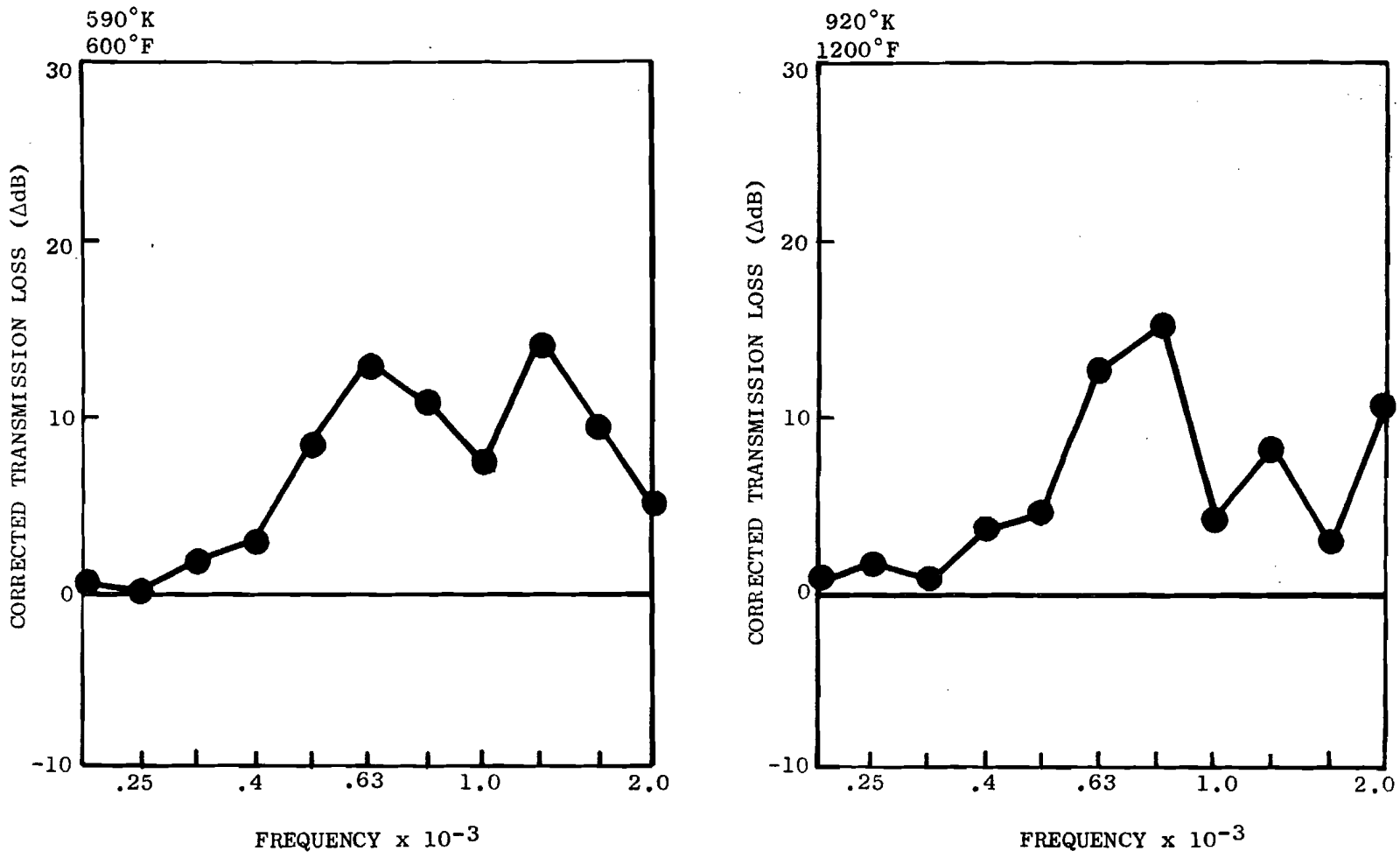

DUCT TEMPERATURES = 590°K & 920°K

Figure 29 Suppression Spectra (ΔT.L. vs Frequency) for Stacked Treatment Suppressor at Duct MACH NO. = 0.4

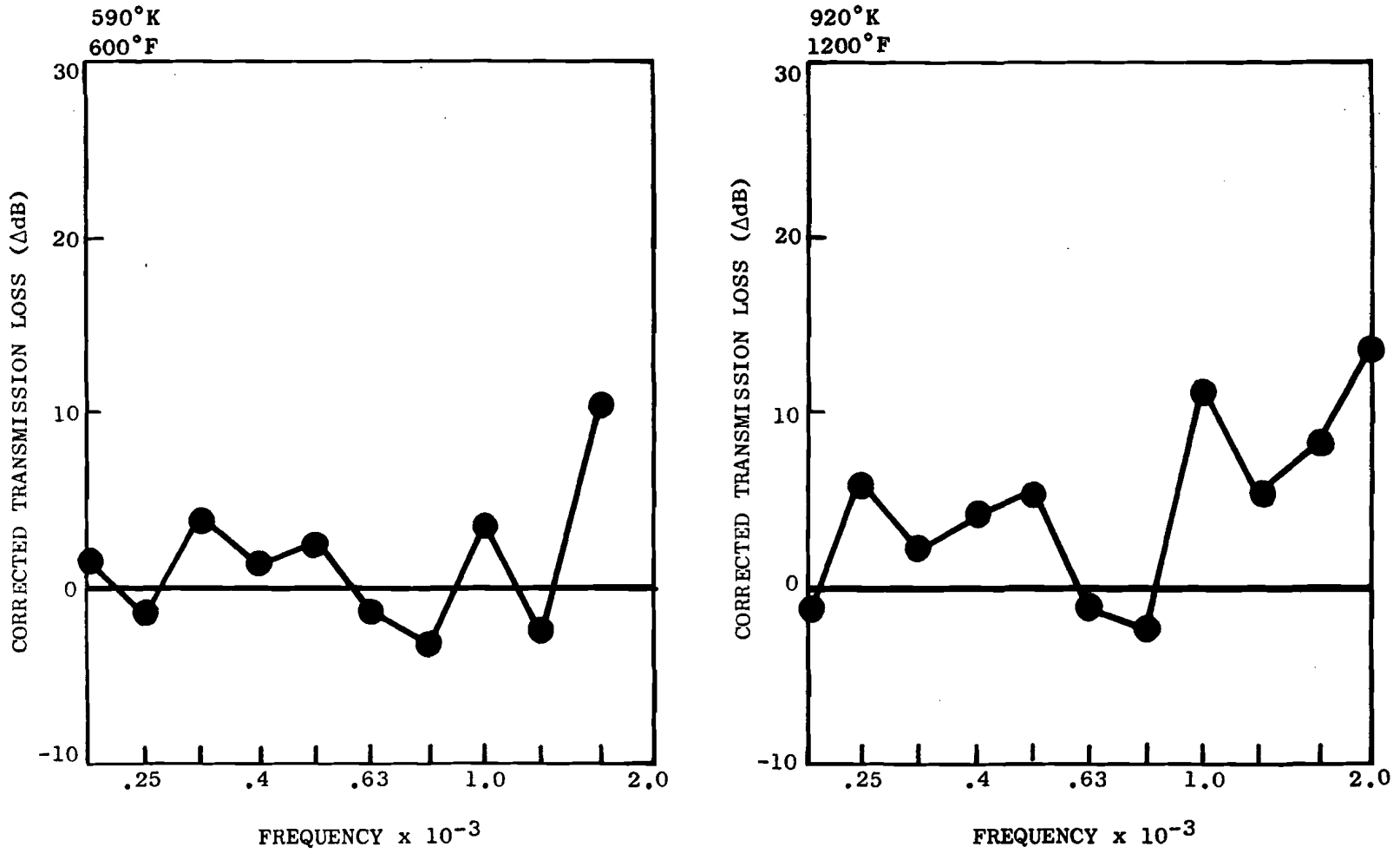

DUCT TEMPERATURES = 590°K & 920°K

Figure 30 Suppression Spectra (ΔT.L. vs Frequency) for Side-Branch Resonator at Duct MACH NO. = 0.2

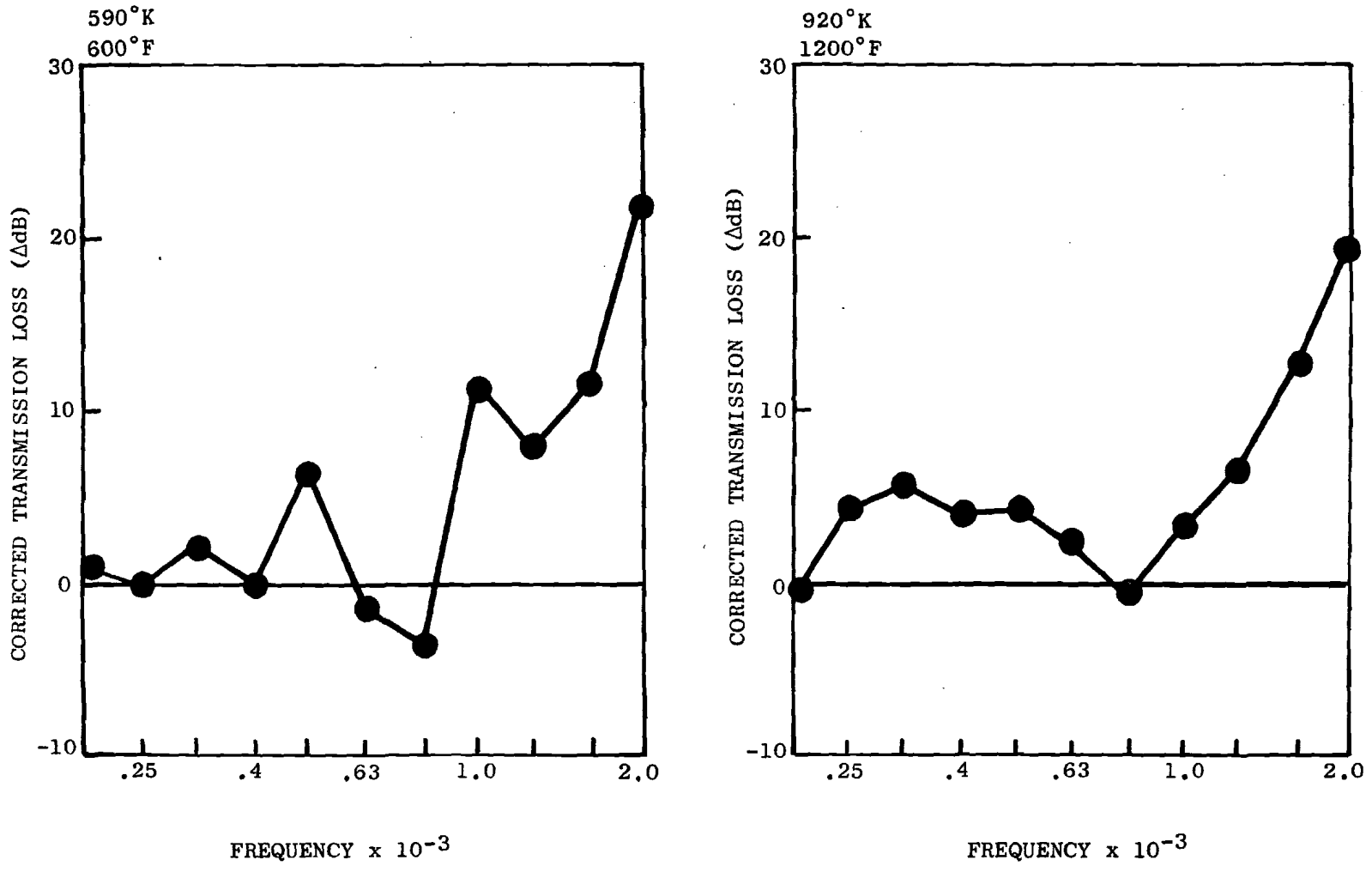

DUCT TEMPERATURES = 590°K & 920°K

Figure 31 Suppression Spectra (ΔT.L. vs Frequency) for Side-Branch Resonator at Duct MACH NO. = 0.3

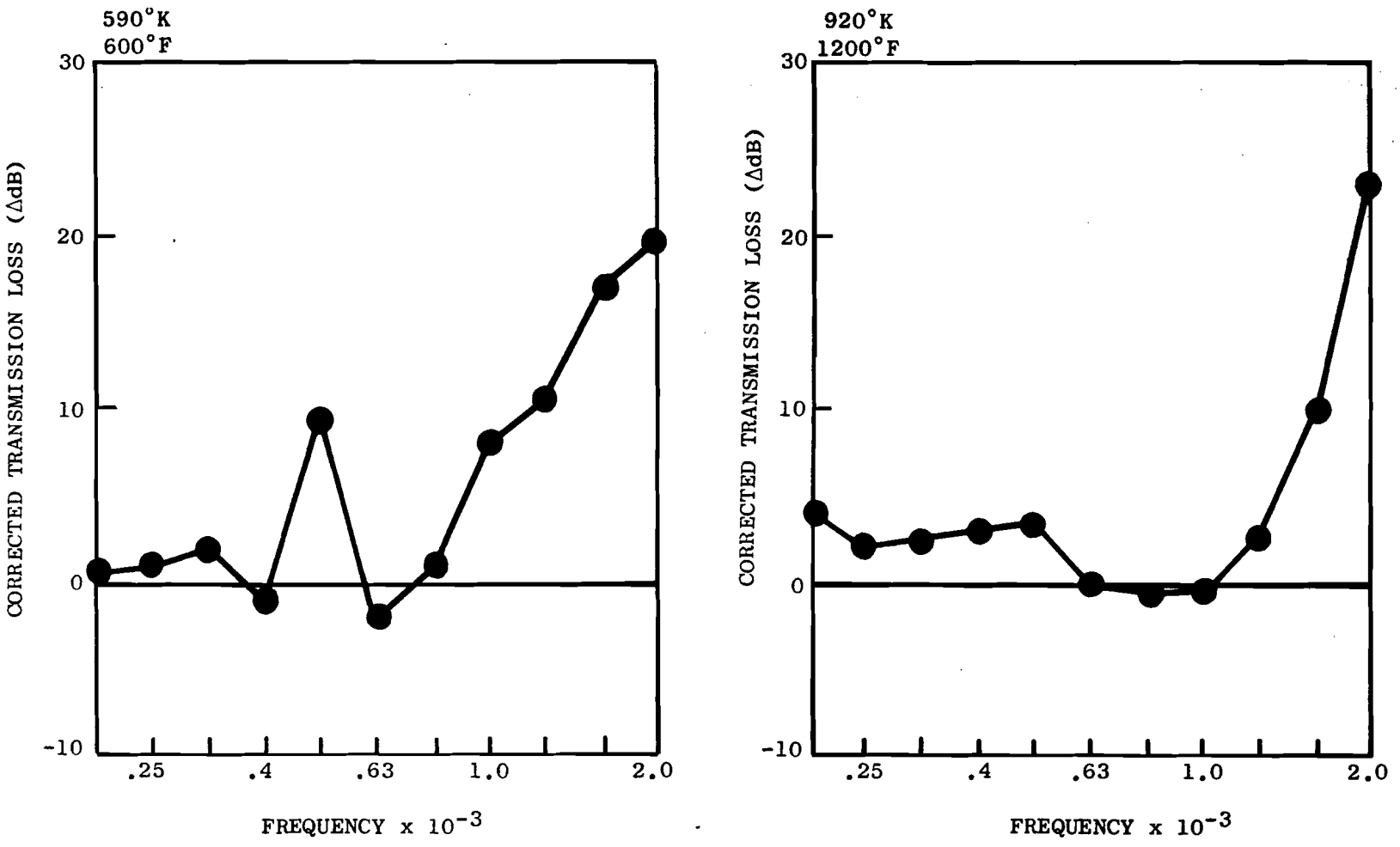

DUCT TEMPERATURES = 590°K & 920°K

Figure 32 Suppression Spectra (Δ T.L. vs Frequency) for Side-Branch Resonator at Duct MACH NO. = 0.4

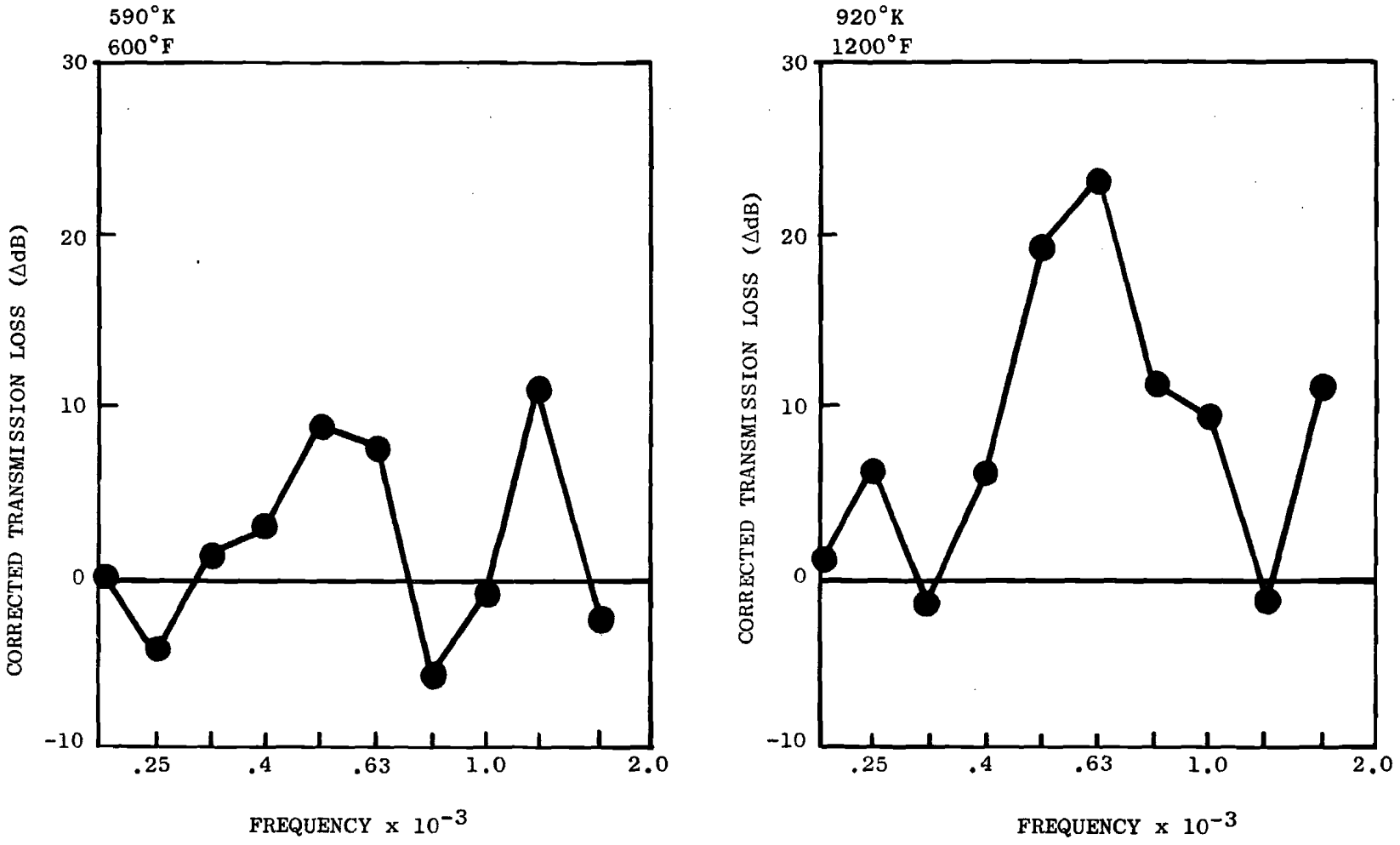

DUCT TEMPERATURES = 590°K & 920°K

Figure 33 Suppression Spectra (ΔT.L. vs Frequency) for Acoustic Rectifier at Duct MACH NO. = 0.2

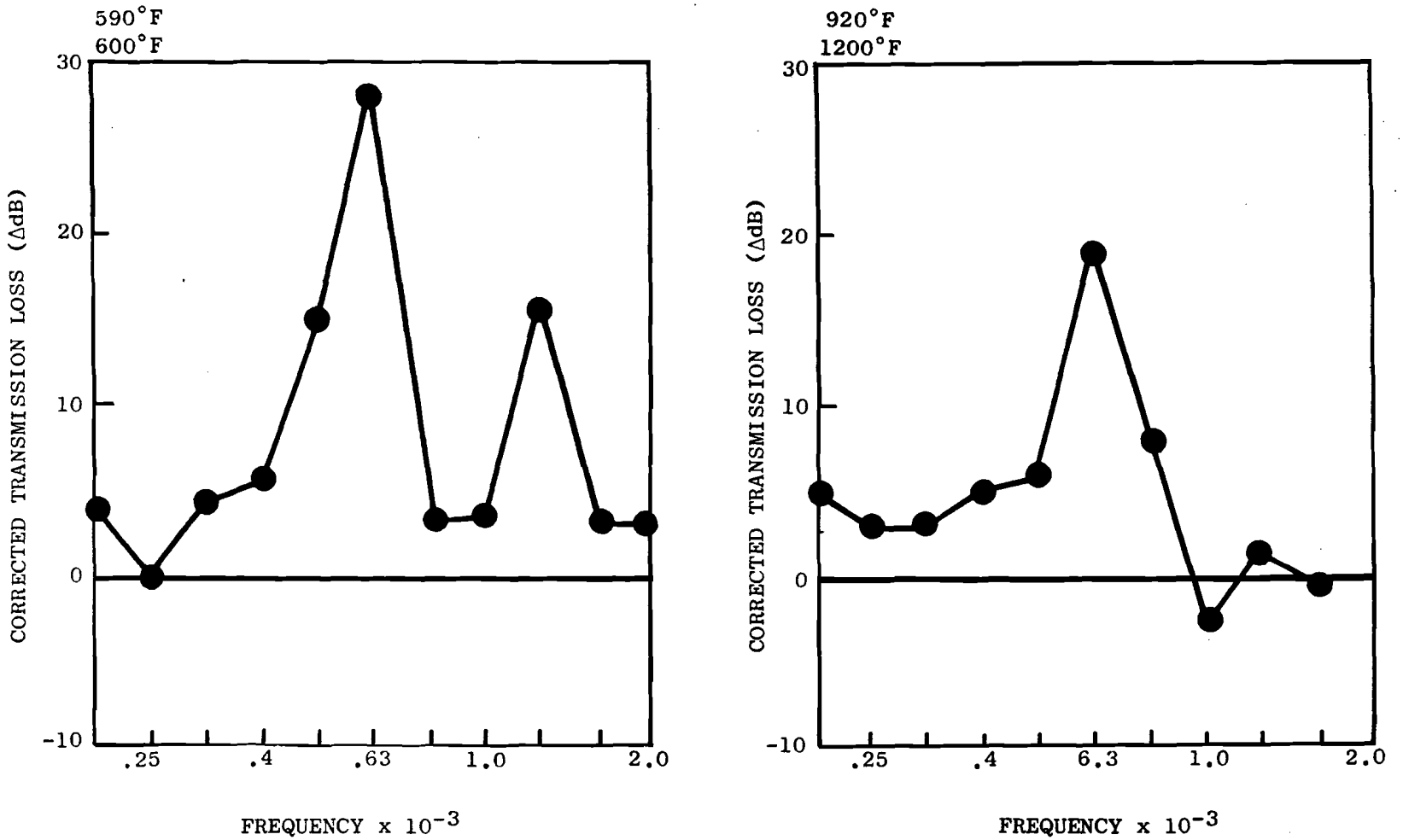

DUCT TEMPERATURES = 590°K & 920°K

Figure 34 Suppression Spectra (ΔT.L. vs Frequency) for Acoustic Rectifier at Duct MACH NO. = 0.3

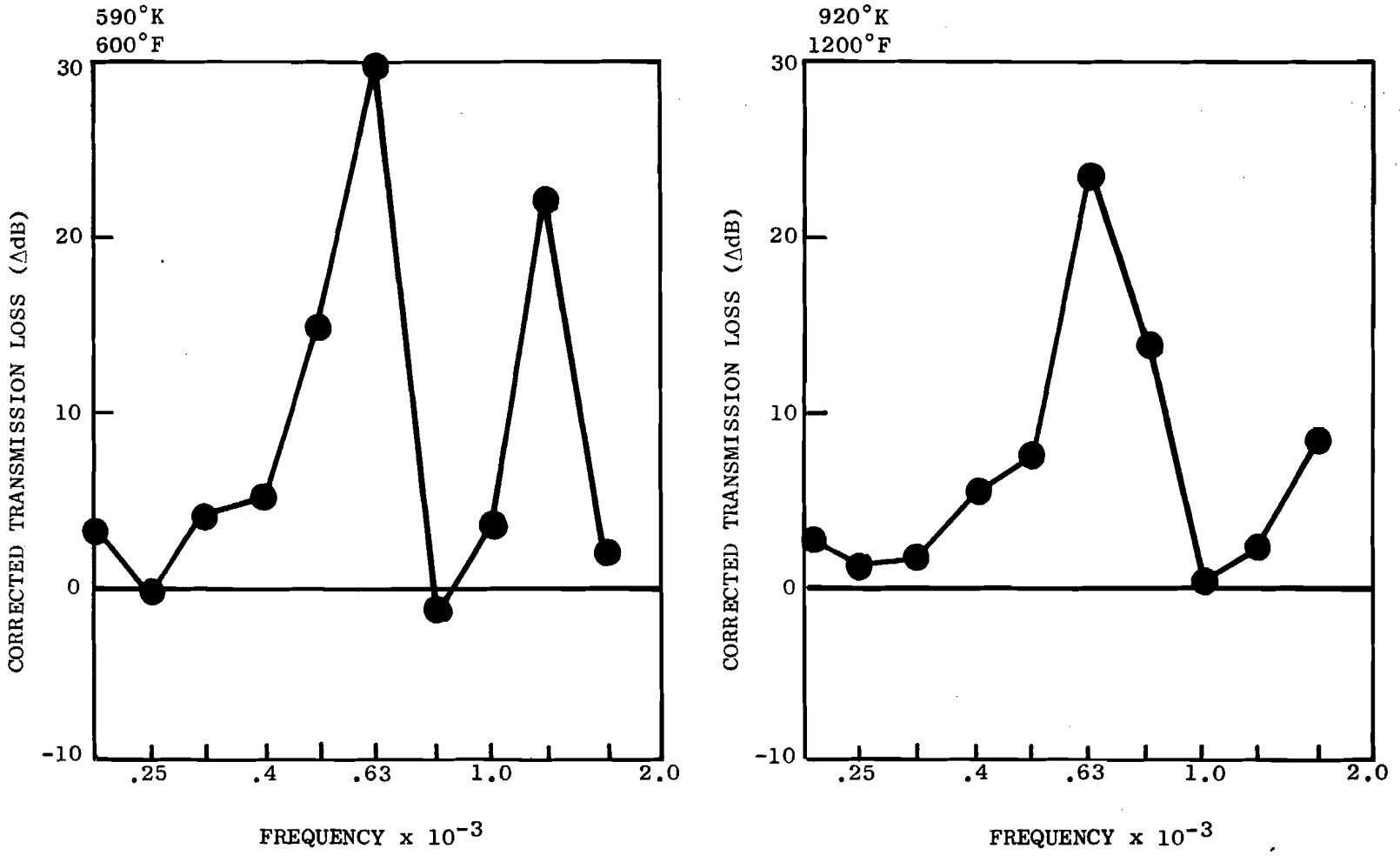

DUCT TEMPERATURES = 590°K & 920°K

Figure 35 Suppression Spectra (ΔT.L. vs Frequency) for Acoustic Rectifier at Duct MACH NO. = 0.4

3.5 DISCUSSION

The corrected transmission loss results show a number of trends and suppression characteristics for each suppressor in the low frequency range from 200 to 2000 Hz.

The stacked treatment suppressor results behaved as predicted. The peak tuning frequency observed at 630 Hz for 590° K agrees with the predicted frequency at design conditions. With the increased temperature, 920° K, the tuning frequency shifted to 800 Hz. Also quarter-wave resonance tuned in at 1250 Hz. For both temperatures, the peak suppression, 25 - 30 dB at $M_n = 0.2$, decreased as the Mach number increased. This trend indicates that the suppressor resistance was overdamped at the tuning frequency. By increasing the porosity of the low frequency cavities, the stacked treatment suppression can be improved. The stacked treatment, while achieving a 10 dB suppression only over a 300 Hz frequency range centered at 630 Hz for 590° K, met the desired suppression goals of approximately 10 dB over 400 Hz centered at 800 Hz for 920° K and $M_n = 0.2$, 0.3, and 0.4 test conditions.

Results for the side-branch resonator treatment show that it tuned-in in the range of 315 to 500 Hz, and the suppression at all test conditions was poor (except above 1000 Hz where the thin treatment contributed to the suppression). The side-branch resonator thin treatment did achieve the goal of 10 dB over 400 Hz at $M_n = 0.3$ and 0.4 for both test temperatures, however suppression in this frequency range (1600 - 2000 Hz) is not very effective if the combustor low frequency peak is not also suppressed.

The acoustic rectifier results indicate that it behaved in a similar manner to the stacked treatment suppression. The Helmholtz tuning frequencies occurred at 630 Hz and a strong quarter wave resonance appeared at 1250 - 1600 Hz. The peak suppression decreased little as Mach number increased, indicating that the tapered necks and bleed system had a positive effect on the suppressor resistance. The suppressor did obtain or exceed approximately 10 dB over a 400 Hz frequency range centered at 630 Hz for 920° K and $M_n = 0.2$ and 0.3, but achieved only a 200 to 300 Hz frequency range for the remaining test points.

3.6 CONCLUSIONS AND RECOMMENDATIONS

The low frequency suppressor study has shown that the goal of 10 dB suppression over a 400 Hz frequency range has been achieved in a configuration that is practical for application to flightworthy engines. The stacked treatment suppressor design can meet and exceed the goals when designed to the desired temperature and Mach number with the proper resistance and reactance impedance components. The side-branch resonator suppressor achieved poor peak suppression in this test series. The acoustic rectifier suppressor demonstrated that it also can be designed to meet or exceed the suppression goals. Since these concepts incorporate thin treatment panels as low frequency

facesheets, the suppressors could be designed to suppress both the low frequency combustor noise and higher frequency turbine noise.

The low frequency suppressor (stacked treatment) was identified, built, and tested and demonstrated to meet the design objective of 10 dB suppression over a frequency bandwidth of 400 Hz below a frequency of 2000 Hz. The porosity of the stacked treatment design was close to the estimated optimum porosity, based on the least-attenuated-mode design criteria. The porosities used were slightly lower than those which would provide peak suppression at a given design frequency. This allowed a thinner panel design, required for engine compatibility, and maintained the suppression bandwidth at a slight expense of peak suppression (which would occur in only a very narrow frequency band. This is essentially the design procedure followed for the QCSEE vehicle core suppressor in which the geometry was constrained by the allowable thickness between core duct passage and outer cowl.

Both the stacked treatment and acoustic rectifier concepts appear to be good choices as compact low frequncy suppressors. Additional work should be done on the stacked treatment concept to obtain better suppression by defining the more desirable impedance components and subsequently a better suppressor geometry by varying such parameters as porosity. Since the acoustic rectifier concept is innovative, additional work beyond the scope of this program should be done to better define the design parameters and to determine more desirable combinations of neck geometries and amounts of bleed. Both the stacked treatment and acoustic rectifier concepts have excellent possibilities as future compact core suppressors.

3.7 PREDICTION METHOD UPDATE

The suppressed combustor noise can be predicted by applying the suppression bandwidths from the stacked treatment of the acoustic rectifier to the predicted combustor noise (see Vol. III, Section 3). The bandwidth chosen should reflect the Mach number and temperature at the operating point where the maximum suppression is desired. If the operating point does not lie close to one of the test points, linear interpolation or extrapolation should be used.

REFERENCES

1. Beranek, L.L., Noise and Vibration Control, ch. 12, McGraw-Hill, New York, 1971.

SECTION 4.0

TURBINE TONE/JET STREAM INTERACTION

4.1 BACKGROUND AND OBJECTIVES

"Haystacking" can be attributed to turbulence scattering of turbine tones by inhomogeneities in the exhaust jet mixing regions. Using a simplified analytical model, it has been shown (Volume II, Section 5) that as a coherent (discrete frequency) signal propagates through a region of turbulence, part of the incident acoustic energy is redistributed into a scattered wave by the turbulence cells. The change of inhomogeneities in time, as seen by the incident wave, produces a change in the frequency of the scattered wave and results in a broadening of the signal bandwidth. The nature of the broadening can be inferred from the form of the time autocorrelation functions of the amplitude and phase fluctuations. In particular, the frequency spread is determined by the correlation time of the turbulence eddies. The amplitude transformation is a strong function of the correlation length, of the eddies, and the turbulence intensity.

In the period since this modulation mechanism was first suggested by General Electric (during the Core Engine Noise Control Program) several investigators have indicated their apparent corroboration (References 1, 2, and 3).

The analytical model splits the far-field signal into two distinct parts:

(a) the unaffected, or residual, portion of the initial wave

(b) the scattered or modulated wave;

The residual portion consists of the surviving discrete frequency signal. The scattered wave, however, reflects the turbulence spectrum and consists of a "haystack" of noise, the peak frequency of which exhibits a Doppler shift due to the fact that the scattering cells are in motion. When the scattered wave contains less acoustic energy than the residual tone, a discrete frequency spike is seen capping the haystack (somewhat obscuring the Doppler shift of the haystack). When the scattered wave contains more energy than the residual tone, there is no visible tone content, and the haystack peak frequency shift can be observed quite clearly (the peak moving to higher frequencies as the observation angle, measured from the inlet, increases-Figure 36).

The objectives of the analytical modelling were to identify the pertinent parameters, to provide a base for data correlations, and to define parametric trends which could be utilized in a continuing study of this phenomenon. The first objective was accomplished as given in Volumes II and

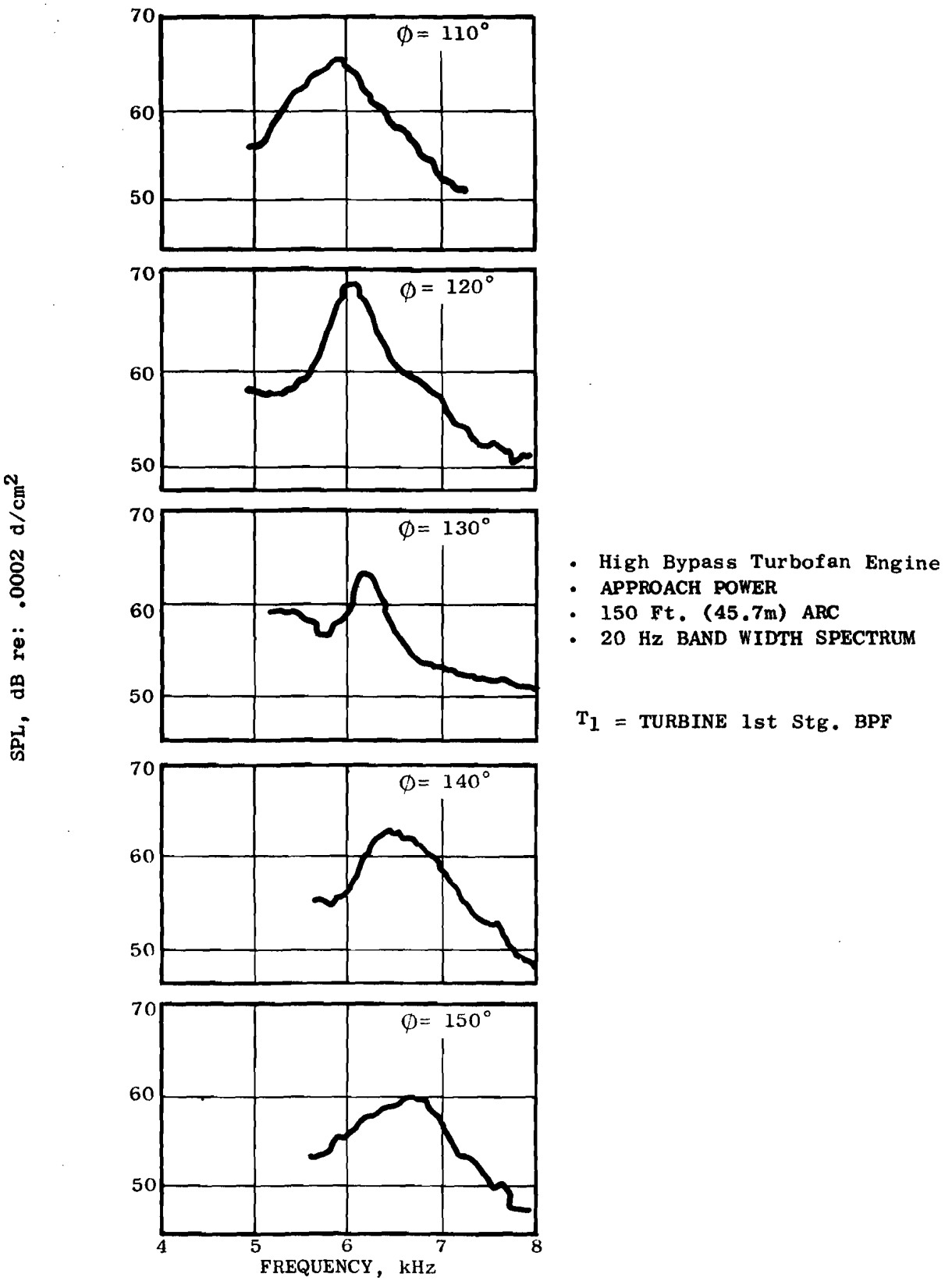

Figure 36 Haystack Peak Frequency Shift with Observer Angle

III. A semi-empirical prediction method was derived from TF34 and Quiet Engine "C" data to predict both the tone amplitude reduction and the frequency spread. The prediction method was held to two variables due to the limited data available: the fan jet stream velocity and the distance between the fan and core exhaust planes.

The purpose of the present work was to conduct a parametric study of the analytical model to quantitatively define the effect of other pertinent variables and to accordingly update the prediction method.

4.2 PARAMETRIC STUDY

Pertinent Equations - The analysis of Phase II models the turbulence cells encountered by a turbine tone as inhomogeneities in density, compressibility and velocity. An inhomogeneous wave equation is obtained which can be solved using a Green's function. The solution is limited to two terms by assuming the Born approximation is valid. Cases where this approximation becomes invalid are discussed by Howe (Reference 4).

The two terms represent the residual tone and the scattered wave. The spectral distribution and the intensity of the scattered wave expressed as fractions of the energy in the incident plane wave are given by the following two equations:

$$\frac{\bar{I}_\omega(\vec{r})}{|A_o^2|/\rho c r^2} \simeq \frac{V \ell^3}{16\pi^2 c\,\omega_c}\Big[k_i^4\langle\gamma_k^2\rangle + k_i^2\langle\gamma_\rho^2\rangle\left(\frac{\omega}{c}\right)^2\cos^2\Theta + 4\left(\frac{\omega}{c}\right)^4\langle M_t^2\rangle\cos^2\Theta\Big]\exp\Big[-\frac{1}{2}\mu_s^2\ell_c^2 - \frac{1}{2}\left(\frac{\Delta_s}{\omega_c}\right)^2\Big] \tag{4-1}$$

$$\frac{\bar{I}_s(\vec{r})}{|A_o^2|/\rho c r^2} \simeq \frac{V}{\sqrt{32\pi}\,\ell_c}\,\frac{\alpha^4}{\sqrt{1+\alpha^2}}\Big\{\eta^4\langle\gamma_k^2\rangle + \eta^2\langle\gamma_\rho^2\rangle\,\frac{1+\eta^2(1+\alpha^2\cos^2\Theta)^2}{1+\alpha^2} + 12\langle M_t^2\rangle\,\frac{1+2\eta^2(1+\alpha^2\cos^2\Theta)^2 + \frac{1}{3}\eta^4(1+\alpha^2\cos^2\Theta)^4}{(1+\alpha^2)^2}\Big\} \tag{4-2}$$

$$\exp\Big[-\frac{\eta^2\alpha^2}{2(1+\alpha^2)}\left(4\sin^2\frac{\Theta}{2} + \alpha^2\sin^2\Theta\right)\Big]$$

where $\bar{I}(\vec{r})$ = the time averaged intensity at $\vec{r}$ for any frequency, $\omega/2\pi$

$\vec{I}_s(\vec{r})$ = overall intensity of the scattered wave at $\vec{r}$

$\vec{r}$ = position vector of observer, (r,ϕ)

r = observation distance

ϕ = angle measured, from inlet

A_o = amplitude of incident plane wave

ρ = fluid density

c = acoustic velocity

k_i = incident wave number, $\frac{\omega_o}{c}$

$\gamma_\kappa, \gamma_\rho, M_t$ = perturbations in compressibility, density and Mach number due to inhomogeneities in the jet mixing region(s)

$<>$ = time and space averaged mean

θ = angle between observer and incident plane wave and

$\vec{\mu}_s$ = $\frac{\omega}{c}\hat{a}_r - \vec{k}_i$

$\hat{a}_r$ = unit vector in the $\vec{r}$ direction

Δ_s = $\omega - \omega_o$

ℓ_c, ω_c = correlation length and frequency of eddies in the mixing region(s)

V = volume of mixing region(s) encountered by the propagating tone

η = ω_o/ω_c

α = $\frac{\omega_c \ell_c}{c}$

The jet Mach numbers of interest here are low and since $\gamma_k, \gamma_\rho \sim O(M_t^2)$, these two equations can be simplified by dropping the first two terms on the right hand sides. The second equation is of primary interest to us and it becomes

$$\Delta_5 = \frac{I_s(\vec{r})}{|A_o^2|/\rho c r^2} \simeq \frac{3}{\sqrt{2\pi}} \frac{V}{\ell_c} \frac{\alpha^4}{\sqrt{(1+\alpha^2)^5}} <M_t^2> [1+2\eta^2(1+\alpha^2\cos^2\Theta)^2 + \frac{1}{3}\eta^4(1+\alpha^2\cos^2\Theta)^4 \exp\left[-\frac{\eta^2\alpha^2}{2(1+\alpha^2)}(4\sin^2\frac{\Theta}{2} + \alpha^2\sin^2\Theta)\right] \quad (4\text{-}3)$$

The exponent on the right hand side arises from the assumption of the form of the spatial - temporal spectral distribution of the inhomogeneities. It can be temporarily removed from the analysis by looking at the $\theta = 0$ case. The results so obtained then reflect the trends for a flat source distribution, that is the actual source distribution must be superimposed on the answers to provide the observed trends.

Putting $\theta = 0$ in equation (4-3) gives:

$$\Delta_5^\circ \simeq \frac{3}{\sqrt{2\pi}} \frac{V}{\ell_c} \frac{\alpha^4}{\sqrt{(1+\alpha^2)}} \langle M_t^2 \rangle_5 [1+2\eta^2(1+\alpha^2)^2 + \frac{1}{3}\eta^4(1+\alpha^2)^4] \qquad (4\text{-}4)$$

The various quantities V, ℓ_c, M_t, α and η must now be defined in terms of known flow parameters and nozzle dimensions.

Shear Layer Model - Engine data indicated that it was the outer stream that controlled the haystacking in turbofans (Volume III, Section 5). Hence a turbulence model is defined for the outer shear layer of a coannular flow configuration and equations (4-1) and (4-4) exercised in a parametric study with this model. The results are considered valid for conventional staggered and coplanar exhausts.

A coannular flow arrangement is characterized by three distinct regimes as shown in Figure 37.

Region I - two distinct shear layers are seen and both potential cores exist.

Region II - the outer region is in transition, while the inner potential core still persists.

Region III - both potential cores have dissipated and the entire region is in transition. The two streams have fully coalesced.

Consideration of existing engine dimensions indicates that turbine tones from high bypass engines will normally encounter the first flow regime. Numerous investigators have shown that the width (b) of the mixing region is a linear function of the axial distance (2) downstream of the nozzle exit for round turbulent jets. For example, Hammersley (Reference 5) presents empirical data showing that for the outer flow,

$$b = .21\ (Z - Z_o) \qquad (4\text{-}5)$$

where Z_o = virtual origin. The virtual origin is actually a function of the fan nozzle diameter, but the variation appears to be small and 0.2 appears to be a good approximation to (Z_o/fan jet diameter).

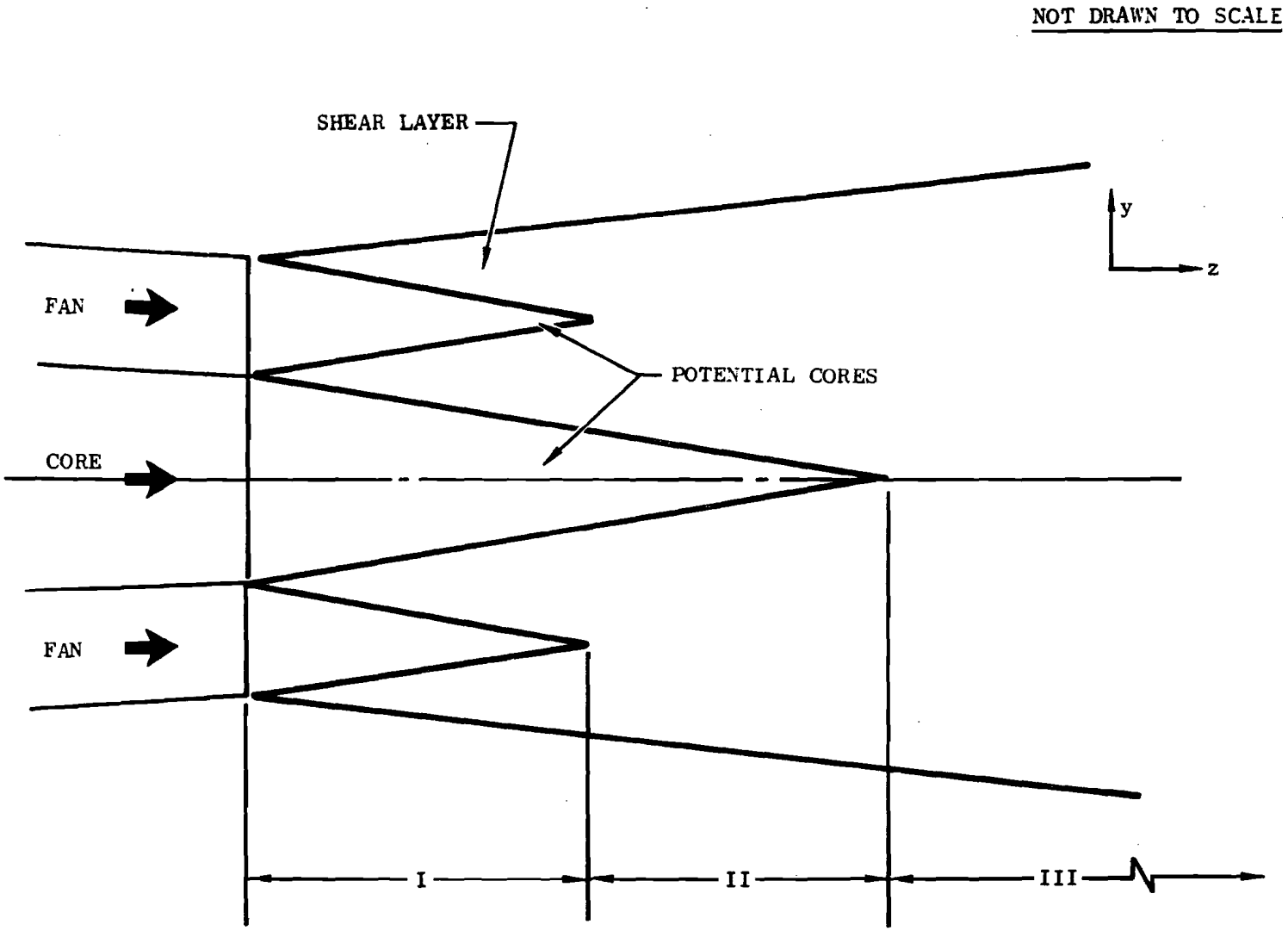

Figure 37 Coannular Flow Regimes

This width can be used to scale eddy length, convection velocity, the integral time scale and the turbulence spectrum. Hammersley's data suggest that for the range of parameters studied

$$\ell_c = .4b \tag{4-6}$$

in the outer layer. Other investigators (see, for example Reference 6) also indicate a weak Mach number dependence in the case of single conical nozzles:

$$\ell_c = \frac{k_1 b}{1+k_2 M_j} \tag{4-7}$$

where M_j = jet exit Mach number

k_1 = slope constant

$k_2 \simeq .38$

This leads to the relationship

$$\ell_c = \frac{.4b}{1+.38M_j} \tag{4-8}$$

The eddies under discussion here are the small scale inhomogeneities that convect along with the flow with a phase velocity approximately equal to the local mean velocity in the shear layer. Thus, the phase velocity will vary between .6 and .7 of the fan exit velocity and as a first order approximation we can conveniently use:

$$V_{phase} = .65\ V_{jet} \tag{4-9}$$

As has been observed by Kolpin (Reference 7), different size eddies have different convective velocities larger eddies travel slower than the smaller (high frequency) eddies. Hence, if the large scale structure noted by Crow and Champagne (Reference 8) were to occur, the interaction effects would change perceptibly, as these large scale eddies convect at about half the jet exit velocity. This structure is normally encountered at higher Mach numbers only.

Once eddy size and convection velocity are known, the correlation frequency is determined from

$$\omega_c = 2\pi \left(\frac{V_{phase}}{\ell_c}\right) \tag{4-10}$$

Thus far, neither the area ratio (fan/core) nor the velocity ratio feature prominently in the turbulence model. Hammersley (Reference 5) concludes that the structure of the mixing region is constant. For the range of variables studies, the structure is independent of velocity ratio and area ratio. This explains why the various parameters scale on the width of the shear layer which is a function only of the axial distance downstream.

It further appears that the turbulence intensity and spectrum are also largely invariant. Data from Engine 'C' (Figure 38) and from Hammersley's model tests show the turbulence velocity (u') initially accelerating in a very short distance to about 15% of the jet exit velocity and then remaining essentially constant throughout Region I. Hence a good approximation for $\langle M_t \rangle$ is 0.15 M_j. There will be no L/D effect until the fan duct is shortened to such an extent that Region II is encountered, in which case $\langle M_t \rangle$ will increase with L.

The distribution of kinetic energy of the fluctuating velocity components over the various frequencies can be represented by a turbulence spectrum such as shown in Figure 39 (Reference 9). The spectrum at any location scales on shear layer width. Typically, the spectrum peaks at a low frequency and the energy density then falls off at about 6dB per octave as in Figure 39. In fact, the exact energy roll-off at high frequencies can be expressed by the 5/3 law (see, for example, References 10 and 11).

$$E(\omega) \propto \omega^{-5/3} \tag{4-11}$$

where E is the turbulent energy per unit frequency. Recalling that the scattering at any angle θ is determined only by a narrow portion of the turbulence spectrum near $\omega_o = |(\omega_o - \omega_c)|$, where $\omega_o = 2\pi$ (BPF), an 8000 Hz tone will then encounter about 6dB less turbulence energy than a 4000 Hz tone. This source distribution effect enters into the amplitude loss determination through the exponent in equation (4-3), supplying a $20\log(\omega_o)$ decay in the form of $\exp(-\eta^2)$, which is a good approximation to the 5/3 law.

Parametric Results - Equations (4-8) through (-10) along with the following assumptions are sufficient to define all the quantities in equation (4-4).

(a) The turbulence intensity is assumed to be remain constant (at 15%) with increasing jet velocity, hence

$$\langle M_t^2 \rangle \propto M_j^2 = (V_{fan}/c)^2 \tag{4-12}$$

(b) The axial coordinate $(Z - Z_o)$ is replaced by $(1 + L/D_o)$ where L is the distance between the fan and nozzle exhaust planes and D_o is a convenient constant.

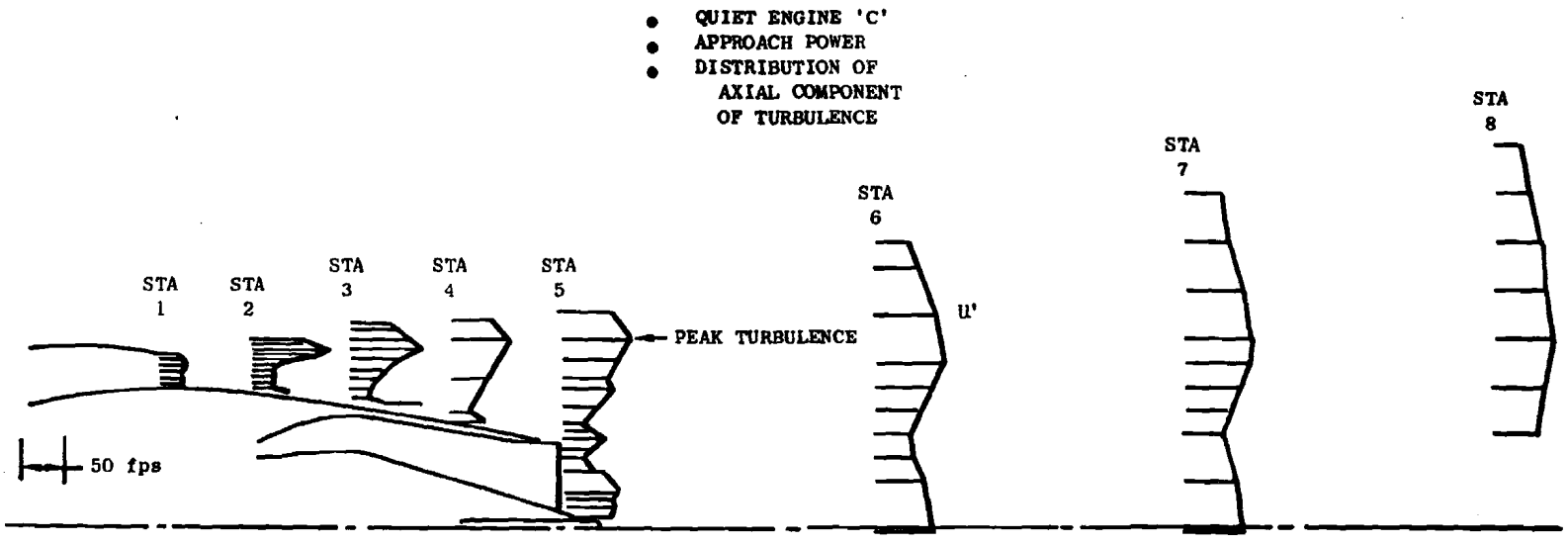

Figure 38 Laser Velocimeter Measurements Showing Axial Turbulence Variation in a Coannular Flow Arrangement

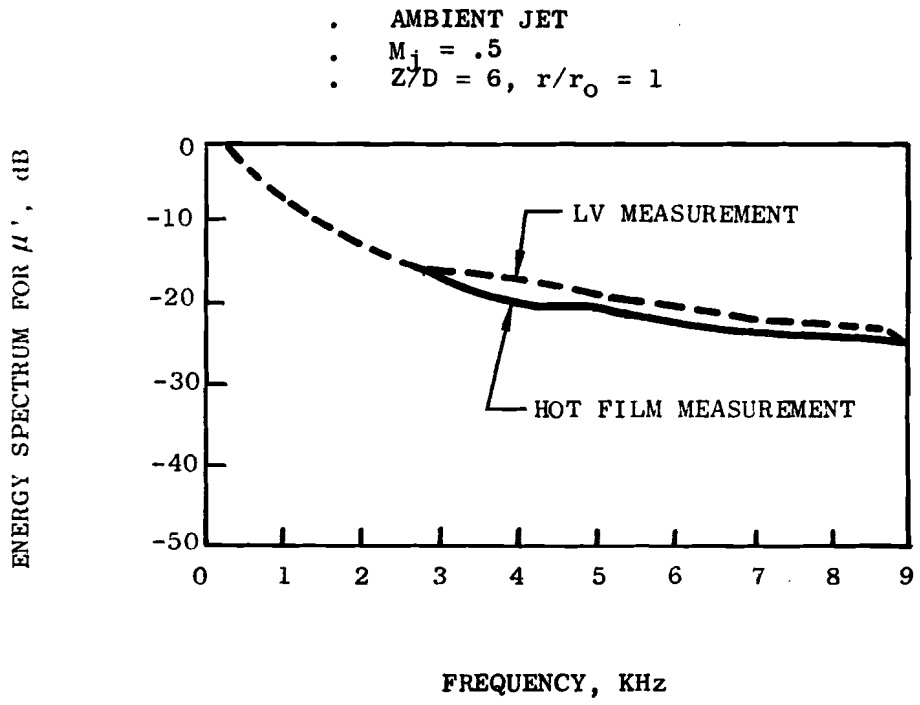

Figure 39 Axial Turbulence Spectrum in a Shear Layer

(c) The volume of turbulence seen by the tone is proportional to the shear layer width,

$$V \propto b \tag{4-13}$$

The results of exercising equation (4-4) parametrically for the distance between fan and core exhaust planes, incident tone frequency and jet velocity are provided in Figures 40 through 42. In addition, the spectral distribution for three different velocities is shown in Figure 43. The spectra were obtained using the $\langle M_t \rangle$ term only from equation (4-1), along with $\theta = 0$. The absolute trends indicated by these figures are, of course, limiting values since the scattering experienced is due to two shear layers (core and fan).

The computer program used in this study is given in Appendix B.

4.3 DISCUSSION

Figures 40 through 42 indicate that

$$\Delta_5^\circ \sim 40\log(1+L/D_o) + 40\log(f_o) + 40\log(V_{fan})^n \tag{4-14}$$

where f_o = incident tone frequency
and $n = 0.8$ for $V_{fan} < 300$ ft/sec (91 m/sec) rising to 1.0 for $V_{fan} = 1000$ ft/sec (305 m/sec).

It was noted earlier that source distribution effects are lost from Δ_5°, due to the $\theta = 0$ assumption in equation (4-4), and must be entered separately to arrive at the observed amplitude loss. For example, the turbulence energy spectral distribution at once reduces the frequency dependence in (4-14) to $20\log_{10}(f_o)$. In addition, there is also a damping effect on the other two terms in (4-14).

Consideration of α and η in equation (4-3) suggests that the source distribution is approximated by $\exp\,[(-\eta^2\alpha^2)/(1+\alpha^2)^2]$.

But $\eta = \omega_o/\omega_c$

$$\alpha = \frac{\omega_c \ell_c}{c} \propto \frac{V_{phase}}{c} \propto \frac{V_{fan}}{c}$$

and $\eta\alpha = \dfrac{\omega_o \ell_c}{c}$

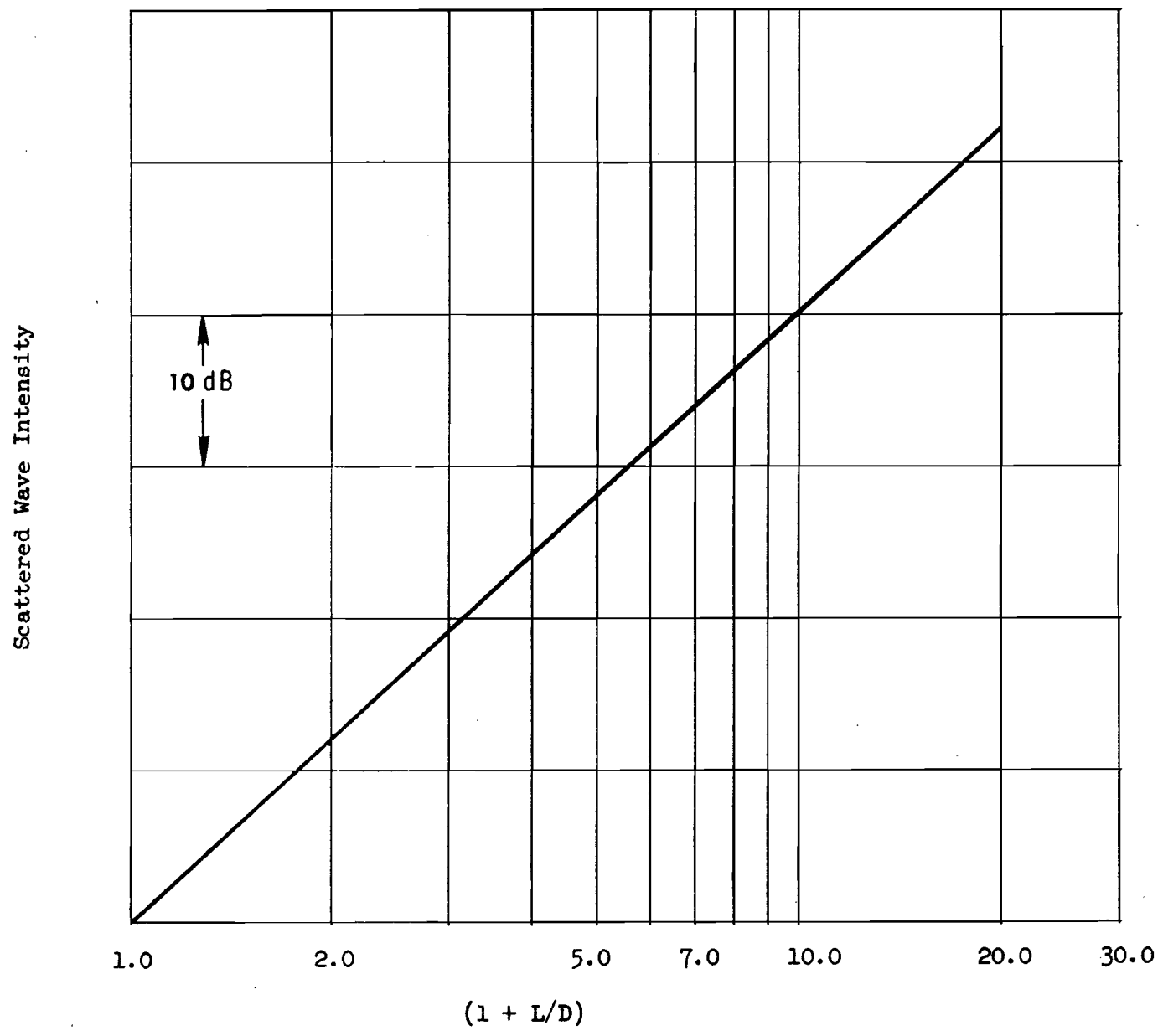

Figure 40 Intensity Variation with Nozzle Exhaust Plane Separation Distance

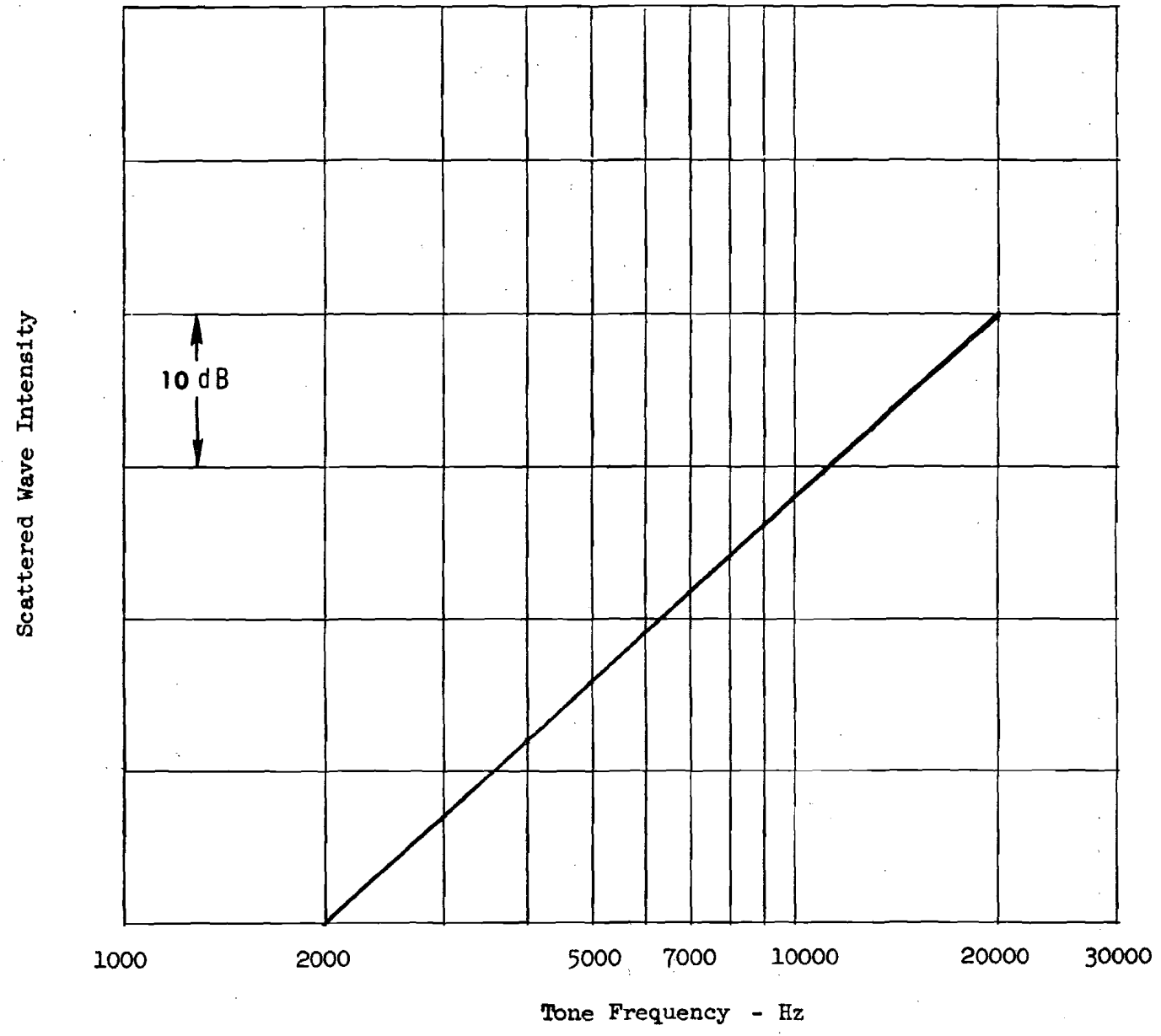

Figure 41 Intensity Variation with Tone Frequency

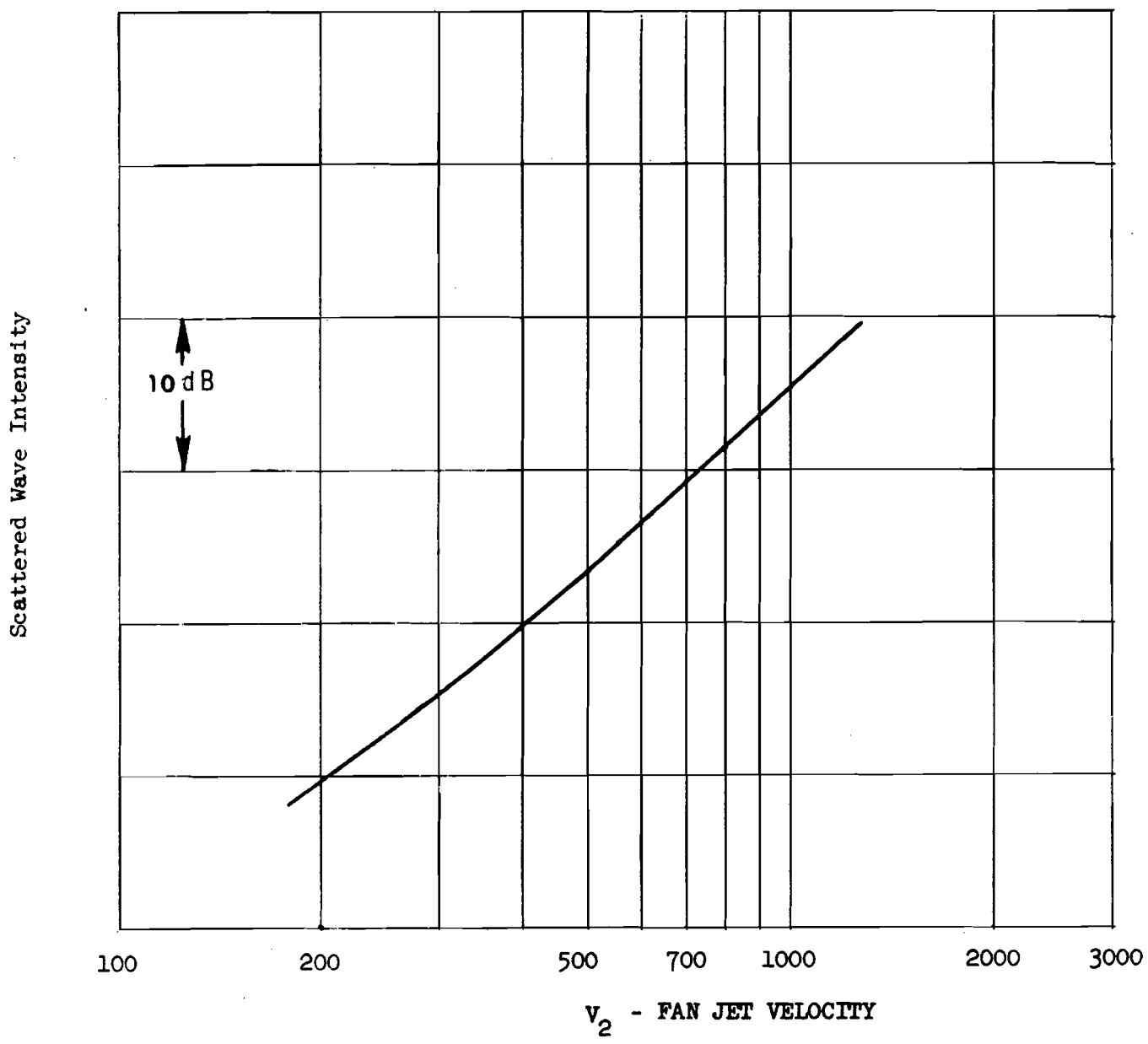

Figure 42 Intensity Variation with Fan Jet Velocity

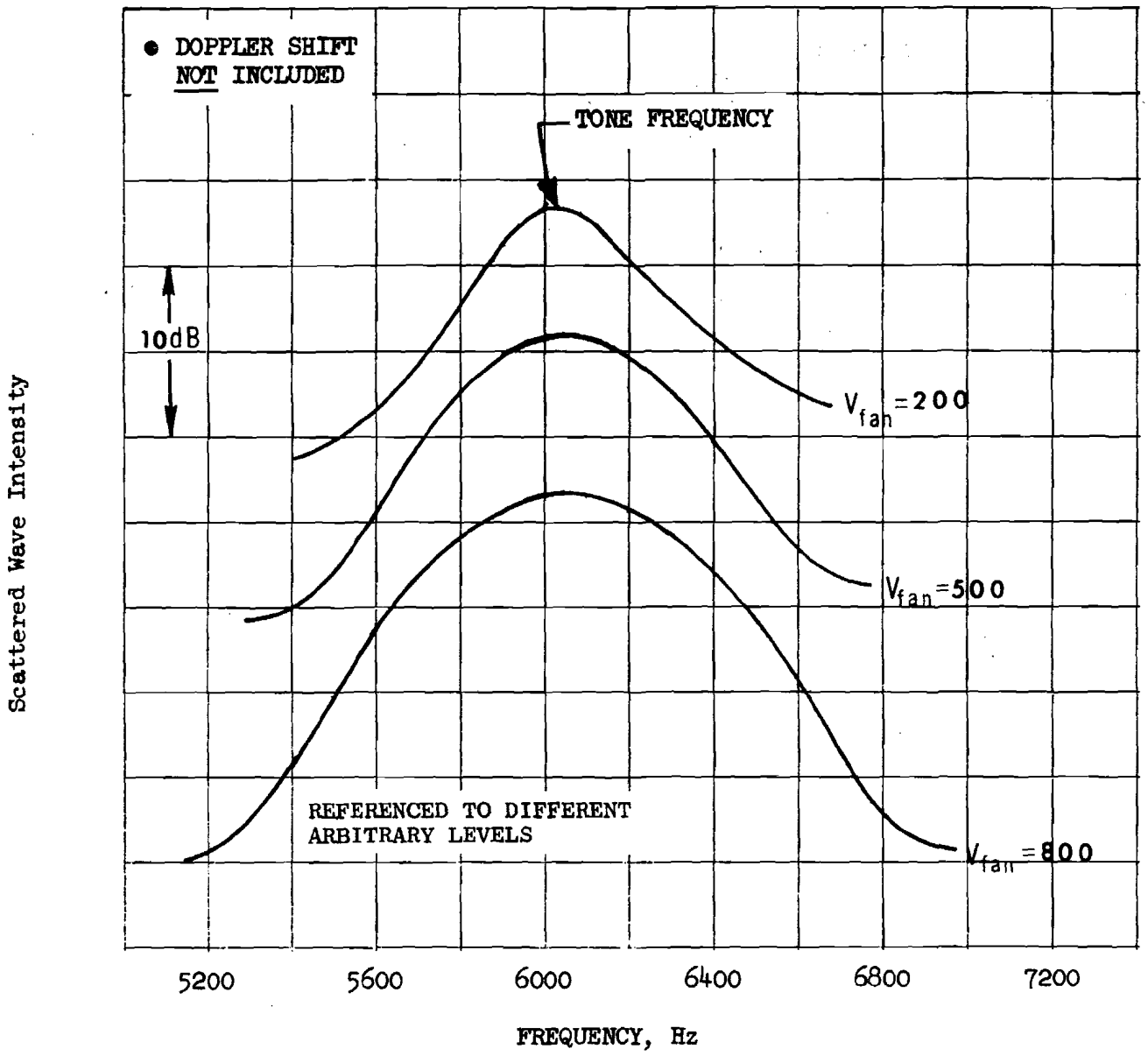

Figure 43 Wave Intensity Spectral Distribution

When these source effects are superimposed on equation (4-14), we get

$$\Delta_5^\circ - 20\log_{10}(1+L/D_o) + 20\log_{10}(f_o) + 20\log_{10}(V_{fan})^{2n-1} \qquad (4\text{-}15)$$

The prediction method includes all the turbulence parameters that are necessary to describe the shear layer. The eddy size and shear layer thickness are both functions of the distance between fan and core nozzle exhaust planes and thus are represented by the $(1+L/D_o)$ term. Similarly, the turbulence Mach number is represented by the jet velocity. Equation (4-15) then provides a rank ordering of the pertinent parameters.

The variable dependence on V_{fan} is predicated on the turbulence intensity remaining constant, that is on the turublence velocity varying linearly with the jet velocity. It remains to be demonstrated whether this actually occurs.

In the prediction method given in Volume III, Section 5, the amplitude loss δ is obtained by:

$$\delta = 20\log_{10}(1+ \frac{L}{D_{fan}}) + 40\log(\frac{V_{fan}}{100})-25 \qquad (4\text{-}16)$$

A frequency dependence could not be included because of the limited amount of data available. However, a $20\log_{10}(f_o)$ correction was suggested based on the classical results of Tatarski (Reference 11). Since V_{fan} and f_o demonstrate a linear dependence on each other, the $(40\log V_{fan})$ term in (4-16) could be taken as $(20\log V_{fan} + 20\log f_o)$. The amplitude losses Δ_5 and δ are equivalent parameters, and therefore the analytic and empirical formulations are seen to be in very good agreement. However the following changes are indicated:

(a) the frequency dependence should be entered $20\log_{10}(f_o/8000)$ since data used in the Volume III correlation centered around a mean frequency of 8000 Hz.

(b) The non-dimensionalizing parameter D_{fan} should be replaced by a constant D_o [6 ft (1.83 m)].

The prediction method provides for increasing frequency spread with δ. The same trends are indicated by equation (4-1), as can be seen from consideration of the various terms. The variation with jet velocity is given in Figure 43. The three scattered wave spectra [for V_{fan} = 200, 500 and 800 ft/sec, (61, 152 and 244 m/sec)2 are referenced to different arbitrary levels in order to demonstrate the variation in the spreading.

In addition, the spectra must be frequency shifted to properly account for the mean motion of the turbulence cells. The scattering equation was derived for zero mean flow velocity, which corresponds to working in a

coordinate system convecting with the local stream velocity in the region of interest. In order to transform the results back to the stationary coordinate frame, a shift must be imposed on the scattered wave. The incident wave is shifted twice - once into the moving coordinate system, and then once out of it, and the transformations are mutually off setting. The calculated and observed frequency shifts for Engine 'A' at approach power are shown in Figure 44.

The analysis indicates minimal effect of velocity ratio and area ratio variations as long as the outer shear layer controls the interaction. Just as obviously, the interaction (haystacking) will be reduced by motion of the ambient surrounding air. The effect can be accounted for by appropriate amendment to the shear layer thickness equation (Reference 5):

$$b = .21\ (Z - Z_o)\ \left(\frac{1-\zeta}{1+\zeta}\right) \qquad (4\text{-}17)$$

where $\zeta = \dfrac{\text{velocity of ambient air}}{\text{velocity of fan stream}}$

The assumptions made in the analysis would appear to define the limits of applicability of the prediction method. Since the tone was assumed to propogate through Regime I, then L is obviously limited:

$$L < \left(\frac{D_{fan} - D_{core}}{.21}\right)$$

The variable dependency of Δ_5^o on V_{fan} suggests applying the prediction equation (4-15) to fan velocities below 1200 ft/sec (305 m/sec) only. Above this, the amplitude loss could be higher than given by (4-15)

The scattering analysis is valid only for tone frequencies such that $\lambda \gtrsim \ell_c$. For frequencies above this, geometrical optics must be applied.

The Green's function used to obtain the scattering term was simplified for far-field conditions, that is $k_i r >> 1$. Also, since the Born approximation was considered valid, γ_κ, γ_ρ and M_t must be small, say less than 0.2.

4.4 CONCLUSIONS

The parametric study of the analytic model suggests the following:

(a) The amplitude loss of the incident tone intensity will vary as $20 \log_{10} (1 + L/D_o)$, $20 \log_{10} (f_o)$ and approximately $20 \log_{10} (V_{fan})$, increasing with all three.

(b) The observed frequency spread will increase with amplitude loss.

(c) The effect of area ratio and velocity ratio will be minimal for large L, when the interaction effect is controlled by the outer shear layer.

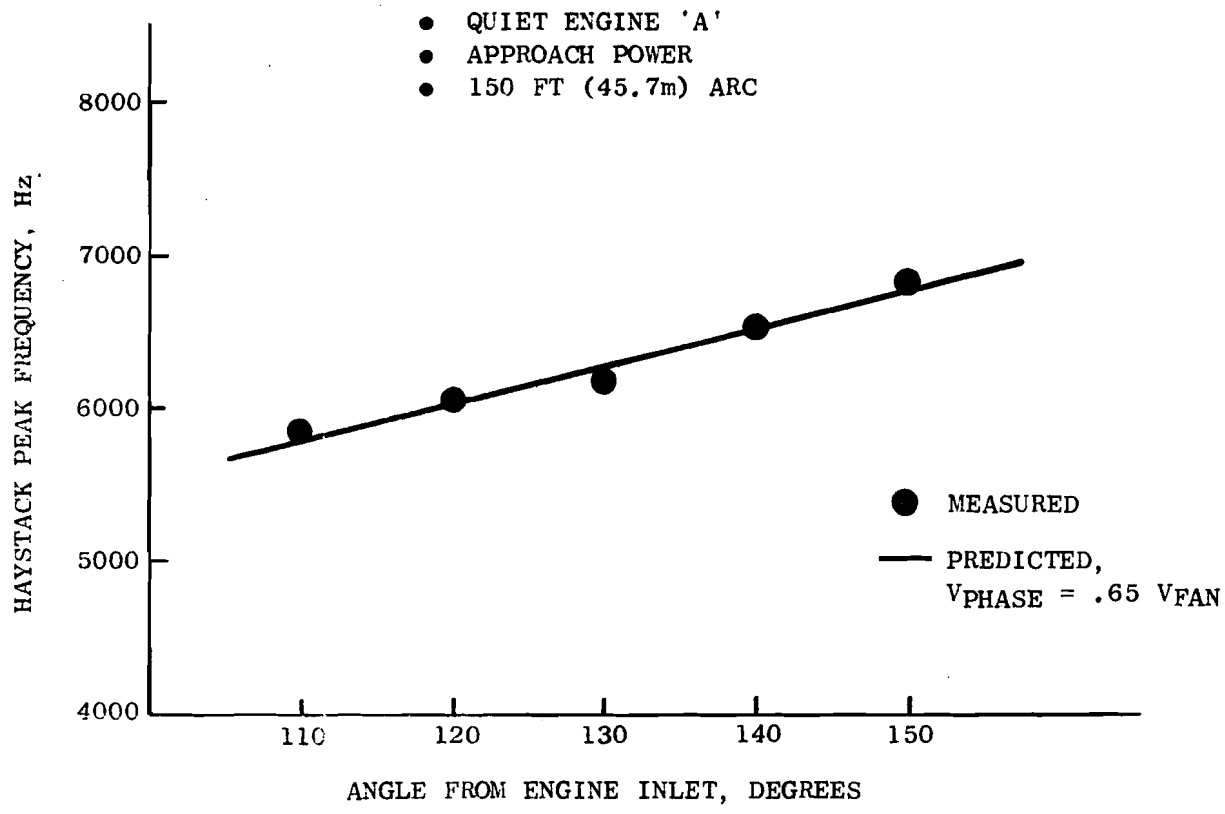

Figure 44 Comparison of Observed and Predicted Haystack Peak Frequency Shift

(d) The scattered wave will exhibit a Doppler shift. The pertinent velocity is the local mean stream velocity.

(e) The haystacking will be reduced inflight by roughly 20 log $[1-\zeta)]$ $(1+\zeta)]$ where ζ is the ratio of flight velocity to fan jet velocity.

4.5 PREDICTION UPDATE

A prediction method was evolved in Volume III, Section 5, using data from Engine 'C' and TF34. The amplitude loss (δ) of the incident tone was determined as a function of V_{fan} and L/D_{fan} and the frequency spread then followed as a function of δ:

$$\delta = 40\log_{10}(V_{fan}/100) + 20\log_{10}(1+L/D_{fan}) - 25 \qquad (4\text{-}16)$$

where δ = drop in 20 Hz narrow-band SPL at 120°, dB

V_{fan} = fan velocity, ft/sec

L = distance between fan and core nozzle exhaust planes, ft.

D_{fan} = fan nozzle exit diameter (outer), ft.

m = slope of haystack sides on a 20 Hz bandwidth spectrum

The data were too limited to yield a separate frequency correction, but a $20\log_{10}(f_o)$ correction was suggested based on the classical works of Tatarski (Reference 11) on turbulence scattering. The parametric study has now provided corroborating evidence as to the frequency effect and the correction is formally entered into equation (4-16) through $20\log_{10}(f_o/8000)$. The normalizing frequency, 8000 Hz, is the mean frequency of the data used in deriving equation (4-16). At the same time, the V_{fan} dependence is reduced to $20\log V_{fan}$ since V_{fan} and f_o demonstrate a linear inter-relationship for engines. All this uses is the fact that the data of Volume III could be fitted equally well by $(20\log V_{fan} + 20\log f_o)$ or by $(40\log V_{fan})$. However, the former is now chosen because of the analytical justification.

The fan nozzle diameter was used as a convenient non-dimensionalizing parameter. The shear layer model of Section 4.2 suggests that the D_{fan} dependence will be very weak, for coplanar exhaust configurations, appearing only in the virtual origin term, Z_o. Whether this diameter becomes a consideration for staggered plane exhausts remains to be seen. The coefficient for the L/D_{fan} term in equation (4-16) was actually determined from consideration of coplanar and a staggered exhaust plane configuration of Engine 'C', hence the D_{fan} <u>was</u> a constant [= 6 ft. (1.83 m.)] in the derivation. The physical geometries of the TF34 and Engine 'C' are sufficiently similar and the data scatter large enough to allow D_{fan} to be 6 ft. (1.83 m.) for the entire correlation. Therefore the $(1 + L/D_{fan})$ term can be replaced by $(1 + L/6)$.

The frequency spread equation (4-18) is being kept the same, as the parametric study does not suggest any obvious changes.

The updated prediction method is then given by:

$$\delta = 20\log_{10}(V_{fan}/100) + 20\log_{10}(1+L/6) + 20\log_{10}(f_o/8000)-25 \quad (4\text{-}18)$$

$$\text{and} \quad 10\log\,(1/m) = 0.85\delta + 8.4 \quad (4\text{-}19)$$

where V_{28} is in ft/sec., L in ft. and f_o in Hz. The amplitude drop (δ) and frequency spread term (m) are defined in Figure 45.

A flow chart for using this prediction method is provided in Figure 46.

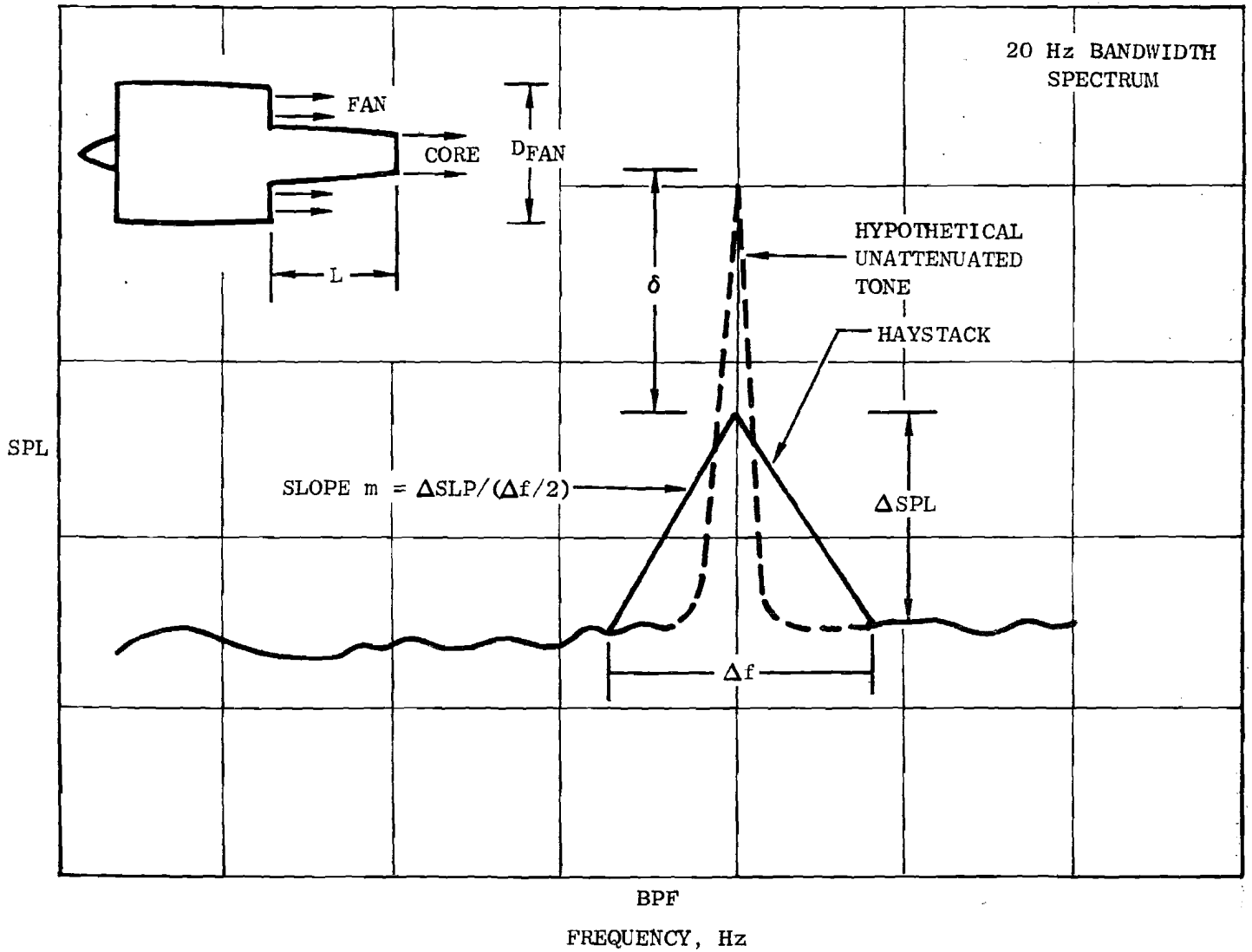

Figure 45 Definition of Interaction Effects

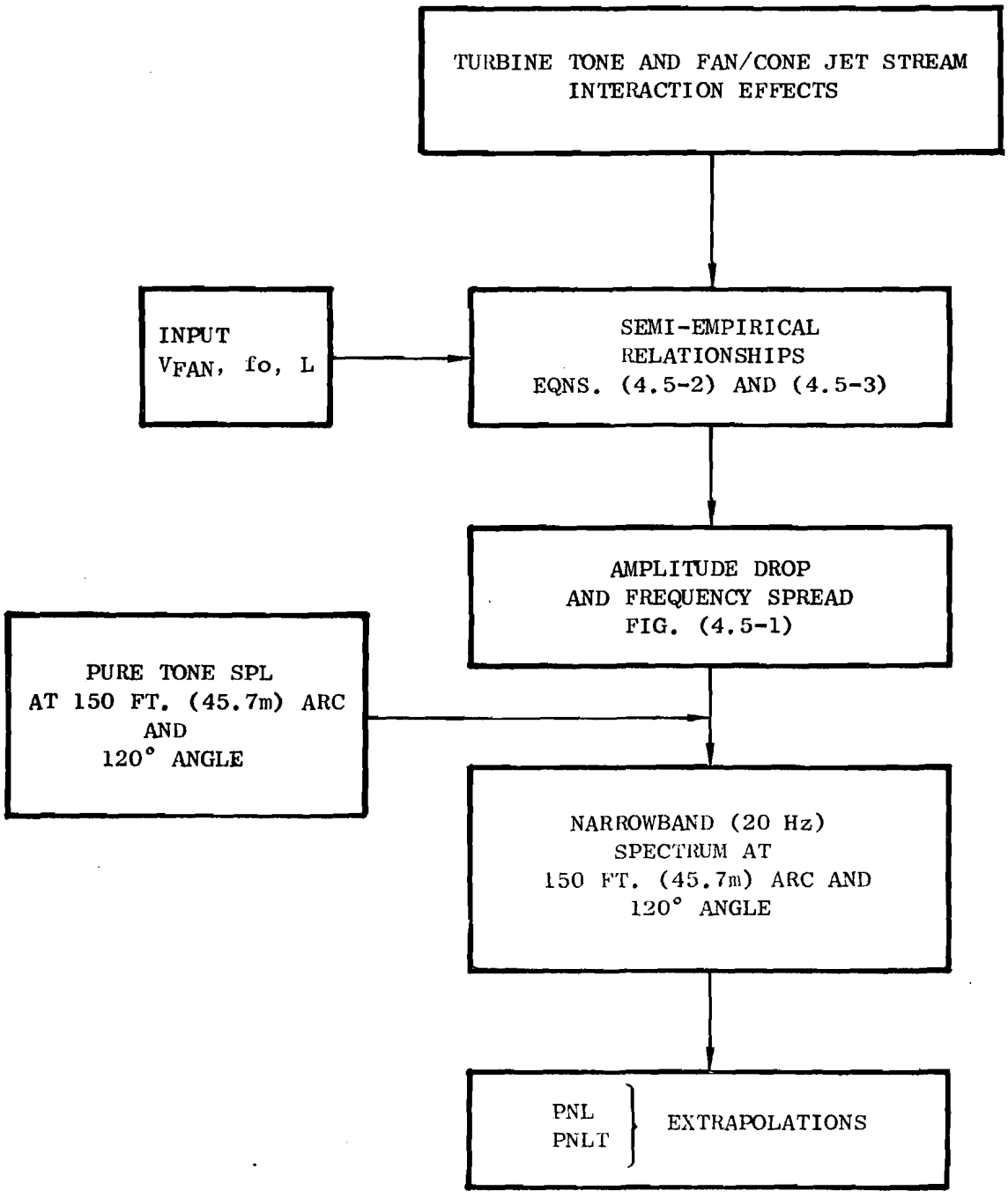

Figure 46 Flow Chart for Estimating Turbine Tone Interaction Effects

REFERENCES

1. Mani, R., "Discrete Frequency Noise Generation from an Axial Fan Blade Row," ASME Paper No. 69-FE-12, 1969.

2. Morfey, C.L., "Rotating Pressure Patterns in Ducts: Their Generation and Transmission," J. Sound Vibra. I, 1964.

3. Motsinger, R.E., Kraft, R.E., and Zwick, J.W., "Design of Optimum Acoustic Treatment for Rectangular Ducts with Flow," to be published as an ASME Paper, International Gas Turbine Conference, 1976.

4. Hoch, R., Thomas, P. and Weiss, E., "An Experimental Investigation of the Core Engine Noise of a Turbofan Engine," AIAA Paper No. 75-526, 1975.

5. Matthews, D.C., and Peracchio, A.A., "Progress in Core Engine and Turbine Noise Technology," AIAA Paper No. 74-928, 1974.

6. Fitremann, J.M., and Ffowcs-Williams, J.E., "Spectral Broadening and Variability of Discrete Turbine Tones Propagating Through Unsteady Flow," University of Cambridge, 1974.

7. Howe, M.S., "Multiple Scattering of Sound by Turbulence and Other Inhomogeneities," J. Sound Vibr. 27, 4, p. 455, 1973.

8. Hammersley, R.J., "An Experimental Investigation of the Turbulent Characteristics of Coannular Jets and their Role in Aerodynamic Noise Generation," PhD Thesis, Nucleur Energy Program, University of Illinois at Urbana-Champaign, Urbana, 1974.

9. Ollerhead, J.B., "On the Prediction of Nearfield Noise of Supersonic Jets," NASA CR-857, 1967.

10. Kolpin, M.A., "Velocity Correlation Measurements in the Mixing Region of a Jet," AGARD Fluid Dynamic Meeting, Report 452, 1963.

11. Crow, S.C. and Champagne, F.H., "Orderly Structure in Jet Turbulence," J. Fluid Mechanics, 48, 3, p. 547, 1971.

12. Knott, P.R., "Supersonic Jet Exhaust Noise Investigation, Volume I - Summary Report," General Electric, Final Report under Air Force Contract Number F33615-73-C-2031, to be published.

13. Hinze, J.O., Turbulence, McGraw Hill, New York, 1959.

14. Tatarski, V.I. Wave Propagation in a Turbulent Medium, transl. from the Russian by R.A. Silverman, Dover Publications, Inc., New York, 1967.

APPENDIX A

ANALYTIC TURBINE TONE PREDICTION

The equations for predicting viscous wake interaction noise in turbines have been programmed and the coding in FORTRAN Y is provided here. The logical flow in the program, TURBINE AERODYNAMICALLY INDUCED NOISE (TAIN), is shown in Figure A-1.

The program has been updated to include leaned vane capability.

Input - The variables required are shown in Table A-1, and an input preparation sheet is provided in Table A-2. This sheet includes a brief explanation for each input variable required. As is noted on input sheet three following the variable DELLAM, if the user wishes to input eigenvalues (λ_{nm}) they should be included in the data deck at this point. To facilitate this process, eigenvalues (LAMBAY (I,J)) and associated coupling coefficients (QAY (I,J)) are output on punched cards in NAMELIST format each time they are calculated within a data case. When the program is initiated, the geometric and aerodynamic parameters are read in from cards and immediately displayed.

Preliminary Calculations - Absolute velocities, relative velocities, chords and phase angles are determined from the input geometric and aerodynamic parameters. Optional calculations include lobe numbers, number of radial inflexions per lobe number, and drag coefficients.

Unsteady Force Distribution - The unsteady circulation generated by viscous wake interaction is computed at discrete radial stations and curve-fitted over the blade span.

Generation Analysis - The various circumferential lobe numbers and associated radial modes are computed internally if not input. The lobe numbers are limited to 100 as the energy transmission decreases with increasing lobe number. The Fourier coefficients for the acoustic pressure are determined for each radial and circumferential mode and the energy summed incoherently to yield the total acoustic energy in the BPF.

Output - The following are printed out:

(i) All input data

(ii) Data common to all generating mechanisms

- Lobe numbers
- Number of rotating line sources
- Chords
- "Drag" coefficients, (pressure loss coeff/solidity)

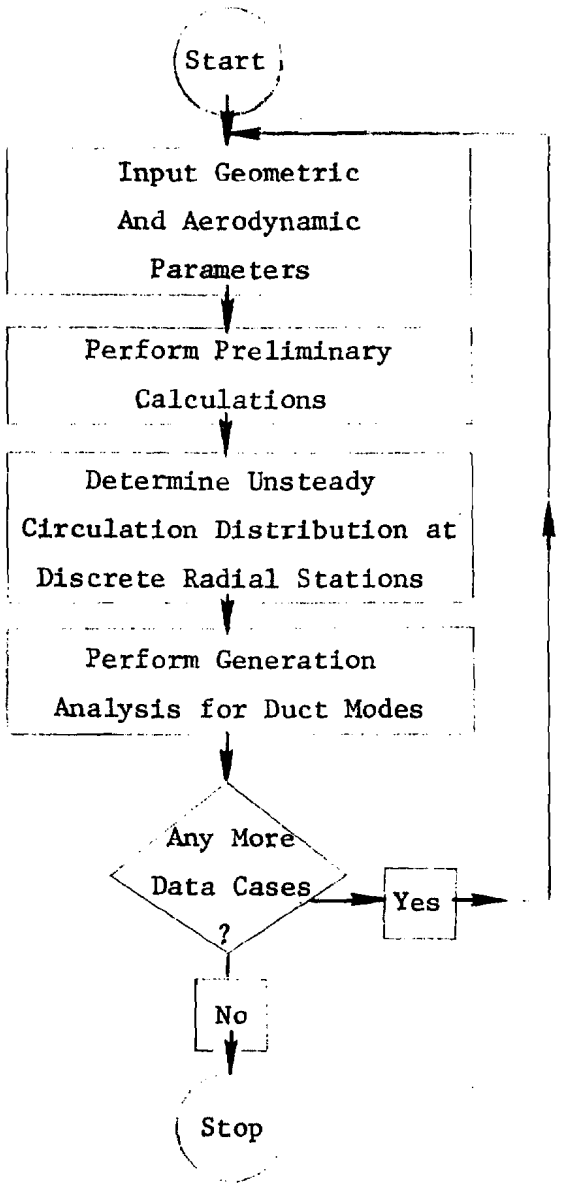

Figure A-1. Flow Chart for TAIN.

TABLE A-1

INPUT PARAMETERS FOR TAIN IV

- The pitch value is required for the following parameters:

  Number of Rotor Blades

  Number of Nozzle Blades

  Speed (rpm)

  Mean Static Pressure (lb/ft^2)

  Mean Static Temp. (° R)

  Trailing edge thickness of upstream blade (in.)

- The values of the following parameters are required for at least three radial stations (hub, pitch, tip). However up to five radial stations may be input. Figure A-2 defines angle sign convention.

  α_h - Physical lean

  β_{1A} - Absolute angle at inlet to upstream row

  β_{1R} - Relative angle at inlet to upstream row

  β_{2A} - Absolute angle
  β_{2R} - Relative angle } at exit from upstream row or at inlet to downstream row

  β_{3A} - Absolute angle at exit from downstream row

  β_{3R} - Relative angle at exit from downstream row

  Mean Radius (in.)

  Upstream Blade Row Solidity

  Downstream Blade Row Solidity

- In addition, input of certain parameters is optional; if not input, they are computed internally.

  Circumferential lobe numbers

  Radial modes (inflexions)

  Profile loss coefficients

  Eigenvalues

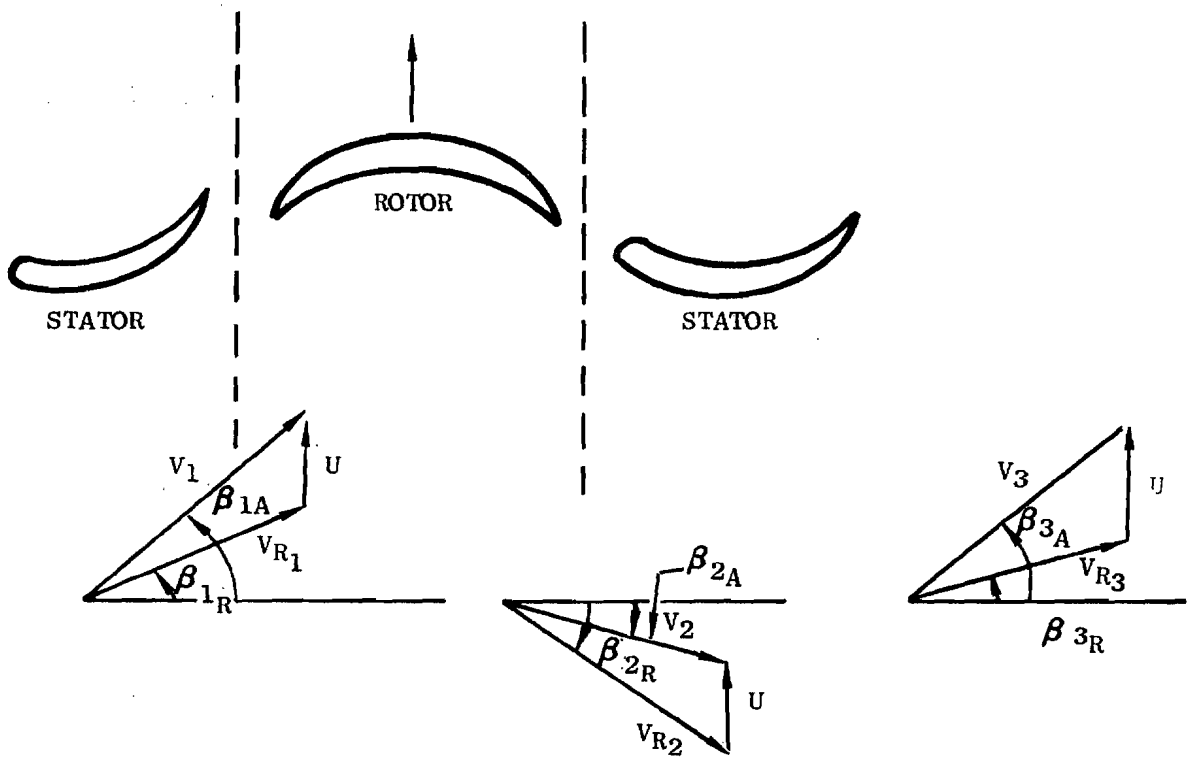

β_{1_A} +ve	β_{2_A} -ve	β_{3_A} +ve
β_{1_R} -ve	β_{2_R} +ve	β_{3_R} -ve

- Absolute Flow Angles are +ve in Direction of Rotation
- Relative Flow Angles are +ve Opposite Direction of Rotation
- Lean is +ve in Direction of Rotation

Figure A-2 Sign Convention for Flow Angles

TABLE A-2

INPUT SHEETS

TURBINE AERODYNAMICALLY INDUCED NOISE

Sept., 1975 | Page 1 of 3

GE Class II | TAIN | TAIN - IV

NAMELIST 1 of 3

```
$INPUT
  cash title
TITLE=60H____________________________________________________________
MODE=6H TURBIN,
     generating interaction
     IRVSWK    -    igv -rotor viscous wake
     ROVSWK    -    rotor-ogv viscous wake
IRVSWK or ORVSWK?
NMECH/MECH=6H______,
 hub radius    tip radius     no. of blades    no. of vanes
  -in-            -in-
HUBRAD=______,  TIPRAD=______,  NBLADE=______,  NVANES=______,
  wheel speed no of lobes harmonic no.
    -rpm-                    (1 for fundamental)
SPEED=______,  NLOBNO=______,  NHARM=______,
input lobe no.'s?
(true or false (T or F)), if true, enter lobe no.'s
INPLOB=____,  LOBNO=____, ____, ____, ____, ____,
input radial inflexions?
(T or F), # if true, enter radial inflextion no.'s
INPNIN=____,      INFLEC=____, ____, ____, ____, ____,
static pressure   static temperature   trailing edge thickness
-lbf/ft^2           -° R-                    -in-
PSTAT=_____,      TSTAT=_____,         TET=_____,
```

TABLE A-2 (Continued)

vane lean?
(T or F)
FLEAN1=_____, EFLEAN= F ,
radial output stations
-in-
NOPRAD/OPRAD=_____, _____, _____, _____, _____, _____, _____, _____,
_____, _____, _____, _____, _____, _____, _____, _____, _____,
radial stations at which aero data are given - first station must be hub
-in-
NRADP/RADTAB=_____, _____, _____, _____, _____,
enter the following for each radial station
physical lean for FLEANL=T only
-deg-
ALPHA=_____, _____, _____, _____, _____
upstream blade row absolute inlet angle
-deg-
BETA1A=_____, _____, _____, _____, _____,
r-o, rotor relative inlet angle
-deg-
BETA1R=_____, _____, _____, _____, _____,
i-r, rotor absolute inlet angle
r-o, rotor absolute exit angle
-deg-
BETA2A=_____, _____, _____, _____, _____,
i-r, rotor relative inlet angle
r-o, rotor relative exit angle
-deg-

TABLE A-2 (Continued)

BETA2R=_____, _____, _____, _____, _____,
i-r, rotor absolute exit angle
r-o, stator absolute exit angle
-deg-
BETA3A=_____, _____, _____, _____, _____,
i-r, rotor relative exit angle
-deg-
BETA3R=_____, _____, _____, _____, _____,
upstream blade row solidity
SIGMA1-_____, _____, _____, _____, _____,
downstream blade row solidity
SIGMA2=_____, _____, _____, _____, _____,
axial blade row spacing, trailing to leading edge
-in-
BP=_____, _____, _____, _____, _____, _____,
input upstream blade row loss coeffs? (T or F)
if true, input (pressure loss coefficient/σ_1)
INPCD1=_____, CD1=_____, _____, _____, _____, _____,
punch eigenvalues?
(T or F)
PUNCH=_____,
delete eigenvalue calculations?
(T or F)
DELLAN=_____,
insert prepunched eigenvalues here if available
$

_____ _____

INPUT additional cases as:
$ INPUT
variables that are changed
$_____ _____

(iii) Data for each interaction

- Unsteady circulation distribution
- Phase angles in radians (leaned vanes only)
- Data for each of the component modes

  Eigenvalue

  Residual associated with eigenvalue (This is the value of the characteristic function evaluated at the calculated eigenvalue and thus indicates the accuracy of the eigenvalue calculation. If eigenvalues are read from cards, the printed residuals do not apply).

  Cut-off speed

  Norm

  Amplitude

  Power

  Power level

  Radial distribution of pressure and pressure level

- Composite data for each lobe number summed over its radial modes (inflexions).

  Power

  Power level

  Radial distribution of pressure and pressure level

- Overall composite data summed over all lobe numbers.

  Power

  Power level

  Radial distribution of pressure and pressure level.

(iv) Eigenvalues and associated coupling coefficients on punched cards in NAMELIST format for future use if these quantities were calculated.

A typical output is shown in Table A-3.

```
*****************
INPUT DATA
*****************

CASE TITLE - NASA III TUR3 N2R2  BASE    PT. 3836

MECHANISM 1 IRVSWK

MODE        TURBIN   HUBRAD      8.900  TIPRAD     12.560  NBLADE       102  NVANES       108  SPEED      3677.
NLOBND           1   NHARM          1  PSTAT    1472.000  TSTAT   540.000  TET     0.020000  INPLOB         F
INPNIN           F   DELLAM         T  INPCD1          F  PUNCH         F  EFLEAN         F  FLEANI         T
NLEANI          20
DPRAD(1- 1)
          12.560
RADTAB(1-3)
           8.900          10.700          12.560
ALPHA(1-3)
           0.             0.              0.
BETA1A(1-3)
         -49.300         -44.800         -43.300
BETA1R(1-3)
          58.600          57.600          60.200
BETA2A(1-3)
          61.400          58.500          58.200
BETA2R(1-3)
         -54.200         -45.300         -36.500
BETA3A(1-3)
         -46.100         -40.000         -38.000
BETA3R(1-3)
          57.000          55.800          58.100
SIGMA1(1-3)
           1.910           2.050           2.130
SIGMA2(1-3)
           1.820           1.650           1.560
BP(1-3)
           0.370           0.330           0.290

*****************
OUTPUT DATA
*****************

                    CIRCUMFERENTIAL LOBES    ROTATING LINE SOURCES
                              6                        6

U/S BLADE ROW CHORD(IN)
           0.989           1.276           1.556
D/S BLADE ROW CHORD(IN)
           0.993           1.088           1.207
U/S BLADE ROW CD
           0.02753         0.01966         0.01724
```

****
MECHANISM 1 I-R VISCOUS WAKE
****

THETAF(I)

-0.0000	-0.0034	-0.0066	-0.0097	-0.0127	-0.0155	-0.0181	-0.0206	-0.0230	-0.0252
-0.0273	-0.0292	-0.0309	-0.0325	-0.0340	-0.0353	-0.0364	-0.0374	-0.0383	-0.0390

PHIR(I)

-0.0000	-0.0034	-0.0066	-0.0097	-0.0127	-0.0155	-0.0181	-0.0206	-0.0230	-0.0252
-0.0273	-0.0292	-0.0309	-0.0325	-0.0340	-0.0353	-0.0364	-0.0374	-0.0383	-0.0390

RL(I)

0.7085	0.7239	0.7393	0.7546	0.7699	0.7853	0.8006	0.8160	0.8313	0.8466
0.8620	0.8773	0.8926	0.9080	0.9233	0.9387	0.9540	0.9693	0.9847	1.0000

AK(I)

0.	0.	0.	0.	0.	0.3198	-0.6762	0.3174	0.	0.

ALPCOE(I)

0.	0.	0.

UNSTEADY CIRCULATION DISTRIBUTION

RADIUS RATIO	CIRCULATION(FT**2/SEC)
0.709	0.2724E 00
0.852	0.2693E 00
1.000	0.2545E 00

COMP	MODE	EGNVAL	RESIDUAL	C/O SPD (RPM)	NORM	AMP	POWER (FT*LBF/SEC)	PWL (DB)	RADR	RADIUS (IN)	PRES (PSF)	SPL (DB)
1	6, 0	7.001	0.	713.	0.3077E-01	0.2604E-04	0.2194E 00	124.74	1.000	12.56	0.5308E 00	122.08
2	6, 1	19.097	0.	1945.	0.1640E-01	0.2260E-04	0.3103E-01	116.24	1.000	12.56	0.2454E 00	115.38
3	6, 2	22.743	0.	2317.	0.8539E-02	0.4091E-04	0.1503E 00	123.09	1.000	12.56	0.5156E 00	121.83
4	6, 3	23.943	0.	2439.	0.4177E-01	0.1581E-04	0.8660E-01	120.70	1.000	12.56	0.3823E 00	119.23
RADIAL COMPOSITE LOBE NO 6							0.4874E 00	128.20	1.000	12.56	0.1674E 01	132.06
OVERALL COMPOSITE							0.4874E 00	128.20	1.000	12.56	0.1674E 01	132.06

PROC TIME = 0 MIN 5 SEC

"TAIN" PROGRAM LISTING

```
$       FORTRAN DECK,MAP                                                TAIN
$       INCODE  IBMF
CTAIN        TAIN - TURBINE AERODYNAMICALLY INDUCED NOISE
C
      CALL INPUT1
    5 CALL INPUT2
      CALL CYCMCH
      GO TO 5
      END
$       FORTRAN DECK,MAP,XREF                                           INPUT
$       INCODE  IBMF
CINPUT       INPUT ROUTINE
C               FORTRAN-Y       22APR1975
C
      SUBROUTINE INPUT1
      COMMON/INPBLK/TITLE(10),MODE,MECH(5),NMECH,HUBRAD,TIPRAD,NBLADE,
     1 NVANES,SPEED,INPLOB,LOBNO(5),NLOBNO,INPNIN,INFLEC(5),NHARM,PSTAT,
     2 TSTAT,TET,DELLAM,LAMBAY(20,5),QAY(20,5),OPRAD(20),NOPRAD,NRADP,
     3 RADTAB(5),BETA1A(5),BETA1R(5),BETA2A(5),BETA2R(5),BETA3A(5),
     4 BETA3R(5),SIGMA1(5),SIGMA2(5),BP(5),INPCD1,CD1(5),PUNCH
     5 ,EFLEAN,ALPHA(5),C,LAMBDA(10,5),RHO,GAM,DYVISC
      LOGICAL INPLOB,INPNIN,DELLAM,INPCD1,PUNCH
      LOGICAL EFLEAN
      COMPLEX LAMBDA
      REAL LAMBAY
      COMMON/IYRBLK/IYR
      DIMENSION NAME(10),ADDRES(10),IDENT(10)
      DIMENSION CATS(10)
      DIMENSION INTIT(10)
      LOGICAL EOF
      COMMON /CLEAN1/ FLEAN1,NLEAN1,RL(20)
      LOGICAL         FLEAN1
      NAMELIST/CO/NBR/ID/NAME,ADDRES,IDENT
      NAMELIST/INPUT/TITLE,MODE,MECH,NMECH,HUBRAD,TIPRAD,NBLADE,NVANES,
     1 SPEED,INPLOB,LOBNO,NLOBNO,INPNIN,INFLEC,NHARM,PSTAT,TSTAT,TET,
     2 DELLAM,LAMBAY,QAY,OPRAD,NOPRAD,NRADP,RADTAB,BETA1A,BETA1R,
     3 BETA2A,BETA2R,BETA3A,BETA3R,SIGMA1,SIGMA2,BP,INPCD1,CD1,PUNCH
     4 ,EFLEAN,ALPHA,LAMBDA,FLEAN1,NLEAN1
      DATA CATS/6H1900DE,6HE/USER,8*1H /
      DATA INTIT(1)/60H*          TAIN NAMELIST        *
     1            /
      CALL NLISTW(INTIT)
      CALL FXOPT(66,1,0,0)
      CALL FXOPT(67,1,1,0)
      CALL FLGEOF(5,EOF)
      CALL WRAP($10)
      CALL CLOCK(DUMY,DUMY,IMON,IDAY)
      IDATE = IYR+100*IDAY+10000*IMON
      READ(5,ID)
      WRITE(6,900) IDATE,NAME,ADDRES,IDENT
  900 FORMAT(1H1,51X,23H    T    A    I    N    /
     1            11HRUN DATE-I6////
     2            45X,10A6//45X,10A6//45X,10A6)
```

```
      GO TO 5

      ENTRY INPUT2
      READ(5,INPUT)
      IF(EOF) GO TO 100
      WRITE(6,905) TITLE,(I,MECH(I),I=1,NMECH)
905   FORMAT(1H1,51X,3(6H******)/56X,10HINPUT DATA/52X,3(6H******)///
     1 18X,13HCASE TITLE - 10A6//47X,10HMECHANISM I1,1X,A6/
     2 (57X,I1,1X,A6))
      WRITE(6,910) MODE,HUBRAD,TIPRAD,NBLADE,NVANES,SPEED,NLOBNO,NHARM,
     1 PSTAT,TSTAT,TET,INPLOB,INPNIN,DELLAM,INPCD1,PUNCH,EFLEAN
     2,FLEAN1,NLEANI
910   FORMAT(/5X,4HMODE,7X,A6,2X,6HHUBRAD,1X,F10.3,2X,6HTIPRAD,1X,F10.3,
     1 2X,6HNBLADE,1X,I10,2X,6HNVANES,1X,I10,2X,5HSPEED,2X,F10.0/
     2 5X,6HNLOBNO,1X,I10,2X,5HNHARM,2X,I10,2X,5HPSTAT,2X,F10.3,2X,
     3 5HTSTAT,2X,F10.3,2X,3HTET,4X,F10.6,2X,6HINPLOB,1X,L10/
     4 5X,6HINPNIN,1X,L10,2X,6HDELLAM,1X,L10,2X,6HINPCD1,1X,L10,2X,
     5 5HPUNCH,2X,L10,2X,6HEFLEAN,1X,L10,2X,6HFLEAN1,1X,L10/,5X,
     6 6HNLEANI,1X,I10/)
      IF(INPLOB) WRITE(6,915) NLOBNO,(LOBNO(I),I=1,NLOBNO)
915   FORMAT(5X,8HLOBNO(1-I1,1H)/3X,5(9X,I10))
      IF(INPNIN) WRITE(6,920) NLOBNO,(INFLEC(I),I=1,NLOBNO)
920   FORMAT(5X,9HINFLEC(1-I2,1H)/3X,5(9X,I10))
      IF(NOPRAD.GT.0) WRITE(6,925) NOPRAD,(OPRAD(I),I=1,NOPRAD)
925   FORMAT(5X,8HOPRAD(1-I2,1H)/(3X,6(9X,F10.3)))
      WRITE(6,930) NRADP,(RADTAB(I),I=1,NRADP)
930   FORMAT(5X,9HRADTAB(1-I1,1H)/3X,5(9X,F10.3))
      WRITE(6,931)  NRADP, (ALPHA(I),I=1,NRADP)
931   FORMAT(5X,8HALPHA(1-I1,1H)/3X,5(9X,F10.3))
      WRITE(6,935) NRADP,(BETA1A(I),I=1,NRADP)
935   FORMAT(5X,9HBETA1A(1-I1,1H)/3X,5(9X,F10.3))
      WRITE(6,940) NRADP,(BETA1R(I),I=1,NRADP)
940   FORMAT(5X,9HBETA1R(1-I1,1H)/3X,5(9X,F10.3))
      WRITE(6,945) NRADP,(BETA2A(I),I=1,NRADP)
945   FORMAT(5X,9HBETA2A(1-I1,1H)/3X,5(9X,F10.3))
      WRITE(6,950) NRADP,(BETA2R(I),I=1,NRADP)
950   FORMAT(5X,9HBETA2R(1-I1,1H)/3X,5(9X,F10.3))
      WRITE(6,955) NRADP,(BETA3A(I),I=1,NRADP)
955   FORMAT(5X,9HBETA3A(1-I1,1H)/3X,5(9X,F10.3))
      WRITE(6,960) NRADP,(BETA3R(I),I=1,NRADP)
960   FORMAT(5X,9HBETA3R(1-I1,1H)/3X,5(9X,F10.3))
      WRITE(6,965) NRADP,(SIGMA1(I),I=1,NRADP)
965   FORMAT(5X,9HSIGMA1(1-I1,1H)/3X,5(9X,F10.3))
      WRITE(6,970) NRADP,(SIGMA2(I),I=1,NRADP)
970   FORMAT(5X,9HSIGMA2(1-I1,1H)/3X,5(9X,F10.3))
      WRITE(6,975) NRADP,(BP(I),I=1,NRADP)
975   FORMAT(5X,5HBP(1-I1,1H)/3X,5(9X,F10.3))
      IF(INPCD1) WRITE(6,980) NRADP,(CD1(I),I=1,NRADP)
980   FORMAT(5X,6HCD1(1-I1,1H)/3X,5(9X,F10.5))
    5 RETURN
100   CONTINUE
   10 CALL USELOG(6HF10051,6HTAIN 4,CATS)
      STOP
      END
```

```
$       FORTRAN DECK,MAP,XREF                                           BLKDAT
$       INCODE  IBMF
CBLKDAT      BLOCK DATA
C                FORTRAN-Y       22APR1975
      BLOCK DATA
      COMMON/INPBLK/TITLE(10),MODE,MECH(5),NMECH,HUBRAD,TIPRAD,NBLADE,
     1 NVANES,SPEED,INPLOB,LOBNO(5),NLOBNO,INPNIN,INFLEC(5),NHARM,PSTAT,
     2 TSTAT,TET,DELLAM,LAMBAY(20,5),QAY(20,5),OPRAD(20),NOPRAD,NRADP,
     3 RADTAB(5),BETA1A(5),BETA1R(5),BETA2A(5),BETA2R(5),BETA3A(5),
     4 BETA3R(5),SIGMA1(5),SIGMA2(5),BP(5),INPCD1,CD1(5),PUNCH
     5 ,EFLEAN,ALPHA(5),C,LAMBDA(10,5),RHO,GAM,DYVISC
      COMPLEX LAMBDA
      LOGICAL INPLOB,INPNIN,DELLAM,INPCD1,PUNCH
      LOGICAL EFLEAN
      REAL LAMBAY
      COMMON/PRCBLK/NRLSAY(5),RADRTB(5),OPRR(20),AK(10),
     1 RHUB,ALPCOE(3),GPRM1,GONE
      COMMON/IYRBLK/IYR
      COMMON /CLEAN1/ FLEAN1,NLEANI,RL(20)
      LOGICAL         FLEAN1
      DATA FLEAN1,NLEANI/F,20/
      DATA MODE/6HCOMPRE/
      DATA INPLOB,INPNIN,DELLAM,INPCD1/4*.FALSE./
      DATA NHARM,C,RHO,GAM,NOPRAD/0,1116.89,0.076475,1.4,0/
      DATA PSTAT,TSTAT/2116.,519./
      DATA PUNCH/.TRUE./
      DATA IYR/75/
      DATA EFLEAN/F/
      END
```

```
$       FORTRAN DECK,MAP                                                LOBNUM
$       INCODE  IBMF
CLOBNUM      LOBE NUMBERS
C                FORTRAN-Y       22APR1975
C
C             THIS PROCEDURE DETERMINES THE FIRST FIVE LOBE NUMBERS,
C             N BEING A PARTICULAR LOBE NUMBER, AND THEIR ASSOCIATED
C             VALUES OF K FROM THE RELATIONSHIP
C
C                    N = NHARM*NBLADE + K*NVANES
C
C             AND PLACES THEM IN NARY AND KARY RESPECTIVELY.
C
      SUBROUTINE LOBNUM(NHARM,NBLADE,NVANES,NARY,KARY)
      DIMENSION NARY(5),KARY(5),ARY(2,11)
      ICONST = NHARM*NBLADE
      IF(NHARM .EQ. 0)  ICONST=NBLADE
      DO 5 J=1,11
      K = J-6
      ARY(1,J) = IABS(ICONST+K*NVANES)
    5 ARY(2,J) = K
```

```
      CALL SORT(ARY,2,11,1,.TRUE.)
      DO 10 I=1,5
      NARY(I) = ARY(1,I)
   10 KARY(I) = ARY(2,I)
      RETURN
      END
```

```
$       FORTRAN DECK,MAP                                                +
$       INCODE  IBMF                                            NRADMO
CNRADMO      RADIAL MODES PER LOBE NO.
C               FORTRAN-Y       22APR1975
C
C            THIS PROCEDURE DETERMINES THE NUMBER OF RADIAL
C            MODES TO BE ANALYZED PER LOBE NUMBER (NRADMO) AS
C            A FUNCTION OF LOBE NUMBER (N) VIA AN EMPIRICAL TABLE.
C
      FUNCTION NRADMO(N)
      DIMENSION IRANGN(10),IRADMO(10)
      DATA NRANGN/9/,(IRADMO(I),I=1,9)/1,2,4,5,6,7,8,9,10/,
     1 (IRANGN(I),I=1,8)/3,6,11,21,31,41,51,70/
      NRNGM1 = NRANGN-1
      DO 5 I=1,NRNGM1
      IF(N.LT.IRANGN(I)) GO TO 10
    5 CONTINUE
      I = NRANGN
   10 NRADMO = IRADMO(I)
      RETURN
      END
```

```
$       FORTRAN DECK,MAP                                                +
$       INCODE  IBMF                                            DECBEL
CDECBEL      INTENSITY LEVEL FUNCTION
C               FORTRAN-Y       22APR1975
C
C            THIS PROCEDURE DETERMINES INTENSITY LEVELS AS FOLLOWS,
C
C                  IF X.NE.0, DECBEL = C*ALOG10(ABS(X)/REF).
C                  IF X.EQ.0, DECBEL = 0.
C
      FUNCTION DECBEL(X,C,REF)
      IF(X.NE.0.) GO TO 5
      DECBEL = 0.
      GO TO 10
    5 DECBEL = C*ALOG10(ABS(X)/REF)
   10 RETURN
      END
```

```
$       FORTRAN DECK,MAP                                                +
$       INCODE  IBMF                                            TIMER
CTIMER        TIMING ROUTINE
C                FORTRAN-Y       22APR1975
      SUBROUTINE TIMER1
      CALL CLOCK(DUMY,T1,DUMY,DUMY)
      GO TO 5
      ENTRY TIMER2
      CALL CLOCK(DUMY,T2,DUMY,DUMY)
      PT = T2-T1
      MIN = PT/60.
      NSEC = AMOD(PT,60.)
      WRITE(6,900) MIN,NSEC
  900 FORMAT(//100X,12HPROC TIME = I3,4H MIN,3X,I2,4H SEC)
    5 RETURN
      END
```

```
$       FORTRAN DECK,MAP                                                +
$       INCODE  IBMF                                            SORT
CSORT         GENERAL ALGEBRAIC SORT ROUTINE
C                FORTRAN-Y       22APR1975
C

C
      SUBROUTINE SORT(ARRAY,N,M,ISRT,ASCND)
      DIMENSION ARRAY(N,M),BUFF(10)
      LOGICAL ASCND
      LNG=M+1
      MM1=M-1
      DO 10 LOOP=1,MM1
      LNG=LNG-1
      LNGM1=LNG-1
      DO 15 J=1,LNGM1
      IF(ASCND) GO TO 20
      IF(ARRAY(ISRT,J).GE.ARRAY(ISRT,LNG)) GO TO 15
      GO TO 25
   20 IF(ARRAY(ISRT,J).LE.ARRAY(ISRT,LNG)) GO TO 15
   25 DO 30 I=1,N
      BUFF(I)=ARRAY(I,LNG)
   30 CONTINUE
      DO 35 I=1,N
      ARRAY(I,LNG)=ARRAY(I,J)
   35 CONTINUE
      DO 40 I=1,N
      ARRAY(I,J)=BUFF(I)
   40 CONTINUE
   15 CONTINUE
   10 CONTINUE
      RETURN
      END
```

```
$       FORTRAN LSTOU                                                   +
$       INCODE  IBMF                                            BESFIT
CBSFT
C             BESFIT - LEAST SQUARES CURVE-FITTING ROUTINE
C             USING ORTHOGONAL POLYNOMIALS WITH STATISTICAL
C             TERMINATION
C
C
      SUBROUTINE BESFIT(N,X,Y,K,D,RES)
      DIMENSION X(1),Y(1),D(21),A(23),B(23),S(23),RES(23),TAB(20),
     1  P0(220),P1(220),R(21,21)
      EQUIVALENCE (P0,R),(P1,R(221))
      DATA (TAB(I),I=1,20)/12.706,4.303,3.182,2.776,2.571,2.447,
     1  2.365,2.306,2.262,2.228,2.201,2.179,2.160,2.145,2.131,2.120,
     2  2.110,2.101,2.093,2.086/
      KT=0
      IF=K
      M=N
      NDEG=M-1
      J=0
      CO=M
      A(1)=0.
      B(1)=0.
      S(1)=0.
      RES(1)=0.
      DO 1 I=1,M
      P0(I)=0.
      P1(I)=1.
      S(1)=S(1)+Y(I)
      A(1)=A(1)+X(I)
    1 RES(1)=Y(I)**2+RES(1)
      A(1)=A(1)/CO
      S(1)=S(1)/CO
      RES(1)=RES(1)-S(1)**2*CO
      RMS=RES(1)/(CO-1.)
    3 J=J+1
      IF(J.LE.22) GO TO 24
   27 K=20
      LL=21
      WRITE(6,29)
      GO TO 4
   24 C1=0.
      XPP=0.
      YP=0.
      DO 2 I=1,M
      Q=P1(I)
      P1(I)=(X(I)-A(J))*Q-B(J)*P0(I)
      P0(I)=Q
      PP=P1(I)**2
      C1=PP+C1
      XPP=XPP+X(I)*PP
```

```
 2 YP=YP+Y(I)*P1(I)
   S(J+1)=YP/C1
   SSR=S(J+1)**2*C1

23 RES(J+1)=RES(J)-SSR
   IF(RES(J+1).GT.0.) GO TO 13
12 K=J
   IF(RES(J).LT.ABS(RES(J+1))) K=J-1
   LL=K+1
43 WRITE(6,14) K
   GO TO 4
13 A(J+1)=XPP/C1
   B(J+1)=C1/C0
   C0=C1
   LL=J+1
   IF(IF.NE.0) IF(LL-IF) 3,3,4
15 NDEG=NDEG-1
   RMS=RES(J+1)/FLOAT(NDEG)
   ISUB=MIN0(NDEG,20)
   T=SQRT(SSR/RMS)
   IF(T.LE.TAB(ISUB)) GO TO 17
22 KT=0
   GO TO 3
17 S(J+1)=0.
   RES(J+1)=RES(J)
   NDEG=NDEG+1
   IF(KT.EQ.1) GO TO 18
21 KT=1
   GO TO 3
18 LL=J-1
   K=J-2
 4 R(1,1)=1.
   R(1,2)=-A(1)
   R(2,2)=1.
   R(2,1)=0.
   IF(K-2) 6,8,8
 8 DO 9 I=3,LL
   R(1,I)=-A(I-1)*R(1,I-1)-B(I-1)*R(1,I-2)
   LOOP=I-2
   R(I-1,I)=R(I-2,I-1)-A(I-1)*R(I-1,I-1)
   R(I,I)=1.
   DO 9 JJ=2,LOOP
   R(JJ,I)=R(JJ-1,I-1)-A(I-1)*R(JJ,I-1)-B(I-1)*R(JJ,I-2)
 9 CONTINUE
 6 DO 10 JJ=1,LL
   D(JJ)=0.
   DO 10 L=JJ,LL
10 D(JJ)=D(JJ)+S(L)*R(JJ,L)
   RETURN
14 FORMAT(28HOBESFIT RETURNED WITH ORDER I2//)
29 FORMAT(30HOBESFIT LIMITED TO 20TH ORDER.//)
   END
```

```
$       FORTRAN DECK,MAP                                                ARCSIN
$       INCODE  IBMF
CARCSIN      ARC SINE  (PRINCIPAL VALUE)                                ARCSIN00
C        FORTRAN-Y   22APR1975
      FUNCTION ARCSIN(X)                                                ARCSIN01
      IF(X.NE.0.0) GO TO 5                                              ARCSIN02
      ARCSIN = 0.0                                                      ARCSIN03
      GO TO 15                                                          ARCSIN04
    5 IF(ABS(X).NE.1.0) GO TO 10                                        ARCSIN05
      ARCSIN = SIGN(1.57.7963,X)                                        ARCSIN06
      GO TO 15                                                          ARCSIN07
   10 ARCSIN = ATAN(X/SQRT(1.-X**2))                                    ARCSIN08
   15 RETURN                                                            ARCSIN09
      END                                                               ARCSIN10
```

```
$       FORTRAN                                                         ALNGAM
$       INCODE  IBMF
CALNGAM      NATURAL LOGARITHM OF GAMMA FUNCTION                        ALNGAM01
C                                                                       ALNGAM02
C                                                                       ALNGAM03
C            THIS PROCEDURE EVALUATES THE NATURAL LOGARITHM OF          ALNGAM04
C            GAMMA(X) FOR ALL REAL X IN THE INTERVAL 10**-8 =X =10**6.  ALNGAM05
C            STIRLING-S FORMULA IS USED FOR THE CENTRAL POLYNOMIAL PART ALNGAM06
C            OF THE PROCEDURE.                                          ALNGAM07
C                                                                       ALNGAM08
C                                                                       ALNGAM09
C                                                                       ALNGAM10
      FUNCTION ALNGAM(X)                                                ALNGAM11
      IF(X.GE.1.E-8.AND.X.LE.1.E6) GO TO 5                              ALNGAM12
      WRITE(6,900) X                                                    ALNGAM13
  900 FORMAT(72H0***ALNGAM ARGUMENT FAULT. PROCEDURE REQUIRES 10**-8 =ARALNGAM14
     1G =10**6. ARG = E15.8,21H. RESULT SET = ARG***)                   ALNGAM15
      ALNGAM = X                                                        ALNGAM16
      GO TO 30                                                          ALNGAM17
    5 IF(X.LT.7.) GO TO 10                                              ALNGAM18
      F = 0.                                                            ALNGAM19
      Y = X                                                             ALNGAM20
      GO TO 25                                                          ALNGAM21
   10 F = 1.                                                            ALNGAM22
      Z = X-1.                                                          ALNGAM23
      DO 15 I=1,7                                                       ALNGAM24
      Z = Z+1.                                                          ALNGAM25
      IF(Z.GE.7.) GO TO 20                                              ALNGAM26
      Y = Z                                                             ALNGAM27
      F = F*Z                                                           ALNGAM28
   15 CONTINUE                                                          ALNGAM29
   20 Y = Y+1.                                                          ALNGAM30
      F = -ALOG(F)                                                      ALNGAM31
   25 Z = 1./Y**2                                                       ALNGAM32
      ALNGAM = F+(Y-0.5)*ALOG(Y)-Y+0.91893853+(((-0.00059523809*Z       ALNGAM33
     1 +0.00079365079)*Z-0.0027777778)*Z+0.083333333)/Y                 ALNGAM34
   30 RETURN                                                            ALNGAM35
      END                                                               ALNGAM36
```

```
$       FORTRAN LSTOU,DECK,XREF                                         CYCMCH
CCYCMCH      CYCLE THROUGH MECHANISMS
C                FORTRAN-Y       22APR1975
C
      SUBROUTINE CYCMCH
      EXTERNAL LINK1F,LINK1I,LINK2F,LINK2I
      COMMON/INPBLK/TITLE(10),MODE,MECH(5),NMECH,HUBRAD,TIPRAD,NBLADE,
     1 NVANES,SPEED,INPLOB,LOBNO(5),NLOBNO,INPNIN,INFLEC(5),NHARM,PSTAT,
     2 TSTAT,TET,DELLAM,LAMBAY(20,5),QAY(20,5),OPRAD(20),NOPRAD,NRADP,
     3 RADTAB(5),BETA1A(5),BETA1R(5),BETA2A(5),BETA2R(5),BETA3A(5),
     4 BETA3R(5),SIGMA1(5),SIGMA2(5),BP(5),INPCD1,CD1(5),PUNCH
     5 ,EFLEAN,ALPHA(5),C,LAMBDA(10,5),RHO,GAM,DYVISC
      LOGICAL INPLOB,INPNIN,DELLAM,INPCD1,PUNCH
      LOGICAL EFLEAN
      COMPLEX LAMBDA
      REAL LAMBAY
      COMMON/CYCBLK/NRLSAY(5),OPRR(20),H,HSQ,FNOMEG,FNOMSQ,RCONST(4),
     1 LSKEIG,AK(3),K
C    CYCMCH
      COMMON /CLEAN1/ FLEAN1,NLEAN1,RL(20)
      LOGICAL FLEAN1
      COMMON /CLEAN3/ MECHL1,KMODE(5)
      LOGICAL LSKEIG
      DIMENSION MECHSM(10),MCHTAG(5),DUMY(5),RADRTB(5),V1(5),V2(5),
     1 ALPHA1(5),ALPHA2(5),DELCU1(5),DELCU2(5),C1(5),C2(5),GAMTAB(5)
      DIMENSION ANGO1(5),ANGO2(5)
      INTEGER TURBIN
      LOGICAL ROTALN,TILT

      DATA MECHSM/6HIRVSWK,6HROVSWK/
      DATA TURBIN/5HTURBIN/
      DATA RDPRDG/0.0174533/
C
C
      DO 10 I=1,NMECH
      DO 5 J=1,2
      IF(MECH(I).NE.MECHSM(J)) GO TO 5
      MCHTAG(I) = J
      GO TO 10
    5 CONTINUE
      WRITE(6,900) MECH(I)
  900 FORMAT(28H0***INVALID MECHANISM. MECH=A6,3H***)
      GO TO 160
   10 CONTINUE
      ROTALN = .FALSE.
      IF(MCHTAG(1).LE.2) ROTALN = .TRUE.
C
C
      IF(.NOT.INPLOB) GO TO 25
      DO 20 I=1,NLOBNO
      IF(.NOT.ROTALN) GO TO 15
      NRLSAY(I) = NBLADE
```

```
      GO TO 20
   15 NRLSAY(I) = LOBNO(I)
   20 CONTINUE

      GO TO 35
   25 IF(.NOT.ROTALN) GO TO 30
      NLOBNO = 1
      LOBNO(1) = NHARM*NBLADE
      IF(NHARM .EQ. 0)  LOBNO(1)=NBLADE
      NRLSAY(1) = NBLADE
      GO TO 45
   30 CALL LOBNUM(NHARM,NBLADE,NVANES,LOBNO,DUMY)
      CALL LOBNUM(1,NBLADE,NVANES,NRLSAY,DUMY)
   35 DO 40 I=1,NLOBNO
      IF(NRLSAY(I).NE.0) GO TO 40
      WRITE(6,905)
  905 FORMAT(36H0***ANALYSIS INDICATES PLANE WAVE***)
      GO TO 160
   40 CONTINUE
   45 WRITE(6,910) (LOBNO(I),NRLSAY(I),I=1,NLOBNO)
  910 FORMAT(1H1,51X,3(6H******)/56X,11HOUTPUT DATA/52X,3(6H******)///
     1 38X,21HCIRCUMFERENTIAL LOBES,5X,21HROTATING LINE SOURCES/
     2 (45X,I5,20X,I5))
      WRITE(6,915)
  915 FORMAT(1H0)
C
C
      IF(INPNIN) GO TO 55
      DO 50 I=1,NLOBNO
   50 INFLEC(I) = NRADMO(LOBNO(I))
C
C
   55 DO 60 I=1,NRADP
   60 RADRTB(I) = RADTAB(I)/TIPRAD
      DO 65 I=1,NOPRAD
   65 OPRR(I) = OPRAD(I)/TIPRAD
C
C ...AERO PARAMETERS...
      BLADES = NBLADE
      VANES = NVANES
      H = HUBRAD/TIPRAD
      HSQ = H**2
      UTIP = SPEED*TIPRAD/114.59156
C                    NOTE ( 114.59156 = 360/PI )
      VISC=2.27E-8*TSTAT**1.5/(TSTAT+198.6)
      GAMEXP = EXP(5500./TSTAT)
      GAMA = 1.+0.4/(1.+0.4*(5500./TSTAT)**2*GAMEXP/(GAMEXP-1.)**2)
      C = SQRT(1716.4829*GAMA*TSTAT)
C                    NOTE ( 1716.4829 = 53.35*GSUBC )
      RHO = PSTAT/(53.35*TSTAT)
      HARM = NHARM
```

```
      IF(NHARM .EQ. 0)  HARM=1.
      FNOMEG = SPEED*HARM*BLADES*TIPRAD/(114.59156*C)
      FNOMSQ = FNOMEG**2
      RCONST(1) = 114.59156*C/(HARM*BLADES*TIPRAD)
      RCONST(2) = 0.95492964/(C*TIPRAD)
C                   NOTE ( 0.95492964 = 3/PI )
      RCONST(3) = 0.33904214E-3*TIPRAD**2*RHO*C**3*FNOMSQ
C                   NOTE ( 0.33904214E-3 = PI/(2*144*GSUBC) )
      RCONST(4) = 0.19179168E-3*HARM*SPEED*BLADES*TIPRAD*RHO*C

C                   NOTE ( 0.19179168E-3 = 2*PI/(SQRT(2)*60*12*GSUBC) )
      HB = TIPRAD-HUBRAD
      IPOINT = MCHTAG(1)
      DO 90 I=1,NRADP
      B1AR = RDPRDG*BETA1A(I)
      B1RR = RDPRDG*BETA1R(I)
      B2AR = RDPRDG*BETA2A(I)
      B2RR = RDPRDG*BETA2R(I)
      B3AR = RDPRDG*BETA3A(I)
      B3RR = RDPRDG*BETA3R(I)
      SANG1 = B1AR+B1RR
      SANG2 = B2AR+B2RR
      SANG3 = B3AR+B3RR
      U = UTIP*RADRTB(I)
      ARG2 = 6.2831853*RADRTB(I)*TIPRAD
      V2A = U*COS(B2RR)/SIN(SANG2)
      V2R = U*COS(B2AR)/SIN(SANG2)
      GO TO(70,80),IPOINT
C   ...U/S VANE - ROTOR OR I-R...
    7. V1(I) = V2A
      ALPHA1(I) = BETA2A(I)
      V2(I) = V2R
      ALPHA2(I) = BETA2R(I)
      V3A = U*COS(B3RR)/SIN(SANG3)
      CZ = V2A*COS(B2AR)
      DELCU1(I) = ABS(CZ*SIN(B1AR)/COS(B1AR)-V2A*SIN(B2AR))
      DELCU2(I) = ABS(V2A*SIN(B2AR)-V3A*SIN(B3AR))
      IF(ROTALN) GO TO 90
      C1(I) = ARG2*SIGMA1(I)/VANES
      C2(I) = ARG2*SIGMA2(I)/BLADES
      IF(INPCD1) GO TO 90
   75 EPS=ABS(BETA1A(I)-BETA2A(I))
      EPSP = 4.1486E-2+EPS*(3.9976E-4+EPS*(-3.4270E-6+EPS*5.4403E-8))
      EPSPP = (1.+EPSP)*(0.975)-1.0
C PROFILE LOSS APPROX. FROM TOTAL LOSS BY ASSUMING AN
C INFINITE ASPECT RATIO
      DH = (2.*HB*ARG2*COS(B2AR)/VANES)/(ARG2*COS(B2AR)/VANES+HB)
      RH = RHO*V2A*DH/(386.088*VISC)
      FM2 = V2A/C
      EPSPPP =((1.E5/RH)**0.25*EPSPP)/(1.-FM2**2/4.+(2.-GAMA)*FM2**4/24.
     1)
      TANB1A = SIN(B1AR)/COS(B1AR)
```

```
      TANB2A = SIN(B2AR)/COS(B2AR)
      ALPHAM = ATAN((TANB1A+TANB2A)/2.)
      CD1(I)=EPSPPP/(SIGMA1(I)*2.0)
      GO TO 90
C   ...ROTOR - D/S VANE OR R-O...
   80 V1(I) = V2R
      ALPHA1(I) = BETA2R(I)
      V2(I) = V2A
      ALPHA2(I) = BETA2A(I)
      V1A = U*COS(B1RR)/SIN(SANG1)
      V1R = U*COS(B1AR)/SIN(SANG1)
      DELCU1(I) = ABS(V1A*SIN(B1AR)-V2A*SIN(B2AR))
      CZ = V2A*COS(B2AR)
      DELCU2(I) = ABS(V2A*SIN(B2AR)-CZ*SIN(B3AR)/COS(B3AR))
      IF(ROTALN) GO TO 90
      C1(I) = ARG2*SIGMA1(I)/BLADES
      C2(I) = ARG2*SIGMA2(I)/VANES
      IF(INPCD1) GO TO 90
   85 EPS=ABS(BETA1R(I)-BETA2R(I))
      EPSP = 4.1486E-2+EPS*(3.9976E-4+EPS*(-3.4270E-6+EPS*5.4403E-8))
      EPSPP = (1.+EPSP)*(0.975)-1.0
      DH = (2.*HB*ARG2*COS(B2RR)/BLADES)/(ARG2*COS(B2RR)/BLADES+HB)
      RH = RHO*V2R*DH/(386.088*VISC)
      FM2 = V2R/C
      EPSPPP =((1.E5/RH)**0.25*EPSPP)/(1.-FM2**2/4.+(2.-GAMA)*FM2**4/24.
     1)
      TANB1R = SIN(B1RR)/COS(B1RR)
      TANB2R = SIN(B2RR)/COS(B2RR)
      ALPHAM = ATAN((TANB1R+TANB2R)/2.)
      CD1(I) = EPSPPP/(SIGMA1(I)*2.)
   90 CONTINUE
      IF(ROTALN) GO TO 91
      WRITE(6,920) (C1(I),I=1,NRADP)
  920 FORMAT(//5X,23HU/S BLADE ROW CHORD(IN)/3X,5(9X,F10.3))
      WRITE(6,925) (C2(I),I=1,NRADP)
  925 FORMAT(5X,23HD/S BLADE ROW CHORD(IN)/3X,5(9X,F10.3))
      IF(.NOT.INPCD1) WRITE(6,930) (CD1(I),I=1,NRADP)
  930 FORMAT(5X,16HU/S BLADE ROW CD/3X,5(9X,F10.5))
   91 IF(.NOT.DELLAM.AND.PUNCH) PUNCH 800,TITLE
  800 FORMAT(10H0123456789,10A6,10H9876543210)
      LSKEIG = .FALSE.
C
C ...CYCLE THROUGH GENERATING MECHANISMS...
      TIPRFT = TIPRAD/12.
      CALL LLINK(5HLINK2)
      CALL LLINK(4HDUM2)
      CALL FSAVE(22,LINK2F,LINK2I,5HLINK2,1)
      CALL LLINK(5HLINK1)
      CALL LLINK(4HDUM1)
      DO 155 M=1,NMECH
      CALL TIMER1
```

```
      IMECH = MCHTAG(M)
      MECHL=MECHSM(IMECH)
      GO TO(105,110),IMECH
C  ...IRVSWK...
  105 WRITE(6,945) M
  945 FORMAT(1H1,2X,3(6H******)/6X,10HMECHANISM I1,5X,
     . 16HI-R VISCOUS WAKE/3X,3(6H******))
      GO TO 111
C  ...ROVSWK...
  110 WRITE(6,950) M
  950 FORMAT(1H1,2X,3(6H******)/6X,10HMECHANISM I1,5X,
     . 16HR-O VISCOUS WAKE/3X,3(6H******))
  111 IF((.NOT.EFLEAN) .AND. (.NOT.FLEAN1)) GO TO 113
      CALL FSAVE(21,LINK1F,LINK1I,5HLINK1,1)
      CALL FRSTR(22,5HLINK2,LINK2F)
      CALL PRECAL($112)
  112 CALL FSAVE(22,LINK2F,LINK2I,5HLINK2,1)
      CALL FRSTR(21,5HLINK1,LINK1F)
      IF(FLEAN1) GO TO 113
      GO TO 155

  113 CALL VISCWK(UTIP,RADRTB,ALPHA1,ALPHA2,V1,V2,SIGMA1,C1,C2,BP,CD1,
     X  NRADP,TET,MODE,GAMTAB,NHARM,TILT)
  145 IF(.NOT.TILT) GO TO 146
      IF(M.EQ.1) GO TO 160
      GO TO 155
  146 WRITE(6,985) (RADRTB(I),GAMTAB(I),I=1,NRADP)
  985 FORMAT(//5X,33HUNSTEADY CIRCULATION DISTRIBUTION//22X,
     1 12HRADIUS RATIO,3X,22HCIRCULATION(FT**2/SEC)//(25X,F6.3,
     2 11X,E11.4))
      DO 150 I=1,NRADP
      IF(GAMTAB(I).NE.0.) GO TO 150
      WRITE(6,990)
  990 FORMAT(/22X,53HNEGLIGIBLE CONTRIBUTION. PROCEEDING TO NEXT MECHANI
     1SM)
      GO TO 155
  150 CONTINUE
      K = 2
      CALL BESFIT(NRADP,RADRTB,GAMTAB,K,AK,DUMY)
      CALL SYNTHZ($160)
      CALL TIMER2
      LSKEIG = .TRUE.
  155 CONTINUE
  160 RETURN
      END
```

```
$       FORTRAN DECK,MAP                                                +
$       INCODE  IBMF                                            SYNTHZ
CSYNTHZ      SYNTHESIZE COMPOSITE
C                FORTRAN-Y       22APR1975
C
      SUBROUTINE SYNTHZ(*)
      COMMON/INPBLK/TITLE(10),MODE,MECH(5),NMECH,HUBRAD,TIPRAD,NBLADE,
     1 NVANES,SPEED,INPLOB,LOBNO(5),NLOBNO,INPNIN,INFLEC(5),NHARM,PSTAT,
     2 TSTAT,TET,DELLAM,LAMBAY(20,5),QAY(20,5),OPRAD(20),NOPRAD,NRADP,
     3 RADTAB(5),BETA1A(5),BETA1R(5),BETA2A(5),BETA2R(5),BETA3A(5),
     4 BETA3R(5),SIGMA1(5),SIGMA2(5),BP(5),INPCD1,CD1(5),PUNCH
     5 ,EFLEAN,ALPHA(5),C,LAMBDA(10,5),RHO,GAM,DYVISC
      LOGICAL INPLOB,INPNIN,DELLAM,INPCD1,PUNCH
      REAL LAMBAY
      COMMON/CYCBLK/NRLSAY(5),OPRR(20),H,HSQ,FNOMEG,FNOMSQ,RCONST(4),
     1 LSKEIG,AK(3),K
      LOGICAL LSKEIG
C    SYNTHZ
      REAL NORM
      LOGICAL TILT,CUTOFF
      COMMON /CBESLF/ PRESNM(20),PRESM(20),PRES(20),SPLNM(20),
     *                SPLM(20),SPL(20),RESDAY(20),LAMBD,LAMBSQ,Q,
     *     JLAM(110),JLAMH(110),YLAM(110),YLAMH(110),CYL(110,2)
      REAL LAMBD,LAMBSQ,JLAM(110),NORM,JLAMH(110)
      COMMON /CLEAN1/ FLEAN1,NLEAN1,RL(20)
      LOGICAL FLEAN1
      COMMON /CLEAN2/ PHIR(20),CCYL(20)
      COMMON /CLEAN3/ MECHL1,KMODE(5)
      DATA OPNPRN,CLSPRN,EQL/074000000000,034000000000,013000000000/
      DATA PRSREF,POWREF/4.1772E-7,7.3756E-14/
C
C
      DO 5 I=1,NOPRAD
    5 PRESNM(I) = 0.
      POWNM = 0.
      ICOMP = 0
      WRITE(6,899)
  899 FORMAT(7H0  COMP,2X,4HMODE,4X,6HEGNVAL,3X,8HRESIDUAL,3X,7HC/0 SPD,
     1 5X,4HNORM,9X,3HAMP,9X,5HPOWER,7X,3HPWL,6X,4HRADR,3X,6HRADIUS,6X,
     2 4HPRES,7X,3HSPL/38X,5H(RPM),28X,12H(FT*LBF/SEC),3X,4H(DB),13X,
     3 4H(IN),6X,5H(PSF),6X,4H(DB)//)
C
C
      DO 65 ILOB=1,NLOBNO
      N = LOBNO(ILOB)
      FN = N
      FNSQ = FN**2
      NP1 = N+1
      NP2 = N+2
      NP4 = N+4
      NP5 = N+5
      MF = INFLEC(ILOB)
```

```
      MFM1 = MF-1
      NRLS = NRLSAY(ILOB)
      KM= KMODE(ILOB)

      IF(DELLAM.OR.LSKEIG) GO TO 10
      CALL EIGEN(H,N,Q,MFM1,LAMBAY(1,ILOB),QAY(1,ILOB),RESDAY,TILT)
      IF(TILT) GO TO 75
      IF(.NOT.PUNCH) GO TO 10
      PUNCH 805,OPNPRN,ILOB,CLSPRN,EQL,(LAMBAY(I,ILOB),I=1,MF)
  805 FORMAT(7H LAMBAY,A1,2H1,I1,2A1,3(E15.8,1H,)/(1X,4(E15.8,1H,)))
      PUNCH 810,OPNPRN,ILOB,CLSPRN,EQL,(QAY(I,ILOB),I=1,MF)
  810 FORMAT(7H    QAY,A1,2H1,I1,2A1,3(E15.8,1H,)/(1X,4(E15.8,1H,)))
C
C
   10 DO 15 I=1,NOPRAD
   15 PRESM(I) = 0.
      POWM = 0.
C
C
      DO 50 IRM=1,MF
      ICOMP = ICOMP+1
      NINFL = IRM-1
      LAMBD = LAMBAY(IRM,ILOB)
      LAMBSQ = LAMBD**2
      Q = QAY(IRM,ILOB)
C
      CFSPED = LAMBD*RCONST(1)
      CFRATO = SPEED/CFSPED
      IF(FNOMEG.GE.LAMBD) GO TO 20
      CUTOFF = .TRUE.
      BETA = SQRT(LAMBSQ-FNOMSQ)
      GO TO 25
   20 CUTOFF = .FALSE.
      BETA = SQRT(FNOMSQ-LAMBSQ)
C
   25 CALL BESSEL(LAMBD,NP4,.TRUE.,JLAM,YLAM,TILT)
      IF(TILT) GO TO 75
      CALL BESSEL(LAMBD*H,NP4,.TRUE.,JLAMH,YLAMH,TILT)
      IF(TILT) GO TO 75
      DO 30 I=1,NP5
      CYL(I,1) = JLAMH(I)-Q*YLAMH(I)
   30 CYL(I,2) = JLAM(I)-Q*YLAM(I)
C
      NORM = ((LAMBSQ-FNSQ)*CYL(NP1,2)**2
     1 -(LAMBSQ*HSQ-FNSQ)*CYL(NP1,1)**2)/(2.*LAMBSQ)
C
      SUM = 0.
      KP1 = K+1
      DO 35 I=1,KP1
      CALL RPYCYG(I,N,LAMBD,H,1.,CYL,RINTG,TILT)
      IF(TILT) GO TO 75
```

```
   35 SUM = SUM+AK(I)*RINTG
      GO TO 37
   36 CALL INTZL(N,KM,SUM)
   37 ANM = RCONST(2)*FLOAT(NRLS)*SUM/(FN*NORM)
C
      POWER = RCONST(3)*ANM**2*(CYL(NP1,2)**2-CYL(N,2)*CYL(NP2,2)
     1 -HSQ*(CYL(NP1,1)**2-CYL(N,1)*CYL(NP2,1)))
      POWM = POWM+POWER
      PWL = DECBEL(POWER,10.,POWREF)

      IF(NOPRAD.EQ.0) GO TO 45
C
      DO 40 I=1,NOPRAD
      CALL BESSEL(LAMBD*OPRR(I),N,.TRUE.,JLAM,YLAM,TILT)
      IF(TILT) GO TO 75
      PRES(I) = RCONST(4)*ABS(ANM*(JLAM(NP1)-Q*YLAM(NP1)))
      PRESM(I) = PRESM(I)+PRES(I)
   40 SPL(I) = DECBEL(PRES(I),20.,PRSREF)
C
   45 WRITE(6,900) ICOMP,N,NINFL,LAMBD,RESDAY(IRM),CFSPED,NORM,ANM,
     1 POWER,PWL
  900 FORMAT(4X,I2,2X,I2,1H,I2,2X,F8.3,2X,E10.3,2X,F6.0,2X,E11.4,2X,
     1 E11.4,2X,E11.4,2X,F7.2)
      IF(NOPRAD.NE.0) WRITE(6,905) (OPRR(I),OPRAD(I),PRES(I),SPL(I),
     1 I=1,NOPRAD)
  905 FORMAT(1H+,92X,F6.3,2X,F7.2,2X,E11.4,2X,F7.2/(93X,F6.3,
     1 2X,F7.2,2X,E11.4,2X,F7.2))
   50 CONTINUE
C
      PWLM = DECBEL(POWM,10.,POWREF)
      DO 55 I=1,NOPRAD
   55 SPLM(I) = DECBEL(PRESM(I),20.,PRSREF)
      WRITE(6,910) N,POWM,PWLM
  910 FORMAT(/10X,25HRADIAL COMPOSITE LOBE NO I3,33X,E11.4,2X,F7.2)
      IF(NOPRAD.NE.0) WRITE(6,915) (OPRR(I),OPRAD(I),PRESM(I),SPLM(I),
     1 I=1,NOPRAD)
  915 FORMAT(1H+,92X,F6.3,2X,F7.2,2X,E11.4,2X,F7.2/(93X,F6.3,
     1 2X,F7.2,2X,E11.4,2X,F7.2))
      DO 60 I=1,NOPRAD
   60 PRESNM(I) = PRESNM(I)+PRESM(I)**2
      POWNM = POWNM+POWM
      WRITE(6,920)
  920 FORMAT(1H0)
   65 CONTINUE
C
      PWLNM = DECBEL(POWNM,10.,POWREF)
      DO 70 I=1,NOPRAD
      PRESNM(I) = SQRT(PRESNM(I))
   70 SPLNM(I) = DECBEL(PRESNM(I),20.,PRSREF)
      WRITE(6,925) POWNM,PWLNM
  925 FORMAT( 10X,17HOVERALL COMPOSITE,44X,E11.4,2X,F7.2)
```

```
      IF(NOPRAD.NE.0) WRITE(6,905) (OPRR(I),OPRAD(I),PRESNM(I),SPLNM(I),
     1 I=1,NOPRAD)
      RETURN
   75 RETURN 1
      END

$       FORTRAN DECK,MAP,XREF
$       INCODE  IBMF                                                    +
CINTZL      INTEG CYL FUNCT.--- LEANED VANES--                      INTZL
      SUBROUTINE INTZL( N,KMODE ,ZINT )
      LOGICAL ENTRY1
      COMMON /CLEAN1/ FLEAN1,NLEANI,RL(20)
      LOGICAL         FLEAN1
      COMMON /CLEAN2/ PHIR(20),CCYL(20)
      COMMON /CLEAN3/ MECHL1,KMD(5)
      COMMON /PRCBLK/ DUM1(30),AK(10),RHUB,ALPCOE(3),GPRM1,GONE
      COMMON /CBESLF/ DUM4(140),LAMBD,LAMBSQ,Q,
     *                JLAM(110),JLAMH(110),YLAM(110),YLAMH(110),
     *                 CYL(220)
      REAL LAMBD,LAMBSQ,JLAM,JLAMH,YLAM,YLAMH
      COMMON /CYCBLK/ DUM2(25),H,DUM3(8),AC(3),K

      COMMON/INPBLK/TITLE(10),MODE,MECH(5),NMECH,HUBRAD,TIPRAD,NBLADE,
     1 NVANES,SPEED,INPLOB,LOBNO(5),NLOBNO,INPNIN,INFLEC(5),NHARM,PSTAT,
     2 TSTAT,TET,DELLAM,LAMBAY(20,5),QAY(20,5),OPRAD(20),NOPRAD,NRADP,
     3 RADTAB(5),BETA1A(5),BETA1R(5),BETA2A(5),BETA2R(5),BETA3A(5),
     4 BETA3R(5),SIGMA1(5),SIGMA2(5),BP(5),INPCD1,CD1(5),PUNCH
     5 ,EFLEAN,ALPHA(5),C,LAMBDA(10,5),RHO,GAM,DYVISC
      LOGICAL INPLOB,INPNIN,DELLAM,INPCD1,PUNCH
      LOGICAL EFLEAN
      COMPLEX LAMBDA
      REAL LAMBAY
      DIMENSION TEMP(2),TEMPS(2)
      DIMENSION SUM(4)
      DIMENSION CYLR(20)

      DATA ENTRY1/T/,PI/3.14159265/
      DATA MECHL2/6HROVSWK/

      IF( .NOT.ENTRY1 ) GO TO 10

      KP1    = K+1
    1 NP1    = N+1
      TEMPS(1)= RL(1)
      TEMPS(2)= RL(NLEANI)
      DO 25 I=1,NLEANI
      ARGB   = LAMBD*RL(I)
      CALL BESSEL(ARGB,NP1,.TRUE.,JLAM,YLAM,TILT)
      CYLR(I)   = JLAM(NP1)-Q*YLAM(NP1)
   25 CONTINUE
      IF( MECHL1.EQ.MECHL2 ) GO TO 11
```

```
C     IGV-ROTOR

      HARN=NHARM
      IF(NHARM.EQ.0.0) HARN=1
      ANG1=-FLOAT(NBLADE*HARN)
      GO TO 26

C     ROTOR-OGV

   11 ANG1  = FLOAT( KMODE*NVANES )
   26 CONTINUE
      FIVE=PI/12.0
      TT=0.0
      XINT=0.0
      DO 200 M=1,36
      TT=TT+FIVE
      ZINT  = 0.
      DO 100 J=1,KP1

C     EVALUATE INTEGRAND AT RL S

      DO 20 I=1,NLEANI
      IF( J.GT.1 ) GO TO 18
   12 PSIR  = ANG1*PHIR(I)
      CANG1=COS(TT+PSIR)
      CCYL(I)= RL(I)*CYLR(I)*CANG1
      GO TO 20
   18 CCYL(I)= RL(I)*CCYL(I)
   20 CONTINUE

C     INTEGRATE USING LSPFIT

      TEMP(1)= 0.
      CALL LSPFIT(RL,CCYL,NLEANI,TEMPS,TEMP,2,-1)
      SUM(J)= TEMP(2)
      ZINT  = ZINT+AC(J)*SUM(J)
  100 CONTINUE
      ZZ=ABS(ZINT)
      IF(ZZ.GT.XINT) XINT=ZZ
C     WRITE(06,300)M,ZINT,TT,PSIR,XINT
C 300 FORMAT(6HM=     ,I4,10H     ZINT=,F14.5,6H   TT=,F14.5,8H   PSIR=,
C    1F14.5,8H   XINT=,F14.5)
  200 CONTINUE
      ZINT=XINT

      RETURN
      END
```

```
$       FORTRAN DECK,XREF,MAP                                          +
$       INCODE  IBMF                                            VISCWK
CVISCWK      VISCOUS WAKE INTERACTION
C                FORTRAN-Y       22APR1975
C
      SUBROUTINE VISCWK(UTIP,RADR,ALPHA1,ALPHA2,V1,V2,SIGMA1,
     1 C1,C2,BP,CD1,NRADR,          TET,MODE,       GAMMA,NHARM,TILT)
      COMMON /QTHETA/THETAE(20)
      COMMON /CLEAN1/ FLEAN1,NLEANI,RL(20)
      LOGICAL         FLEAN1
      COMMON /CLEAN2/ PHIR(20),CCYL(20)
      COMMON /PRCBLK/ DUM1(30),AK(10),RHUB,ALPCOE(3),GPRM1,GONE
      COMMON /CYCBLK/ DUM2(25),H,DUM3(8),AC(3),K
      DIMENSION PHI(5)
      DIMENSION RADR(1),ALPHA1(1),ALPHA2(1),V1(1),V2(1),SIGMA1(1),
     1 C1(1),C2(1),BP(1),CD1(1),GAMMA(1)
      LOGICAL TILT
      REAL J(2)
      DOUBLE PRECISION SUM
      INTEGER TURBIN
      DATA PI/3.14159/
      DATA TURBIN/6HTURBIN/
    5 RC01=0.6
      RC02=1.391*PI
      RC03=0.283
      IPOINT = 2
   11 CONTINUE
      DO 3 I=1,5
    3 PHI(I)=0.0
      IF(.NOT.FLEAN1) GO TO 1
C     INITIALIZE INTEGRATION RADII AND LEAN PARAMETERS
C     CALCULATE ANGULAR DISPLACEMENT.

      NL     = NLEANI-1
      DR     = (1.-H)/FLOAT(NL)
      RL(1)  = H
      DO 1 I=2,NLEANI
      RL(I)  = RL(I-1)+DR
    1 CONTINUE
      DO 2 I=1,NLEANI
      RL1    = RL(I)
      ALPR   = ALPCOE(1)+RL1*(ALPCOE(2)+ALPCOE(3)*RL1)
      ARG    = PI-ALPR
      TERM   = H/RL1*SIN(ARG)
      GR     = ALPR-ARCSIN( TERM )
      THETAE(I)= AK(6)+RL1*(AK(7)+AK(8)*RL1)
      PHIR(I)= GR+THETAE(I)
```

```
    2 CONTINUE
      CALL LSPFIT(RL,PHIR,NLEANI,RADR,PHI,NRADR,0)
      WRITE(06,12)(THETAE(I),I=1,20),(PHIR(I),I=1,20),(RL(I),I=1,20),
     1 (AK(I),I=1,10),(ALPCOE(I),I=1,3)
   12 FORMAT(1H1,9HTHETAE(I)/2(10F10.4/),7HPHIR(I)/2(10F10.4/),5HRL(I)/
     1 2(10F10.4/),5HAK(I)/10F10.4/9HALPCOE(I)/3F10.4)
      WRITE(06,13)
   13 FORMAT(1H1)
   10 DO 40 I=1,NRADR
      C1SEMI = C1(I)/2.
      C2SEMI = C2(I)/2.
      ALPH1R = 0.0174533*ALPHA1(I)
      ALPH2R = 0.0174533*ALPHA2(I)
      CSALP1 = COS(ALPH1R)
      U = UTIP*RADR(I)
      BETA = ALPH1R+ALPH2R
      OMEGA = C2SEMI*PI*U*SIGMA1(I)/(C1SEMI*V2(I))
      B = BP(I)+C1SEMI*CSALP1+C2SEMI*COS(ALPH2R)
      XPOC1S = (C2SEMI/C1SEMI)*(B/(C2SEMI*CSALP1)+V1(I)/(2.*V2(I)))-RC01
      GO TO(15,20),IPOINT
   15 DELTA = 0.3
      GO TO 25
   20 DELTA = 0.2
      CD5=CD1(I)
   25 FK1 = RC02*V1(I)*CD1(I)*SIN(BETA)*SIGMA1(I)*SQRT(XPOC1S)/
     1 (V2(I)*(XPOC1S+DELTA)*CSALP1)*COS(PHI(I))
      FK2 = -PI*(RC03*SIGMA1(I)/CSALP1)**2*CD1(I)*XPOC1S
      SUM = 0.
      DO 30 M=1,40
      FM=M
      FMOMEG = FM*OMEGA
   26 CONTINUE
      CALL BESSEL(FMOMEG,1,.FALSE.,J,DUMY,TILT)
      IF(TILT) GO TO 45
      FJSSQ = ((J(2)**2+J(1)**2)*(0.1811+FMOMEG))/
       (0.1811+(0.1811*PI+1.)*FMOMEG+2.*PI*FMOMEG**2)
      TERM = FK1*EXP(FM**2*FK2)*SQRT(FJSSQ)
      SUM = SUM+TERM
C     IF(NHARM .NE. 0)  GO TO 35
      IF(DABS(TERM/SUM).LE.1.E-3) GO TO 35
   30 CONTINUE
      WRITE(6,900)
  900 FORMAT(61H0***SUBROUTINE VISCWK. SERIES CONVERGENCE FAULT. RETURNI
     1NG***)
      TILT = .TRUE.
      GO TO 45
   35 GAMMA(I) = (C2SEMI*V2(I)/12.)*SUM
   40 CONTINUE
   45 RETURN
      END
```

```
$       FORTRAN DECK,MAP                                                EIGENL
$       INCODE  IBMF
CEIGEN       EIGENVALUE ROUTINE
C                FORTRAN-Y       22APR
C
C      THIS PROCEDURE DETERMINES THE CONSECUTIVE EIGENVALUES LAMBAY(),
C      ASSOCIATED RESIDUALS RESDAY(),AND COUPLING COEFFICIENTS QAY() OF
C      THE CHARACTERISTIC EQUATION
C
C         Y-(LAMBD    *H)*J-(LAMBD    ) - Y-(LAMBD    )*J-(LAMBD    *H) = 0
C          N       N,M      N       N,M      N       N,M   N       N,M
C
C      FOR A GIVEN RADIUS RATIO H AND SEQUENCE OF MODE NUMBERS N,M
C      (M=MI,MI+1,....,MF) WHERE N AND M =0.
C
C            SUBPROGRAM REFERENCES - CHARFN (EVALUATES CHAR FUNCTION).
C
C
C
       SUBROUTINE EIGEN(H,N,MI,MF,LAMBAY,QAY,RESDAY,TILT)
       DIMENSION QAY(1),RESDAY(1),CONVEC(5)
       DOUBLE PRECISION LAM(3),EPS(3),A,B,C,DISC
       REAL LAMBAY(1),LAMBD,LAMBDZ
       LOGICAL TILT,FLAG
       DATA DELAM/1./,DELAM2/0.5/
       TILT=.FALSE.
       FLAG=.FALSE.
       ICNT=0
       MP1=MI+1
       NROOTS=MF-MI+1
C
C
C
       IF(N.NE.0.OR.MI.NE.0) GO TO 1
C      LAMBD 0,0
       WRITE(6,901)
  901  FORMAT(107H0***SUBROUTINE EIGEN. EIGENVALUE AND COUPLING COEFFICIE
     1NT ARE NOT DEFINED FOR MODE NUMBER 0,0. RETURNING***)
       GO TO 55
     1 IF(N.GT.0) GO TO 2
C      LAMBD 0,MI (MI 0)
       NSNCH=1
       LAMBD=1.
       GO TO 5
C      LAMBD N,MI (N 0,MI=0,1,2,....)
     2 NSNCH=0
       LAMBD=FLOAT(N)
     5 CALL CHARFN(H,LAMBD,N,TILT,EPSN,C)
       IF(TILT) GO TO 55
       IF(EPSN.EQ.0.) GO TO 45
       IF(FLAG) GO TO 15
```

```
      FLAG=.TRUE.
   10 EPSNZ=EPSN
      LAMBDZ=LAMBD
      LAMBD=LAMBDZ+DELAM
      GO TO 5
   15 IF(EPSN*EPSNZ.LT.0.) NSNCH=NSNCH+1
      IF(NSNCH.EQ.MP1) GO TO 20
      GO TO 10

C
   20 LAM(1)=LAMBDZ
      LAM(2)=LAMBDZ+DELAM2
      LAM(3)=LAMBD
      EPS(1)=EPSNZ
      CALL CHARFN(H,SNGL(LAM(2)),N,TILT,EPS2,Q)
      IF(TILT) GO TO 55
      IF(EPS2.EQ.0.) GO TO 50
      EPS(2)=EPS2
      EPS(3)=EPSN
      NITER=0
   25 NITER=NITER+1
      LAMBDZ=LAMBD
      IF(NITER.LE.20) GO TO 25
      WRITE(6,900) ICNT,CONVEC
  900 FORMAT(89H0***SUBROUTINE EIGEN. CONVERGENCE NOT ACHIEVED IN 20 ITE
     1RATIONS. ITERATE HISTORY FOLLOWS./5X,6HLAMBD(I2,3H)=
     2 5(1X,E15.8)/1X,31HCONTINUING WITH LAST ITERATE***)
      GO TO 45
   25 A=((LAM(2)-LAM(1))*EPS(3)+(LAM(1)-LAM(3))*EPS(2)+(LAM(3)-LAM(2))*
     1  EPS(1))/((LAM(3)-LAM(2))*(LAM(2)-LAM(1))**2)
      B=((LAM(2)-LAM(1))*(2.*LAM(3)-LAM(2)-LAM(1))*EPS(3)
     1  -(LAM(3)-LAM(1))**2*EPS(2)+(LAM(3)-LAM(2))**2*EPS(1))/
     2  ((LAM(3)-LAM(2))*(LAM(2)-LAM(1))**2)
      C=(LAM(3)-LAM(1))*EPS(3)/(LAM(2)-LAM(1))
      DISC=DSQRT(B**2-4.*A*C)
      HLAM1=-2.*C/(B+DISC)
      HLAM2=-2.*C/(B-DISC)
      ROOT1=LAM(3)+HLAM1
      ROOT2=LAM(3)+HLAM2
      IF(ROOT1.GT.LAM(1).AND.ROOT1.LT.LAM(3)) GO TO 30
      LAMBD=ROOT2
      GO TO 35
   30 IF(ROOT2.GT.LAM(1).AND.ROOT2.LT.LAM(3)) GO TO 31
      LAMBD=ROOT1
      GO TO 35
   31 IF(B.LT.0.) GO TO 32
      LAMBD=ROOT1
      GO TO 35
```

```
32 LAMBD=RCOT2
35 IF(NITER.GE.16) CONVEC(NITER-15)=LAMBD
   CALL CHARFN(H,LAMBD,N,TILT,EPSN,Q)
   IF(TILT) GO TO 55
   IF(EPSN.EQ.0.) GO TO 45
   IF(ABS((LAMBD-LAMBDZ)/LAMBDZ).LE.1.E-4) GO TO 45
   IF(LAMBD.LT.LAM(2)) GO TO 40
   LAM(1)=LAM(2)
   LAM(2)=LAMBD
   EPS(1)=EPS(2)

   EPS(2)=EPSN
   GO TO 21
40 LAM(3)=LAM(2)
   LAM(2)=LAMBD
   EPS(3)=EPS(2)
   EPS(2)=EPSN
   GO TO 21
50 LAMBD=LAM(2)
   EPSN=0.
45 ICNT=ICNT+1
   LAMBAY(ICNT)=LAMBD
   QAY(ICNT)=Q
   RESDAY(ICNT)=EPSN
   IF(ICNT.EQ.NRCOTS) GO TO 60
   LAMBD=LAMBD+1.
   MP1=MP1+1
   FLAG=.FALSE.
   GO TO 5
55 TILT=.TRUE.
60 RETURN
   END


$       FORTRAN DECK,MAP                                                  +
$       INCODE  IFMF                                                CHARFN
CCHARFN      CHARACTERISTIC FUNCTION
C                FORTRAN-Y       22APR1975
C
C              THIS PROCEDURE EVALUATES THE CHARACTERISTIC FONCTION
C
C           Y-(LAMBDA    *H)*J-(LAMBDA    ) - Y-(LAMBDA    )*J-(LAMBDA    *H)
C            N        N,M      N        N,M      N        N,M   N        N,M
C
C              AND ASSOCIATED COUPLING COEFFICIENT Q FOR A GIVEN
C              H,LAMBDA,AND N (0 =N =1 0).
C
      SUBROUTINE CHARFN(H,LAMBDA,N,TILT,FUNC,Q)
      DIMENSION YLAM(100),YLAMH(100)
      REAL LAMBDA,JLAM(1:2),JLAMH(1:2)
      LOGICAL TILT
      TILT=.FALSE.
```

```
      NM1=N
      NP1=N+2
      CALL BESSEL(LAMBDA,N+1,.TRUE.,JLAM,YLAM,TILT)
      IF(TILT) GO TO 10
      CALL BESSEL(LAMBDA*H,N+1,.TRUE.,JLAMH,YLAMH,TILT)
      IF(TILT) GO TO 10
      IF(N.GT.0) GO TO 5
      FUNC=JLAM(2)-YLAM(2)*JLAMH(2)/YLAMH(2)
      Q=JLAM(2)/YLAM(2)
      GO TO 10
    5 FUNC=(JLAM(NM1)-JLAM(NP1))-(YLAM(NM1)-YLAM(NP1))*(JLAMH(NM1)
     1 -JLAMH(NP1))/(YLAMH(NM1)-YLAMH(NP1))
      Q=(JLAM(NM1)-JLAM(NP1))/(YLAM(NM1)-YLAM(NP1))
   10 RETURN
      END


$       FORTRAN DECK,MAP                                                +
$       INCODE  IBMF                                            RPYCYG
CRPYCYG      POLYNOMIAL-CYLINDER FUNCTION INTEGRAL
C               FORTRAN-Y       22APR1975
C
C            THIS PROCEDURE EVALUATES THE REAL INTEGRAL
C
C                        *RUPPER
C                       *
C              RINTG = * R**P*Z  (LAMBDA*R)*DR
C                       *        N
C                      *RLOWER
C
      SUBROUTINE RPYCYG(P,N,LAMBDA,RLOWER,RUPPER,CYL,RINTG,TILT)
      INTEGER P,PM1
      REAL LAMBDA
      DIMENSION CYL(110,2)
      LOGICAL TILT
      DIMENSION SUM(2),R(2)
      REAL INTZNP
C
C ...ARGUMENT CHECK...
      IF(P.GE.1.AND.N.GE.0) GO TO 5
      WRITE(6,900) N,P,LAMBDA,RLOWER,RUPPER
  900 FORMAT(41H0***SUBROUTINE RPYCYG. ARGUMENT FAULT. N=I3,3H,P=I2,
     1 8H,LAMBDA= E15.8,8H,RLOWER=F8.5,8H,RUPPER=F8.5,14H. RETURNING***)
      TILT = .TRUE.
      GO TO 70
C
C ...PI 1...
    5 NMP = N-P
      PI01 = 1.
      DO 10 J=1,P
   10 PI01 = PI01*FLOAT(NMP+2*J-1)
```

```
C
C ...INDICES...
      PM1 = P-1
      NP2 = N+2
      NPP = N+P
      IPOINT = MOD(NPP,2)+1
      GO TO(15,20),IPOINT
C    ..(N+P) EVEN..
   15 INDX1 = NPP/2-1
      GO TO 25
C    ..(N+P) ODD..
   20 INDX1 = (NPP-1)/2-1

C
C ...LIMITS LOOP...
   25 R(1) = RLOWER
      R(2) = RUPPER
      RCO1 = -1./LAMBDA
      DO 65 I=1,2
C    ..COMPONENT 1..
      SUM(I) = R(I)**P*CYL(NP2,I)/LAMBDA
      IF(PM1.LT.1) GO TO 40
C    ..COMPONENT 2 (SUMMATION OVER K=1,P-1)..
      DO 35 K=1,PM1
      PIO2 = 1.
      DO 30 J=1,K
   30 PIO2 = PIO2*FLOAT(NMP+2*J-1)
      INDX = NP2+K
      SUM(I) = SUM(I)+R(I)**(P-K)*CYL(INDX,I)*PIO2/LAMBDA**(K+1)
   35 CONTINUE
C    ..COMPONENT 3..
   40 INTZNP = 0.
      IF(INDX1.LT.1) GO TO 50
      INDX2 = INDX1+1
      DO 45 KK=1,INDX2
      K = KK-1
      INDX = NPP-2*K
   45 INTZNP = INTZNP+CYL(INDX,I)
      INTZNP = 2.*RCO1*INTZNP
   50 GO TO(60,55),IPOINT
   55 INTZNP = INTZNP+RCO1*CYL(1,I)
      GO TO 65
   60 CALL ASTRUM(LAMBDA*R(I),HOLAMR,TILT)
      IF(TILT) GO TO 70
      INTZNP = INTZNP+R(I)*(CYL(1,I)+1.5707963*(HOLAMR*CYL(2,I)
     -HOLAMR*CYL(1,I)))
   65 SUM(I) = SUM(I)+PM1*INTZNP/LAMBDA**P
      RINTG = SUM(2)-SUM(1)
   70 RETURN
      END
```

```
$       FORTRAN DECK,MAP
$       INCODE  IBMF
CRSTRUV      REAL STRUVE FUNCTIONS - H0(X),H1(X) -
C                FORTRAN-Y       22APR1975
C
      SUBROUTINE RSTRUV(X,HOX,H1X,TILT)
      LOGICAL TILT
      REAL JX(31)
      DIMENSION YX(2)
      LOGICAL NEGX
      TILT = .FALSE.
C
C ***ARGUMENT TYPE***
      ABSX = ABS(X)
      IF(ABSX.NE.0.) GO TO 5
C    ..SPECIAL CASE. X=0..
      H0X = 0.
      H1X = 0.
      GO TO 45
    5 NEGX = .FALSE.
      IF(X.LT.0.) NEGX = .TRUE.
      IF(ABSX.GE.10.) GO TO 40
C
C ***ABS(X) 1 ***
      CALL BESSEL(ABSX,30,.FALSE.,JX,DUMY,TILT)
      IF(TILT) GO TO 50
      IF(.NOT.NEGX) GO TO 15
      DO 10 I=2,30,2
   10 JX(I) = -JX(I)
C    ..H0(X) - AMS 55(12.1.19)..
   15 SUM = JX(2)
      DO 20 K=1,14
      TERM = JX(2*K+2)/FLOAT(2*K+1)
      IF(ABS(TERM/SUM).LE.1.E-6) GO TO 25
      SUM = SUM+TERM
   20 CONTINUE
   21 WRITE(6,900) X
  900 FORMAT(25H0***SUBROUTINE RSTRUV. X=E15.8,40H. SERIES CONVERGENCE F
     1AULT. RETURNING***)
      GO TO 50
   25 SUM = SUM+TERM
      H0X = 1.2732395*SUM
C    ..H1(X) - AMS 55(12.1.20)..
      SUM = JX(3)/3.
      DO 30 K=2,15
      TERM = JX(2*K+1)/FLOAT(4*K**2-1)
      IF(ABS(TERM/SUM).LE.1.E-6) GO TO 35
      SUM = SUM+TERM
   30 CONTINUE
      GO TO 21
```

```
   35 SUM = SUM+TERM
      H1X = 0.6366198*(1.-JX(1))+1.2732395*SUM
      GO TO 45
C
C ***ABS(X) =10***

   40 CALL BESSEL(ABSX,1,.TRUE.,JX,YX,TILT)
      IF(TILT) GO TO 50
C    ..H0(X),H1(X) - AMS 55(12.1.30),(12.1.31),(12.1.18)..
      T = 1./ABSX
      TSQ = T**2
      HOX = YX(1)+0.6366198*T*(1.-TSQ*(1.-TSQ*(9.-225.*TSQ)))
      IF(NEGX) HOX = -HOX
      H1X = YX(2)+0.6366198*(1.+TSQ*(1.-TSQ*(3.-45.*TSQ)))
C
   45 RETURN
   50 TILT = .TRUE.
      CALL FXEM(66)
      GO TO 45
      END
```

```
$       FORTRAN DECK,MAP,DEBUG,LSTOU,XREF                                BESSEL
$       INCODE  IBMF
CBESSEL      1ST-2ND KIND BESSEL FUNC (REAL ARG)                         BESSE001
C               FORTRAN-Y       22APR1975
C                                                                        BESSE002
C            THIS PROCEDURE EVALUATES BESSEL FUNCTIONS OF THE FIRST      BESSE003
C            AND SECOND KINDS OF REAL POSITIVE ARGUMENT X AND REAL       BESSE004
C            INTEGER ORDERS P=0,1,2,...,N. SCKIND IS A LOGICAL INDICATOR BESSE005
C            SPECIFYING WHETHER OR NOT SECOND KIND FUNCTIONS ARE         BESSE006
C            DESIRED. FIRST AND SECOND KIND FUNCTIONS ARE RETURNED IN    BESSE007
C            REAL VECTORS J AND Y RESPECTIVELY FROM LOW TO HIGH ORDER    BESSE008
C            (N+1 ELEMENTS EACH). THE LOGICAL INDICATOR TILT WILL BE     BESSE009
C            .TRUE. ON RETURN FROM BESSEL IF FATAL DIFFICULTIES ARISE.   BESSE010
C                                                                        BESSE011
C                                                                        BESSE012
C                                                                        BESSE013
C                                                                        BESSE014
C                                                                        BESSE015
C                                                                        BESSE016
C                                                                        BESSE017
C         ***AUXILIARY SUBPROGRAMS***                                    BESSE018
C              ALNGAM - NATURAL LOG OF GAMMA FUNCTION                    BESSE019
C                                                                        BESSE020
C                                                                        BESSE021
C                                                                        BESSE022
C                                                                        BESSE023
      SUBROUTINE BESSEL(X,N,SCKIND,J,Y,TILT)                             BESSE024
      REAL J(1)                                                          BESSE025
      DIMENSION Y(1)                                                     BESSE026
      LOGICAL SCKIND,TILT                                                BESSE027
      DIMENSION F(300)                                                   BESSE028
      REAL JOX                                                           BESSE029
      CALL FXOPT(69,1,1,0)
      TILT = .FALSE.                                                     BESSE030
C                                                                        BESSE031
C ***ARGUMENT CHECK***                                                   BESSE032
      IF(X.GE.0.0.AND.N.LE.100) GO TO 5                                  BESSE033
      WRITE(6,900) X,N,SCKIND                                            BESSE034
  900 FORMAT(25H0***SUBROUTINE BESSEL. X= E15.8,3H N=I3,8H SCKIND=L2,    BESSE035
     1 29H ARGUMENT FAULT. RETURNING***)                                 BESSE036
      GO TO 165                                                          BESSE037
    5 IF(X.NE.0.) GO TO 20                                               BESSE038
C                                                                        BESSE039
      J(1) = 1.                                                          BESSE040
      IF(N.EQ.0) GO TO 15                                                BESSE041
      NP1 = N+1                                                          BESSE042
      DO 10 I=2,NP1                                                      BESSE043
   10 J(I) = 0.                                                          BESSE044
   15 IF(.NOT.SCKIND) GO TO 160                                          BESSE045
      WRITE(6,905) X,N,SCKIND                                            BESSE046
  905 FORMAT(25H0***SUBROUTINE BESSEL. X= E15.8,3H N=I3,8H SCKIND=L2,    BESSE047
     1 47H Y(0,0) GOES TO NEGATIVE INFINITY. RETURNING***)               BESSE048
      GO TO 165                                                          BESSE049
C                                                                        BESSE050
C                                                                        BESSE051
```

```
   20 CALL OVERFL(IOVFL)                                                BESSE052
      RC01 = ALOG10(0.5*X)                                              BESSE053
      RC02 = 0.57721566+ALOG(0.5*X)                                     BESSE054
      INDXAP = IFIX(X)+2                                                BESSE055
      M = MAX0(N,IFIX(X))-10                                            BESSE056
      NP1 = N+1                                                         BESSE057
C                                                                       BESSE058
C                                                                       BESSE059
   25 M = M+10                                                          BESSE060
      MP1 = M+1                                                         BESSE061
      DO 30 I=1,MP1                                                     BESSE062
      MPRM = MP1-I                                                      BESSE063
C             (MPRM=M,M-1,M-2,...,2,1,0)                                BESSE064
      FMPRM = MPRM                                                      BESSE065
      EXPJNX = FMPRM*RC01-0.43429448*ALNGAM(FMPRM+1.)                   BESSE066
      IF(EXPJNX.GT.(-20.)) GO TO 35                                     BESSE067
   30 CONTINUE                                                          BESSE068
      WRITE(6,910) X,N,SCKIND                                           BESSE069
  910 FORMAT(25H0***SUBROUTINE BESSEL. X= E15.8,3H N=I3,8H SCKIND=L2,   BESSE070
     1 35H J(X) AMPLITUDE FAULT. RETURNING***)                          BESSE071
      GO TO 165                                                         BESSE072
   35 MPRMP1 = MPRM+1                                                   BESSE073
      IF(MPRM.GE.N) GO TO 45                                            BESSE074
      MPRMP2 = MPRM+2                                                   BESSE075
      DO 40 I=MPRMP2,NP1                                                BESSE076
   40 J(I) = 0.                                                         BESSE077
C                                                                       BESSE078
C ***FIRST KIND FUNCTION J(X)***                                        BESSE079
C                                                                       BESSE080
   45 L = MPRMP1                                                        BESSE081
      IF(MOD(L,2).NE.0) L = L+1                                         BESSE082
      IFLAG = 1                                                         BESSE083
C                                                                       BESSE084
   50 L = L+4                                                           BESSE085
      IF(L.LE.250) GO TO 55                                             BESSE086
      WRITE(6,915) X,N,SCKIND                                           BESSE087
  915 FORMAT(25H0***SUBROUTINE BESSEL. X= E15.8,3H N=I3,8H SCKIND=L2,   BESSE088
     1 50H INTERNAL STORAGE (F ARRAY) EXCEEDED. RETURNING***)           BESSE089
      GO TO 165                                                         BESSE090
   55 LM1 = L-1                                                         BESSE091
      LP1 = L+1                                                         BESSE092
      F(L+2) = 0.                                                       BESSE093
      F(LP1) = 1.E-30                                                   BESSE094
      DO 60 II=1,L                                                      BESSE095
      I = L-II+2                                                        BESSE096
C             (I=L+1,L,L-1,...,4,3,2)                                   BESSE097
      F(I-1) = 2.*FLOAT(I-1)*F(I)/X-F(I+1)                              BESSE098
      CALL OVERFL(IOVFL)                                                BESSE099
   60 CONTINUE                                                          BESSE106
      IF(X.LT.10.) GO TO 64                                             BESSE107
```

```
C
C                                                                       BESSE108
      IF(IFLAG.EQ.2) GO TO 63                                           BESSE109
      T = 1./X                                                          BESSE110
      TSQ = T*T                                                         BESSE111
      JOX = (1.+TSQ*(-0.625E-1+TSQ*(0.10351562E0+TSQ*(-0.54284668E0     BESSE112
     1 +TSQ*(0.58496996E1-TSQ*0.1068679E3)))))* SQRT(0.6366198*T)       BESSE113
     2 * COS(1./T+T*(-0.125E0+TSQ*(0.65104167E-1+TSQ*(-0.20957031E0     BESSE114
     3 +TSQ*(0.16380463E1-TSQ*0.23475128E2))))-0.78539815)              BESSE115
   63 SUM = F(1)/JOX                                                    BESSE116
      IF(ABS(SUM).NE.0.) GO TO 66                                       BESSE117
      WRITE(6,921) X,N,SCKIND,JOX                                       BESSE118
  921 FORMAT(25H0***SUBROUTINE BESSEL. X= E15.8,3H N=I3,8H SCKIND=L2/   BESSE119
     1 5X,55H UNDERFLOW FAULT IN PHASE-AMPLITUDE APPROXIMATION (JOX=    BESSE120
     2  E15.8,15H). RETURNING***)                                       BESSE121
      GO TO 165                                                         BESSE122
C                                                                       BESSE123
   64 SUM = 1.E-30                                                      BESSE124
      DO 65 II=1,LM1,2                                                  BESSE125
      I = L-II                                                          BESSE126
C               (I=L-1,L-3,L-5,....,5,3,1)                              BESSE127
   65 SUM = SUM+F(I)                                                    BESSE128
      SUM = 2.*SUM-F(1)                                                 BESSE129
   66 APROX1 = F(INDXAP)/SUM                                            BESSE130
      GO TO(70,75),IFLAG                                                BESSE131
   70 APROX2 = APROX1                                                   BESSE132
      IFLAG = 2                                                         BESSE133
      GO TO 50                                                          BESSE134
   75 DELTA = APROX1-APROX2                                             BESSE135
      ERR=ABS(DELTA/APROX2)                                             BESSE136
      IF(ERR .LE. 9.E-6)  GO TO 90
      IF(IOVFL .NE. 1)  GO TO 80
      IF(ERR .LE. 9.E-4)  GO TO 90
      WRITE(6,920) X,N,SCKIND,ERR
  920 FORMAT(25H0***SUBROUTINE BESSEL. X= E15.8,3H N=I3,8H SCKIND=L2/   BESSE102
     1 5X,56H OVERFLOW FAULT IN BACKWARD RECURRENCE FOR J(X). ERROR= ,
     X  F10.8)
      GO TO 90
   80 APROX2=APROX1
      GO TO 50                                                          BESSE139
C                                                                       BESSE140
   90 DO 95 I=1,LP1                                                     BESSE141
   95 F(I) = F(I)/SUM                                                   BESSE142
      K = NP1                                                           BESSE143
      IF(L.LT.N) K = LP1                                                BESSE144
      DO 100 I=1,K                                                      BESSE145
  100 J(I) = F(I)                                                       BESSE146
  105 IF(.NOT.SCKIND) GO TO 160                                         BESSE147
C                                                                       BESSE148
```

```
C ***SECOND KIND FUNCTION Y(X)***
  110 IF(L.LT.6) GO TO 25
C
      SUM = F(3)
      LO2 = L/2
      DO 125 I=2,LO2
      TERM = (-1.)**(I-1)*F(2*I+1)/FLOAT(I)
      IF( ABS(TERM/SUM).LE.1.E-6) GO TO 130
      SUM = SUM+TERM
  125 CONTINUE
      GO TO 25
  130 SUM = SUM+TERM
      Y(1) = 0.6366198*(RCO2*F(1)+2.*SUM)

      IF(N.EQ.0) GO TO 160
C
      SUM = F(4)-F(2)
      LM2O2 = (L-2)/2
      DO 145 I=2,LM2O2
      TERM = (-1.)**I*(F(2*I)-F(2*I+2))/FLOAT(I)
      IF( ABS(TERM/SUM).LE.1.E-6) GO TO 150
      SUM = SUM+TERM
  145 CONTINUE
      GO TO 25
  150 SUM = SUM+TERM
      Y(2) = 0.6366198*(RCO2*F(2)-F(1)/X+SUM)
      IF(N.EQ.1) GO TO 160
C
      DO 155 I=3,NP1
      Y(I) = 2.*FLOAT(I-2)*Y(I-1)/X-Y(I-2)
      CALL OVERFL(IOVFL)
      IF(IOVFL.NE.1) GO TO 155
      IM1 = I-1
      WRITE(6,925) X,N,SCKIND,IM1
  925 FORMAT(25H0***SUBROUTINE BESSEL. X= E15.3,3H N=I3,8H SCKIND=L2/
     1 5X,56H OVERFLOW FAULT IN FORWARD RECURRENCE FOR Y(X) AT ORDER I3)
  155 CONTINUE
C
  160 RETURN
  165 TILT = .TRUE.
      CALL EXERM( 66 )
      GO TO 160
      END
```

```
$       FORTRAN DECK,MAP                                                  +
$       INCODE  IBMF                                                 PRECAL
CPRECAL      PRELIMINARY CALCULATIONS
C                 FORTRAN-Y   22APR1975
C
      SUBROUTINE PRECAL(*)
      COMMON/INPBLK/TITLE(10),MODE,MECH(5),NMECH,HUBRAD,TIPRAD,NBLADE,
     1 NVANES,SPEED,INPLOB,LOBNO(5),NLOBNO,INPNIN,INFLEC(5),NHARM,PSTAT,
     2 TSTAT,TET,DELLAM,LAMBAY(20,5),QAY(20,5),OPRAD(20),NOPRAD,NRADP,
     3 RADTAB(5),BETA1A(5),BETA1R(5),BETA2A(5),BETA2R(5),BETA3A(5),
     4 BETA3R(5),SIGMA1(5),SIGMA2(5),BP(5),INPCD1,CD1(5),PUNCH
     5 ,EFLEAN,ALPHA(5),C,LAMBDA(10,5),RHO,GAM,DYVISC
      LOGICAL EFLEAN,INPLOB,INPNIN,DELLAM,INPCD1,PUNCH
      COMPLEX LAMBDA
      COMMON/PRCBLK/NRLSAY(5),RADRTB(5),OPRR(20),AK(10),
     1 RHUB,ALPCOE(3),GPRM1,GONE
C    PRECAL
      COMMON /CLEAN1/ FLEAN1,NLEANI,RL(20)
      LOGICAL FLEAN1
      DIMENSION DUMY(5),V1(5),V2(5),ALPHA1(5),ALPHA2(5),C1(5),C2(5),
     1 GAMTAB(5),RES(3),THETAE(5),ALPHAR(5)
      LOGICAL TILT
      INTEGER TURBIN,ROVSWK
      DATA PI,RDPRDG/3.14159,0.0174533/
      DATA TURBIN/6HTURBIN/
      DATA IRVSWK,ROVSWK/6HIRVSWK,6HROVSWK/
C
C
      IF(.NOT. INPLOB)  GO TO 10
      DO 5  I=1,NLOBNO
    5 NRLSAY(I)=LOBNO(I)
      GO TO 15
   10 CALL LOBNUM(NHARM,NBLADE,NVANES,LOBNO,DUMY)
      CALL LOBNUM(1,NBLADE,NVANES,NRLSAY,DUMY)
   15 DO 20  I=1,NLOBNO
      IF(NRLSAY(I) .NE. 0)  GO TO 20
      WRITE(6,905)
  905 FORMAT(36H0***ANALYSIS INDICATES PLANE WAVE***)
      GO TO 130
   20 CONTINUE
C
C
      IF(INPNIN) GO TO 30
      DO 25 I=1,NLOBNO
   25 INFLEC(I) = NRADMO(LOBNO(I))
C
C
   30 DO 35 I=1,NRADP
      ALPHAR(I) = RDPRDG*ALPHA(I)
   35 RADRTB(I) = RADTAB(I)/TIPRAD
```

```
      IF(NOPRAD.EQ.0) GO TO 45
      DO 40 I=1,NOPRAD
   40 OPRR(I) = OPRAD(I)/TIPRAD
C
C    *CURVE FIT PHYSICAL LEAN ANGLES*
      DO 41 I=1,NRADP
      IF(ALPHAR(I).EQ.0.) GO TO 41
      K = 2
      CALL BESFIT(NRADP,RADRTB,ALPHAR,K,ALPCOE,RES)
      IF(K.LE.1) ALPCOE(3) = 0.
      IF(K.EQ.0) ALPCOE(2) = 0.
      GO TO 45
   41 CONTINUE
      ALPCOE(1) = 0.
      ALPCOE(2) = 0.
      ALPCOE(3) = 0.
C
C
   45 BLADES = NBLADE
      VANES = NVANES
      UTIP = SPEED*PI*TIPRAD/360.
      DYVISC=2.27E-8*TSTAT**1.5/(TSTAT+198.6)
      GAMEXP = EXP(5500./TSTAT)
      GAMA = 1.+0.4/(1.+0.4*(5500./TSTAT)**2*GAMEXP/(GAMEXP-1.)**2)
      C = SQRT(1716.4829*GAMA*TSTAT)
C                    NOTE ( 1716.4829 = 53.35*GSUBC )
      RHO = PSTAT/(53.35*TSTAT)
      RHUB = HUBRAD/TIPRAD
      ARG = RDPRDG*BETA2A(1)
      BRG=RDPRDG*BETA2R(1)
      RCO3=(BP(1)/RADTAB(1))*SIN(BRG)/COS(BRG)
      RCO1 = (BP(1)/RADTAB(1))*SIN(ARG)/COS(ARG)
      SNALP = SIN(ALPHAR(1))
      CSALP = COS(ALPHAR(1))
      ALPPRM = ALPCOE(2)+2.*ALPCOE(3)*RADRTB(1)
      RCO2 = RCO1*COS(ATAN(ALPPRM+(-ALPPRM*CSALP+SNALP/RADRTB(1))/
     1 SQRT(1.-SNALP**2)))
      IF(MECH.NE.IRVSWK) GO TO 50
      IPOINT = 1
      GO TO 60
   50 IF(MECH.NE.ROVSWK) GO TO 55
      IPOINT = 2
      GO TO 60
   55 WRITE(6,910) MECH
  910 FORMAT(//5X,27H*INVALID MECHANISM. MECH = A6,1H*)
      GO TO 130
    6 DO 75 I=1,NRADP
      B1AR = RDPRDG*BETA1A(I)
      B1RR = RDPRDG*BETA1R(I)
      B2AR = RDPRDG*BETA2A(I)
      B2RR = RDPRDG*BETA2R(I)
      B3AR = RDPRDG*BETA3A(I)
```

```
      B3RR = RDPRDG*BETA3R(I)
      SANG1 = B1AR+B1RR
      SANG2 = B2AR+B2RR
      SANG3 = B3AR+B3RR
      U = UTIP*RADRTB(I)
      ARG2 = 2.*PI*RADRTB(I)*TIPRAD
      V2A = U*COS(B2RR)/SIN(SANG2)
      V2R = U*COS(B2AR)/SIN(SANG2)
      HB = TIPRAD-HUBRAD
      SNALP = SIN(ALPHAR(I))
      CSALP = COS(ALPHAR(I))
      GO TO(65,70),IPOINT
C     *I-R*
   65 V1(I) = V2A
      ALPHA1(I) = BETA2A(I)
      V2(I) = V2R
      ALPHA2(I) = BETA2R(I)
      V3A = U*COS(B3RR)/SIN(SANG3)
      CZ = V2A*COS(B2AR)
      DELCU1 = ABS(CZ*SIN(B1AR)/COS(B1AR)-V2A*SIN(B2AR))
      DELCU2 = ABS(V2A*SIN(B2AR)-V3A*SIN(B3AR))
      C1(I) = ARG2*SIGMA1(I)/VANES
      C2(I) = ARG2*SIGMA2(I)/BLADES
      ALPPRM = ALPCOE(2)+2.*ALPCOE(3)*RADRTB(I)
      THETAE(I)=(BP(I)/RADTAB(I))*SIN(B2AR)/COS(B2AR)-RCO1
      IF(INPCD1) GO TO 75
   66 EPS = BETA1A(I)+BETA2A(I)
      EPSP = 4.1486E-2+EPS*(3.9976E-4+EPS*(-3.4270E-6+EPS*5.4403E-8))
      EPSPP = (1.+EPSP)*(0.975)-1.0
      DH = (2.*HB*ARG2*COS(B2AR)/VANES)/(ARG2*COS(B2AR)/VANES+HB)
      RH = RHO*V2A*DH/(336.088*DYVISC)
      FM2 = V2A/C
      EPSPPP =((1.E5/RH)**0.25*EPSPP)/(1.-FM2**2/4.+(2.-GAMA)*FM2**4/24.
     1)
      TANB1A = SIN(B1AR)/COS(B1AR)
      TANB2A = SIN(B2AR)/COS(B2AR)
      ALPHAM = ATAN((TANB1A+TANB2A)/2.)
      CD1(I)=EPSPPP/(SIGMA1(I)*2.0)
      GO TO 75
C     *R-O*
   70 V1(I) = V2R
      ALPHA1(I) = BETA2R(I)
      V2(I) = V2A
      ALPHA2(I) = BETA2A(I)
      V1A = U*COS(B1RR)/SIN(SANG1)
      V1R = U*COS(B1AR)/SIN(SANG1)
      DELCU1 = ABS(V1A*SIN(B1AR)-V2A*SIN(B2AR))
      CZ = V2A*COS(B2AR)
      DELCU2 = ABS(V2A*SIN(B2AR)-CZ*SIN(B3AR)/COS(B3AR))
      C1(I) = ARG2*SIGMA1(I)/BLADES
```

```
      C2(I) = ARG2*SIGMA2(I)/VANES
      THETAE(I)=(BP(I)/RADTAB(I))*SIN(B2RR)/COS(B2RR))-RCO3
      IF(INPCD1) GO TO 75

   71 EPS = BETA1R(I)+BETA2R(I)
      EPSP = 4.1486E-2+EPS*(3.9975E-4+EPS*(-3.4270E-6+EPS*5.4403E-8))
      EPSPP = (1.+EPSP)*(0.975)-1.0
      DH = (2.*HB*ARG2*COS(B2RR)/BLADES)/(ARG2*COS(B2RR)/BLADES+HB)
      RH = RHO*V2R*DH/(386.088*DYVISC)
      EPSPPP =((1.E5/RH)**0.25*EPSPP)/(1.-FM2**2/4.+(2.-GAMA)*FM2**4/24.
     1)
      FM2 = V2R/C
      TANB1R = SIN(B1RR)/COS(B1RR)
      TANB2R = SIN(B2RR)/COS(B2RR)
      ALPHAM = ATAN((TANB1R+TANB2R)/2.)
      CD1(I)=EPSPPP/(SIGMA1(I)*2.0)
   75 CONTINUE
      IF(FLEAN1) GO TO 80
      AK(6) = 0.
      AK(7) = 0.
      AK(8) = 0.
      THETAE(NRADP) = 0.
      GO TO 85
   80 K = 2
      CALL BESFIT(NRADP,RADRTB,THETAE,K,AK(6),RES)
      IF(K.LE.1) AK(8) = 0.
      IF(K.EQ.0) AK(7) = 0.
      IF(FLEAN1) GO TO 129
C
C     *EIGENVALUE BOUNDARY CONDITION*
   85 GO TO(86,87),IPOINT
   86 ARG = ALPHAR(NRADP)+THETAE(NRADP)
      SNARG = SIN(ARG)
      CSARG = COS(ARG)
      ARG2 = ALPCOE(2)+2.*ALPCOE(3)+AK(7)+2.*AK(8)
      GPRM1 = ARG2+RHUB*(-ARG2*CSARG+SNARG)/
     . SQRT(1.-(RHUB*SNARG)**2)
      GONE = ALPHAR(NRADP)+THETAE(NRADP)-ARCSIN(RHUB*SNARG)
      GO TO 100
   87 GPRM1 = GPRMR(1.)-(AK(7)+2.*AK(8))
      GONE = GOFR(1.)-THETAE(NRADP)
C
C
  100 CALL VISCWK(UTIP,RADRTB,ALPHA1,ALPHA2,V1,V2,SIGMA1,C1,C2,BP,
     . CD1,NRADP,AK,ALPCOE,TET,MODE,IPOINT,GAMTAB,NHARM,TILT)
      IF(TILT) GO TO 130
      DO 120 I=1,NRADP
      IF(GAMTAB(I).NE.0.) GO TO 120
      WRITE(6,945)
  945 FORMAT(/49X,23HNEGLIGIBLE CONTRIBUTION)
```

```
      GO TO 130
  120 CONTINUE
      K = 2
      CALL BESFIT(NRADP,RADRTB,GAMTAB,K,AK,RES)
      IF(K.LE.1) AK(3) = 0.
      IF(K.EQ.0) AK(2) = 0.
      AK(4) = K
C
  129 RETURN

  130 RETURN 1
      END


$     FORTRAN DECK,MAP                                                  GOFR
$     INCODE  IBMF
CGOFR       G(R) FOR LEANED VANE
C                FORTRAN-Y   22APR1975
      FUNCTION GOFR(R)
      COMMON/PRCBLK/NRLSAY(5),RADRTB(5),OPRR(20),AK(10),
     1 RHUB,ALPCOE(3),GPRM1,GONE
      IF(R.GT.RHUB) GO TO 5
      GOFR = 0.0
      GO TO 10
    5 ALPHAR = ALPCOE(1)+R*(ALPCOE(2)+R*ALPCOE(3))
      GOFR = ALPHAR-ARCSIN(RHUB*SIN(ALPHAR)/R)
   10 RETURN
      END


$     FORTRAN DECK,MAP                                                  GPRMR
$     INCODE  IBMF
CGPRMR      G-(R) FOR LEANED VANE
C                FORTRAN-Y   22APR1975
      FUNCTION GPRMR(R)
      COMMON/PRCBLK/NRLSAY(5),RADRTB(5),OPRR(20),AK(10),
     1 RHUB,ALPCOE(3),GPRM1,GONE
      IF(R.GE.RHUB) GO TO 5
      GPRMR = 0.0
      GO TO 10
    5 ALPHAR = ALPCOE(1)+R*(ALPCOE(2)+R*ALPCOE(3))
      SINALP = SIN(ALPHAR)
      COSALP = COS(ALPHAR)
      DALPDR = ALPCOE(2)+2.*ALPCOE(3)*R
      GPRMR = DALPDR-RHUB*(COSALP*DALPDR-SINALP/R)/
     1 (R*SQRT(1.-(RHUB*SINALP/R)**2))
   10 RETURN
      END
```

APPENDIX B

INTERACTION EFFECTS

The parametric study was accomplished using Program HAYSTK. The coding provided is in Fortran IV for time-share usage.

Input - Data input is through lines 100 - 140. Lines 100, 110 & 120 provide the physical and aerodynamic parameters. Lines 130 and 140 define the shear layer model.

A1 - shear layer thickness spread rate

A2 - constant in (A + L/D), set to 1

A3 - constant defining relationship between shear layer thickness and turbulence volume.

D2 - fan nozzle exit diameter, ft.

F1 - incident tone frequency, Hz

F2 - output frequency, set to zero in data input

T2 - fan stream static temperature, ° R

V2 - fan stream velocity, ft/sec

X2 - distance between core and nozzle exhaust planes, ft.

Y2 - ratio of V_{phase}/V_{fan}

Y3, Y4 - constants defining eddy size as a function of shear layer thickness and jet exit Mach number.

In addition, the angle between the incident wave direction and observer can be set in line 145 (P2) in degrees.

Output - May be controlled through addition and deletion of Print statements. The following are pertinent:

B1 - shear layer thickness, ft.

B2 - α

B3 - η

F4 - correlation frequency, $\omega_c/2\pi$, Hz

S1 - $10 \log_{10} (1 + L/D_o)$

S3 - $10 \log_{10}$ (Angle Factor for S6)

S6 - $10 \log_{10} [I_s/(A_o/\rho c r^2)$ for $\theta = 0]$, this is the scattered overall intensity

S7 - $10 \log_{10}$ (angle factor for S8)

S8 - $10 \log_{10} [I(\omega)/A_o^2/\rho c r^2)$, this is the spectral distribution of the scattered wave.

X4 - correlation length of eddies, ℓ_c, ft

TYPICAL OUTPUT " HAYSTK "

THETA	ANGLE FACTOR	DELTA
0.	63.0	45.1
10.0	10.1	7.8

TONE FREQ= 6300.0 JET VEL= 509.0 (1+L/D)= 2.7

ALPHA= 1.85 ETA= 15.31

CORR. L= 0.8041 CORR. FREQUENCY= 411.4

FREQUENCY	ANGLE FACTOR	INTENSITY
5900.0	-9.1	-20.9
5920.0	-8.2	-20.0
5940.0	-7.4	-19.1
5960.0	-6.6	-18.2
5980.0	-5.8	-17.4
6000.0	-5.1	-16.6
6020.0	-4.5	-15.9
6040.0	-3.8	-15.2
6060.0	-3.3	-14.6
6080.0	-2.7	-14.0
6100.0	-2.3	-13.5
6120.0	-1.8	-13.0
6140.0	-1.5	-12.6
6160.0	-1.1	-12.2
6180.0	-0.8	-11.8
6200.0	-0.6	-11.5
6220.0	-0.4	-11.3
6240.0	-0.2	-11.0
6260.0	-0.1	-10.9
6280.0	-0.0	-10.7
6300.0	-0.0	-10.7
6320.0	-0.0	-10.6
6340.0	-0.1	-10.7
6360.0	-0.2	-10.7
6380.0	-0.4	-10.8
6400.0	-0.6	-11.0
6420.0	-0.8	-11.2
6440.0	-1.1	-11.4
6460.0	-1.5	-11.7
6480.0	-1.8	-12.0
6500.0	-2.3	-12.4
6520.0	-2.7	-12.8
6540.0	-3.3	-13.3
6560.0	-3.8	-13.8
6580.0	-4.5	-14.4
6600.0	-5.1	-15.0
6620.0	-5.8	-15.6
6640.0	-6.6	-16.3
6660.0	-7.4	-17.1
6680.0	-8.2	-17.9
6700.0	-9.1	-18.7

```
*RESAVE HAYSTK
DATA SAVED-HAYSTK
*
```

PROGRAM LISTING " HAYSTK "

```
 LS@ISTH
09/02/75 eb 09.00

10C   PARAMETRIC STUDY OF HAYSTACKING ANALYSIS
20C   INPUT: TONE FREQUENCY
100 DATA F1,F2/6300.,0./
110 DATA T2,V2/525.,509./
120 DATA D2,X2/6.11,10./
130 DATA Y2,Y3,Y4/.65,.4,.38/
140 DATA A1,A2,A3/.21,1.0,1.0/
145 P2=0.
146 P9=P2
150 C=49.01*SQRT(T2)
160 Z2=V2/C
170C   REM TURBULENCE M3 ASSUMED CONSTANT
180 Z3=0.15*Z2
190 B1=A1*(X2+0.2*D2)
200 X4=Y3*B1/(1.0+Y4*Z2)
210 V4=Y2*V2
220 F4=V4/X4
230 B2=2.0*3.14159*Y2*Z2
240 B3=F1/F4
250 V=A3*B1
251 X1=1.0+X2/6.0
289 C2=B2**2
290 C3=B3**2
292 X5=(3.0/SQRT(2.0*3.14159))*V*Z3**2/X4
294 S5=10.0*ALOG(X5)/ALOG(10.0)
295 PRINT," THETA          ANGLE FACTOR          DELTA"
298 I1=10
299 IF(P2.GT.0)I1=1
300 DO 50 I=1,I1
310 P2=FLOAT((I-1)*10)
311 IF(P9.GT.0)P2=P9
315 P3=3.14159*P2/180.0
320 P4=P3/2.0
330 G3=-C2*C3*(4.0*(SIN(P4))**2+C2*(SIN(P3))**2)/(2.0*(1.+C2))
340 F3=(1.0+2.0*C3*(1.0+C2*COS(P3))**2+C3**2*(1.0+C2*COS(P3))
345&**4/3.0)
350 H3=C2**2/SQRT  ( (1.0 +C2) ** 5)
360 X3=H3*F3*EXP(G3)
361 IF(X3.LE.10E-09)GO TO 50
362 S3=10.0*ALOG(X3)/ALOG(10.0)
364 X6=X5*X3
366 S6=10.0*ALOG(X6)/ALOG(10.0)
367 PRINT 40,P2,S3,S6
370 50 CONTINUE
400 PRINT 10,F1,V2,X1
410 10 FORMAT(1X,"TONE FREQ= ",F7.1,5X,"JET VEL= ",F7.1,5X,
```

```
420&"(1+L/D)=",F7.1)
430 PRINT 20,B2,B3
440 20 FORMAT(1X,"ALPHA= ",F6.2,2X,"ETA= ",F6.2)
450 PRINT 30,X4,F4
460 30 FORMAT(1X,"CORR. L= ",F7.4,2X,"CORR. FREQUENCY= ",F7.1)
490 40 FORMAT(1X,F6.1,10X,F6.1,10X,F6.1)
495 P4=0.
496 P3=0.
500 PRINT," FREQUENCY    ANGLE FACTOR      INTENSITY"
510 K=IFIX(F4/20.0)
520 DO 100 I=1,(2*K+1)
530 W2=2.0*3.14159*(F1-20.0*FLOAT(K-I+1))
540 W1=2.0*3.14159*F1
545 W4=2.0*3.14159*F4
550 B4=(W2-W1)**2
560 B5=(B4+4.0*W2*W1*(SIN(P4))**2)/C**2
570 G4=-0.5*B5*X4**2-0.5*B4/W4**2
580 X7=(COS(P3))**2*EXP(G4)
581 S7=10.0*ALOG(X7)/ALOG(10.0)
590 X8=V*X4**3*(W2/C)**4*Z3**2*X7/(4.0*3.14159**2*W4)
592 S8=10.0*ALOG(X8)/ALOG(10.0)
600 F2=W2/(2.0*3.14159)
610 PRINT 40,F2,S7,S8
650 100 CONTINUE
700 STOP
800 END

ready

*BYE
  usage:   1.3 cpu-sec,   1.9 i/o-sec,   27.3 k*sec,   0.07 con-hrs.
  off even-b at  9.034 on 09/02/75.  0.0017 nbu  $   0.41


CP DISCONNECTS
```